THE CHEMICAL KINETICS OF THE HYDROGENATION OF COAL EXTRACT SOLUTIONS

A thesis submitted by

Stephen Gerard Jones

for the degree of

Doctor of Philosophy (Ph.D),

August 1979

THE CHEMICAL KINETICS OF THE HYDROGENATION OF COAL EXTRACT SOLUTIONS

A thesis submitted by Stephen Gerard Jones

for the degree of Doctor of Philosophy (Ph.D)

August 1979

SUMMARY

The chemical kinetics of the hydrogenation of coal extract solutions have been studied in a semi-continuous stirred tank reactor with slurried catalyst.

The reactor system and experimental programme were designed so that many of the process variables affecting the rate of hydrogenation of coal extract solutions and suspected reaction intermediates could be investigated. These variables included reaction time, temperature, pressure, catalyst loading and coal concentration and their effects on hydrofining, catalyst deactivation and product composition were also studied.

The results showed that at the catalyst loadings generally employed, the rate limiting steps were chemical reaction on the catalyst surface and mass transfer from the gas-liquid interface into the bulk liquid.

The overall reaction was found to be first order with respect to coal material remaining, the rate constant showing an Arrhenius temperature dependence giving a high apparent activation energy.

The kinetics could be adequately described in terms of a series of distillation fractions of different boiling range. On this basis, a scheme has been proposed for the reactions involved in the hydrogenation of coal extract solution.

The rate constants for each step in the scheme were determined and a mathematical model was developed. The yields predicted by the model were in good agreement with the experimental results. It was also shown that the reaction scheme was applicable to the hydrogenation of coal extract solutions in other reactor systems.

KEYWORDS:- Coal
Hydrogenation
Kinetics

For

Samantha, Abi and Daniel

"We are as much gainers by finding
a new property in the old earth as
by acquiring a new plant."

Emerson.

ACKNOWLEDGEMENTS

The experimental work for this thesis was carried out entirely at the National Coal Board's Coal Research Establishment and constituted part of the research programme of the Coal Refining Department. The views contained in the thesis are those of the author and not necessarily those of the Board.

I am sincerely grateful to Professor Mike Page, my University Supervisor, not only for his help and advice but especially for the encouragement he has given me over the last four years. I also owe a debt of thanks to Wally Wyss and, formerly, Frank Derbyshire, my External Supervisors. Also, the thesis would never have begun had it not been for the enterprise of Glyn Davies, Head of the Hydrogenation Section at C.R.E.

The thesis has been typed with much patience by Jane Robinson, to whom I am grateful.

Some of the analyses were carried out by CRE Chemistry and Product Development Departments, and Dave Collop and Trish Pruden of the Physics Department have given me the benefit of their mathematical expertise, especially in writing the computer programmes.

I express my humble thanks to all those who have been involved in proof-reading and to those who have given me the benefit of their advice.

Finally, I would like to apologise for the monosyllabic text (which is entirely the fault of my three children and their bedtime stories!) and to my wife, Liz, for my single-mindedness during the writing of the thesis, which would have taken a lot longer without her understanding.

CONTENTS

PAGE NUMBER

LIST OF TABLES

LIST OF FIGURES

Figure Number

In Appendices:

CHAPTER 1

INTRODUCTION

Recent estimates have shown that coal reserves in the United Kingdom alone are sufficient to last at least 300 years whereas it is predicted that petroleum production will reach a peak during the 1980's. Direct coal combustion and atomic energy are the main alternatives for industrial and domestic energy so that diminishing petroleum production will have greatest impact on the petrochemical and automotive fuel markets.

Although liquid hydrocarbons suitable for these markets were being manufactured from coal in the 1930's and 40's, the processes employed were not economic compared with those developed for treating inexpensive crude oil. It is only now, with rising petroleum costs, that coal conversion processes are becoming economically viable and the subject of this thesis represents part of the renewed effort in coal conversion technology.

A process has been developed at the Coal Research Establishment where coal is dissolved in a coal-derived oil, with the elimination of most of the ash, to produce a coal extract solution. This material is considered to be a convenient feedstock for hydrogenation as its ash-free nature allows the use of typical, highly active petroleum processing catalysts.

In order to produce distillable liquid hydrocarbons from coal it is necessary to convert the large, highly aromatic, hydrogen-deficient coal molecules to smaller, distillable hydrocarbon molecules by cracking and simultaneous hydrogen addition.

In the design of any coal conversion process, it is important to obtain fundamental information regarding the physical and chemical processes involved. The latter comes under the realm of chemical kinetics and this can be used to answer process-design questions for various types of reactions and reactors and also to give an insight into possible reaction paths.

The main objectives of this work, therefore, were as follows:

(1) To set up a facility to study the kinetics of the hydrogenation of coal feedstocks.

(2) To study the effect on coal hydrogenation of process variables.

(3) To evaluate rate functions.

(4) To propose a kinetic model to describe the major reaction paths.

(5) To carry out further experiments to test the validity of the model.

(6) To relate the results obtained to other systems.

CHAPTER 2

LITERATURE REVIEW

2.1 Background

North Sea oil production will pass through a maximum in 1981[1], and according to some estimates[2] all available natural gas and oil throughout the world will be consumed by the year 2020 if the present petrochemical industry growth rate (currently about 3% per year) is maintained. Recent estimates of World and European reserves of oil, natural gas and coal[3] are given in Table LR1:

	Oil	Natural Gas	Economically recoverable coal
World	209,018	113,878	786,650
East & West Europe	5,212	5,613	87,065

TABLE LR1. World and European Fossil Fuels Reserves (1977) in m.tons coal equivalent

The alternatives to oil and natural gas in the U.K. are coal, nuclear power and, to a lesser extent, wind, wave and solar energy and biomass. Current projections estimate that coal will last for at least 300 years in this country. The production of substitute feed-stocks from these alternative resources is, therefore, of fundamental importance and research work in each of these branches is being vigorously pursued. This study will be concentrating on the conversion of coal by catalytic hydrogenation.

2.2 History of Coal Hydrogenation Processes

The first experiments in the hydrogenation of coal into liquid products were performed in 1869 by Berthelot[4] using hydrogen iodide. He obtained a 67% aromatic oil yield at 270°C. In 1913, Bergius[5] patented a method of direct hydrogenation of coal at 100 atmospheres and 450°C which led to the Bergius process[6] of 1921, operated by

Bergin AG. Here, the coal-oil mixture was hydrogenated at 200 atmospheres and 480°C using a titaniferous ore (Luxmasse) catalyst.

In 1919, independent work by I.G. Farbenindustrie had begun in Germany and after the development of sulphur resistant catalysts in 1926, a plant was opened at Leuna in 1927 to produce 100,000 tons/year of liquid fuels.(7) This was a two-stage process. The first stage was carried out at 700 atmospheres and 450°C using a once through, cheap Bayermasse catalyst. The middle oil produced was then hydrogenated in the second stage of the process at 300 atmospheres using a more active catalyst. In 1944, there were 18 plants in Germany with a total capacity of about 4 m.tons/year.

In the U.K., work on coal hydrogenation began in 1920 by the British Fuel Research Station. In 1926 a 1 ton/day Bergius plant was installed.(8) In 1935 a plant was opened at ICI, Billingham to produce 100,000 tons/year of liquid fuels.(9) The process involved liquid phase hydrogenation of coal to middle oil and gasoline followed by vapour phase hydrogenation of middle oil to produce more gasoline. Tin catalysts were used in the process which was operated at 250 atmospheres and 450°C.

After the Second World War, the changing economical conditions resulted in the closing down of most coal hydrogenation plants, although research continued or was resumed in the 1950's and 60's by many countries, notably Germany, India, Australia, Japan, USSR and USA.

Since the oil crisis of 1973, research in coal conversion has escalated greatly and many new processes are under investigation. The different processing schemes fall into three general categories. First, a single-stage process of extraction with catalytic hydro-

genation such as in the fixed-bed catalyst reactors developed by the Gulf Oil Corporation and the United States Bureau of Mines. Second, a three-stage process of solvent extraction followed by separate catalytic hydrocracking such as the Consol Process.

The third category is based on the Fischer-Tropsch synthesis, the Sasol process in South Africa being the first of the "new generation" of coal to oil plants to run on a commercial basis. The process involves the production of synthesis gas followed by its conversion to low boiling liquids using a fluidised catalyst bed and to higher boiling liquids using a fixed bed.

The other processes may operate commercially before the end of the century.

2.3 Nature of Coal

2.3.1 Formation

Coal is a carbonaceous, non-homogeneous, highly variable fossilized material formed millions of years ago from decayed plant remains. Under the influence of heat, pressure and geologic time the plant fragments were altered, minerals were transformed and volatile components driven off. The extent to which this process of coalification continued determined the type or "rank" of the coal formed.

A low rank coal, eg. a lignite, contains less carbon and more oxygen (typically 65%C, 30%O) than a high rank coal, eg. an anthracite (typically 95%C, 2%O). British coals fall predominantly into the class known as hard coals, with carbon contents ranging from about 80% to 95%.

2.3.2 Structure and Composition

Coal is believed to consist largely of aromatic and hydroaromatic ring systems linked by direct carbon-carbon bonds, aliphatic groups or ether linkages.

Several structural models have been put forward for coal. The "turbostratic-lamellar" model of Blayden[10] looked upon coal molecules as polycondensed aromatics (lamellae). A number of lamellae showing parallel orientation coalesce to form one crystallite. The model of Hirsch[11], distinguished between three structures: (1) The open structure typical of low rank coals. Lamellae are connected by cross-links and randomly orientated giving a porous structure, (2) the liquid structure, typical of the bituminous coals. Lamellae are more orientated and pores are practically absent. (3) The anthracitic structure, where lamellae are highly orientated.

From spectrometric studies Dryden[12] found that about 70% of all carbon atoms in coal are in aromatic rings, but only about 23% of hydrogen atoms are attached to aromatic carbon atoms, ie. the aromatic systems are heavily substituted.

Ayre[13] suggested that the number of aromatic rings per cluster in coal was constant at 4 or 5 up to 85% carbon content, then increased rapidly with rank.

In 1963, van Krevelen[14] suggested a simple structural unit to correlate the available information about coal structure:

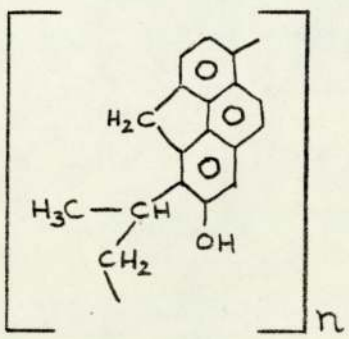

This unit ignores the presence of sulphur and nitrogen, which generally represent only a small part of coal composition (see Section 2.3.3).

It should be understood that such a unit represents an average of all the features present and does not necessarily or even probably exist as such in any coal.

Wynne-Jones[15] found values of molecular weight for pyridine extracts of between 400 and 1200 (depending on coal rank). From these results, he calculated the number average molecular weight of coal to be about 2000. Hayatsu[16] gave the structural formulae of 18 aromatic units believed to be indigenous to bituminous coal. They were benzene, naphthalene, phenanthrene, fluoranthene, fluorenone, anthraquinone, benzanthraquinone, dibenzofuran, benzonaphthofuran, xanthone, benzoxanthone, dibenzo-p-dioxin, benzothiophene, dibenzothiophene, pyridine, quinoline, carbazole and acridone.

From N.M.R. studies, Pugmire[17] found a significant amount (estimated at about 5%) of normal paraffinic material present in coals both as free paraffins and as alkyl substituents or aromatic and hydroaromatic materials.

2.3.3 Heteroatoms in Coal

2.3.3.1 Oxygen

The oxygen content of coals varies with rank, falling from about 30% in lignites to as little as 2% in anthracites[19]. Low and high rank bituminous coals contain about 14.0 and 2.2% oxygen respectively.

Lignites contain various oxygen groups including -COOH, but in bituminous coals a large proportion of the oxygen is present as -OH and the remainder mainly as -O- in linkages or as C=O. Orchin[18] and others have found about 5% hydroxyl oxygen in a coal containing 84% carbon.

2.3.3.2 Nitrogen

Nitrogen in coal again varies with rank, according to Shacklock[20], but the effect is small, most coals having a nitrogen content in the range 0.6-1.8%.

Birkofer[21] divided the nitrogen in coal into four categories. (1) The water phase which contained purine bases, structures with urea units, amino acids and peptides (35%); carbazole structures (10%); low molecular weight cyclic bases and phenylamines (3%). (2) The chloroform phase including nonbasic nitrogen compounds, fatty amines and hydrophobic bases (23%). (3) Residual coal - high molecular weight nitrogen compounds (3%). (4) Compounds yielding free nitrogen (26%).

Hill[22] stated that in bituminous coals nitrogen occurs mainly in the heterocyclic ring structures whereas sulphur and oxygen may be present in linking groups.

2.3.3.3 Sulphur

The amount of sulphur present in different coals is very variable, but in general, European coals have a lower sulphur content than U.S.A. coals.

Sulphur occurs in coal as organic chemical combinations, as pyrites and/or marcasites, and as sulphates[23].

Lissner[24] found that organic sulphur in coal exists in four forms: $\geq C-SH$, $\geq C-S-S-C\leq$, $>CH-SH$ and $>CH-S-CH<$.

2.3.4 Mineral Matter in Coal

Coal is invariably associated with mineral matter, which varies greatly in amount and composition. It occurs in two forms; intrinsic - originating from the inorganic matter originally present in the vegetation which produced the coal - and extrinsic, representing material introduced to the area of the coal seam from the surrounding rocks.

Mineral matter usually contains SiO_2, Al_2O_3, Fe_2O_3, CaO, MgO, TiO_2, alkalies and many less common elements in small quantities.

2.3.5 Structure of Coal Extract

Snape[25] has compared the structure of anthracene oil extracts of high and low rank coals using information obtained from elemental analyses, molecular weight determinations, NMR and phenolic -OH determinations. The extracts contained about 80% coal, 20% oil.

He concluded that (1) high rank extract solutions have more condensed aromatic structures containing 4.5 rings per cluster compared to 3-3.5 rings per cluster for low rank extracts. (2) High rank extract solutions have a smaller degree of substitution on the aromatic skeleton than low rank extract solutions. (3) High rank extract solutions have a higher aromaticity than low rank extract solutions.

For each extract solution, two average molecules were proposed representing two views on coal structure viz. (i) The aromatic clusters are joined by methylene bridges and heterocyclic links, (ii) The aromatic clusters are joined by hydro-aromatic structures such as polynaphthenics.

(i) Methylene bridge model

High rank coal extract solution:

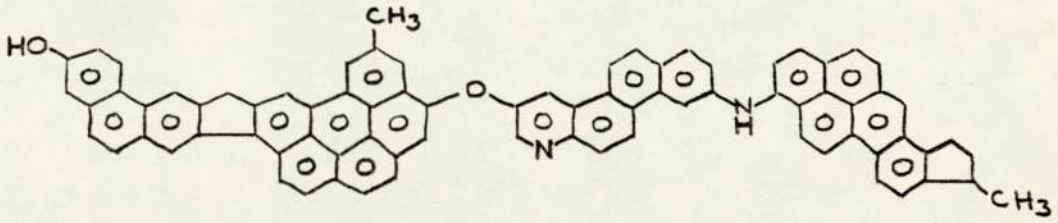

Low rank coal extract solution:

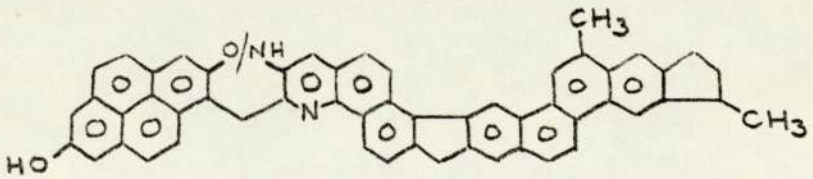

(ii) Hydroaromatic model

High rank coal extract solution:

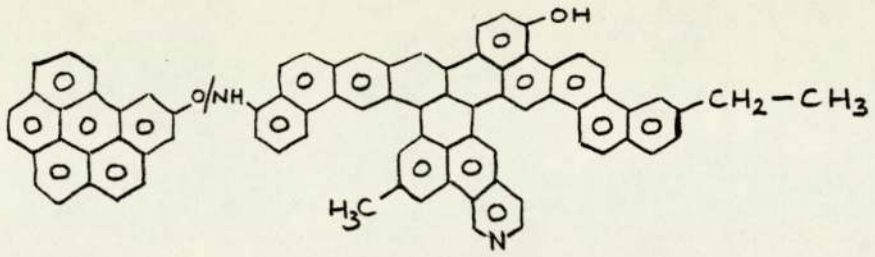

Low rank coal extract solution:

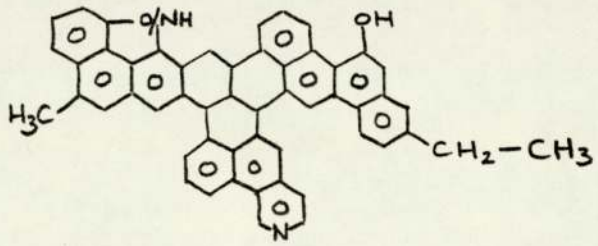

2.3.6 Molecular Weight of Coal Extracts

In the work of Snape[25], it was found that the number average molecular weights of high and low rank coal extracts were 660 and 570 respectively. This agreed with the work of Golumbic[26] who found the molecular weights of various extracts to be less than 1000. Wynne-Jones[15] estimated the molecular weight of pyridine extracts to be between 400 and 1200, depending on coal rank.

It should be pointed out that all these values refer to the molecular weight of the portion of extract which was soluble in the solvent used for the determination, so that the values of molecular weight of the whole extract may be considerably higher than those given here.

2.4 Feedstocks

2.4.1 Coal Solubility

Oele[27] distinguished between four types of coal extraction. (1) Non-specific extraction by solvents such as alcohol, benzene and ether. (2) Specific extraction with nucleophilic solvents such as the

pyridine bases, aliphatic amines and mononuclear phenols. (3) Extractive disintegration with polynuclear aromatic solvents including phenanthrene, naphthols, pitch and pitch oils. (4) Extractive chemical disintegration with polynuclear hydro-aromatic solvents of the tetralin type.

Only a small amount of coal is dissolved in non-specific extraction and is therefore relatively unimportant.

Between 20 and 40% of coal is dissolved in specific extraction which is carried out at temperatures below 200°C. Dryden[28] has measured the extraction capacity of many solvents.

In extractive disintegration, anthracene oil is widely used as the coal extraction solvent because it is coal-derived, it is a good solvent for coal and it has hydrogen-donating properties. Anthracene oil is obtained from coal tar. Its chemical composition is complex and has been extensively studied by Kruber[29]. He has listed many of the hundreds of aromatic compounds present, including dihydroanthracenes, methylphenanthrenes, phenylnaphthalenes, quinolines and fluorenes.

Extractive disintegration is carried out at temperatures above 200°C and yields are high. At 350-380°C, Gillet[30] found that up to 90% coal dissolved in anthracene oil. However he also found that the solution was temporary and that the disintegrated coal could be flocculated by the addition of light solvents. On addition of oleic acid at 350°C, this flocculation was eliminated. The extraction yield also depended on coal rank[31], reaching a maximum at 88% carbon content, and temperature. Maximum extraction was achieved between 370 and 400°C.

Extractive chemical disintegration is a high temperature (>300°C) process. Davies[32] found that hydrogenated anthracene oil was a better coal solvent than fresh anthracene oil. This was due to the presence

of fairly high concentrations of polynuclear hydroaromatics effecting liquefaction by a process involving the thermal dissociation of coal with hydrogen donation by the solvent.

Orchin[33] has summarized the effectiveness of a coal solvent with respect to its structure. (1) The least effective solvent is a high boiling aromatic compound. (2) A better solvent is a high boiling aromatic compound possessing good hydrogen-donor properties. (3) The best solvent has the properties of (2) and includes aromatic hydroxyl groups in the structure.

The kinetics of coal extraction have been studied by several authors, all of whom state that the rate of extraction is independent of added catalyst.

Curran[34] studied extraction using a number of pure solvents and postulated a free radical mechanism where coal was extracted in two steps. Both steps were thought to be first order, but the first proceeded at ten times the rate of the second. Oele[27] also found extraction in anthracene and β-naphthol solvents to be a two-step process, but the first step was zero order while the rate of the second depended on the fraction of material extracted.

More recently Squires[35] and Cronauer[36] have studied extraction by anthracene oil and hydrogenated anthracene oil respectively. They both proposed a three step mechanism of the type

coal $\longrightarrow$ preasphaltene $\longrightarrow$ asphaltene $\longrightarrow$ oil

where the last step was the slowest. Preasphaltene is defined as material soluble in pyridine but insoluble in benzene and asphaltene as material soluble in benzene but insoluble in n-hexane.

2.4.2 Hydrogen Solubility

Very little work has been reported on the solubility of hydrogen in coal feedstocks, petroleum products and other organic compounds under conditions of high temperature and pressure.

According to Ipatieff[37], hydrogen was more soluble in alicyclic than in aromatic compounds. The solubility in aromatic compounds decreased with increase in the number of methyl side-chains. At 100°C, 100 bar, the solubility of hydrogen in hydrocarbons of the aromatic and naphthenic series obeyed Henry's Law, but at higher pressures, the solubility coefficient increased with pressure. In other work, Ipatieff determined the solubility at high temperatures and pressures (up to 300°C, 300 bar) of hydrogen in benzole, toluole, xylole, gasoline fractions and kerosene[38] and in various gasolines and kerosenes, cracking residue, shale and peat[39]. In the latter work, some heats of solution were also quoted. The main conclusions to be drawn from these works were:
(1) The solubility of hydrogen increases with temperature and pressure.
(2) The solubility decreases with the complexity of the composition of the molecule, being the greatest for benzole and gasoline.

Frolich[40] determined the solubility of hydrogen in cyclohexane, heavy naphtha, gas oil and other solvents at high pressures (up to 200 bar). He concluded that if hydrogen did not form a chemical compound with the solvent, it followed Henry's Law over a wide pressure range.

Rapoport[41] gives values for the solubility of hydrogen and other gases in the hydrogenate, slurry oil and wash oil of a coal slurry hydrogenation process under the conditions 550 bar hydrogen pressure, 475-480°C. A red-mud catalyst was used. The solubilities quoted were 0.05, 0.06 and 0.31 $cm^3/g/bar$ respectively.

More recent work has been carried out by Guin[42] and by Prather[43] both of whom studied the solubility of hydrogen in creosote oil at high temperatures and pressures. Both confirmed the inverse temperature behaviour found by Ipatieff with the solubility at 400°C being greater than that at 100°C at the same pressure. Guin

quoted the hydrogen solubility in creosote oil (which is similar to anthracene oil) at 3000 psi, 400°C at 0.0028 gH_2/g oil.

2.4.3 Production of Coal Extracts

At the Coal Research Establishment, a pilot plant has been operating for several years producing essentially ash-free coal extract solution. This was considered an ideal starting material for the study of catalytic coal hydrogenation. In the extraction process,[44] a coal-anthracene oil slurry is heated to 400°C under sufficient pressure to ensure that the oil remains in the liquid phase (about 7 bar). Mineral matter and undissolved coal are separated by filtration and the resulting filtrate is converted to a solid extract solution by evaporation of a considerable proportion of oil which is then recycled. The amount of dissolved coal in the extract solution is up to 60% dry-mineral-matter-free coal. When hydrogenated anthracene oil solvent is used, the yield increases to 85%.

The process was developed from that of Pott-Broche[45] where coal was extracted with a gas-oil fraction (from the hydrogenation of coal tar) at 425°C and 10-30 bar for one hour. The filtered product had a higher hydrogen and lower oxygen and sulphur content than the coal and was ash-free. The extract yield was about 70-80%.

The Consol process[46] also made use of the Pott-Broche process. In most other extraction processes, however, simultaneous hydrogenation is carried out to produce greater yields and a better recycle solvent. The Spencer or Pittsburg-Midway process[47,48] and that of the Southern Services Company[49] use the Uhde approach, also operated in Germany. Here, high hydrogen pressures (100-200 bar) are used and more than 90% of the coal is dissolved. The ash is separated from the product and recycled as a catalyst. The Clean Fuels West process[50]

is similar, but no catalyst is used, the process being designed for coals with large amounts of catalyst poisons.

Exxon's approach[51] is again similar, except that unusually severe conditions are employed yielding a recycle solvent of high quality which can convert coal in the presence of hydrogen to a relatively light liquid.

The H-Coal and Synthoil processes and that of the Lummus company have modified the Uhde approach by the addition of catalyst to the dissolution step to promote better hydrogenation of the solvent.

2.5 Catalysis

2.5.1 Catalysts for the Hydrogenation of Coal

A vast amount of research has been undertaken on the selection of suitable hydrogenation catalysts. Since the subject does not form an integral part of this thesis, it will not be covered here in detail.

Catalysts typically contain varying amounts of hydrogenation to cracking activity, depending on the requirements of the process. Precious metals such as palladium and platinum are good hydrogenation components, while cracking components have ranged from montmorillonite to aluminosilicates and zeolites. The most widely used catalyst for the production of low boiling liquids from coal appears to be cobalt-molybdenum, on a silica-alumina support, which displays both hydrogenation and cracking properties. For example, Kawa[52] found this the best catalyst in batch systems out of the 85 tested. However, much work is being carried out on novel catalysts which may eventually prove to be superior to the cobalt-molybdenum system.

Ash, mineral matter and trace metals have also been found to be catalytically active. Gatsis[53] has patented the use of ash from coal

decarbonization as a hydrogenation catalyst. Since this could be produced by the process itself, Gatsis claimed that no deactivation by poisoning or coking occurred. Mukherjee[54] has shown that kaolinite (the major component of coal mineral matter) influenced the production of gas and benzene-soluble products in coal hydrogenation. Trace metals such as iron and titanium have also been found to act as catalysts for coal hydrogenation[54,55,56] iron being converted to catalytically active FeS by sulphur in the coal.

The solvent used in the process can also act as a catalyst. Gleim[57] found that certain solvents promoted the transfer of hydrogen from the gas phase to the coal, which eliminated the use of an added catalyst for this step.

2.5.2 Catalytic Effect of Autoclave Walls

Autoclaves are made of many different materials, although most are of stainless steel. Ipatieff[58] found that hydrogenation gave different products in different autoclaves. He found that, of those tested, a stainless steel autoclave which was not new gave the best yield of p-menthane in the hydrogenation of p-cymene. It was suggested that this was due to the nickel present in the steel.

In the thermal cracking of indan, Slotboom[59] found that the conversion increased from almost zero as the gold plated stainless steel autoclave aged. However, he suggested that the effect was due to free radicals on the coke formed on the walls of the autoclave. The presence of free radicals was detected by E.S.R. measurements.

2.5.3 Catalyst Deactivation

Catalyst deactivation is caused by three types of components; nitrogen and sulphur compounds, trace metals and carbon or coke.

Trimm[60] listed a number of alkaline nitrogen impurities which neutralized the acidic properties of a catalyst. They included pyridines and quinolines. Deem[61] stated that diphenyl sulphide, thiophenol and diphenyl sulphoxide were active poisons although deactivation by sulphur could be largely eliminated by the use of sulphide[62] or carbonyl[63,64] catalysts.

Kovach[65] found that poisoning of the catalyst could be either temporary or permanent. Heavy carbonaceous materials were temporary poisons and the activity of the catalyst could be restored by air regeneration. However, some components in coal permanently deactivated the catalyst. The latter effect has been attributed to minerals, metals and large porphyrin-type molecules which blocked catalyst pores.

Kang[66] considered that the deactivation of cobalt-molybdenum catalyst in the H-Coal Process was initially due to carbon deposition and that further deactivation was caused by metals deposition. Others[62,67] have suggested that the deactivation of fresh catalyst was caused by coke deposition alone.

Metal deposits were harmful during catalyst regeneration[62,67,68] when solid phase reactions took place between the carrier, the catalyst metals and the deposited metals[62] with a reduction in surface area[68].

The ash levels in the feed may also be important. McColgan[67] found that successful regeneration could be achieved after processing a feed containing 0.013% w/w ash but not with 0.7% ash. It has been suggested that deposited metals could act as polymerization catalysts, increasing carbon deposition[62]. Lipovich[69] found that thiophene made a strong contribution to the formation of carbonaceous deposits on cobalt-molybdenum catalysts.

2.6 Hydrogenation of Pure Compounds.

The hydrogenation of individual compounds representative of structures thought to be present in coal is a valuable contribution to the mechanistic study of coal hydrogenation. Although much work has been done in the general hydrogenation field, less has been carried out using similar conditions to those used in coal hydrogenation.

2.6.1 Hydrogenation of Naphthalene

The main products in the hydrogenation of naphthalene are tetralin and decalin irrespective of the conditions or catalyst used. Friedman[70] found that tetralin yields ranged from 16% with $Co_2(Co)_8$ at 200°C and 200 bar to 84% with a complex metal catalyst at 210°C, 70 bar. Decalin yields ranged from 13%[71] to 46% with a platinum on Al_2O_3 catalyst at 450°C, 75 bar[72]. The best catalyst was probably MoS_3 at 400°C, 100 bar[73], when an appreciable conversion to tetralin was achieved at a fast rate. Qader[74] has found that while phenol and 1% sulphur (as dibenzothiophene) increased naphthalene conversion, carbazole, quinoline and 2% or more sulphur reduced it.

2.6.2 Hydrogenation of Tetralin

Decalin is usually the main product from the hydrogenation of tetralin. Frye[72] obtained 52% decalin and also 11% naphthalene. Potgieter[75] found that a $SnCl_2$ catalyst was inferior to Co_2O_3 for the reaction of tetralin to decalin and for the dehydrogenation of tetralin. He also found that the production of naphthalene, which often occurred because of the hydrogen-donating properties of tetralin[76], was either reversible or irreversible depending on the catalyst used. Hall[73] reported that the hydrogenation of tetralin at temperatures above 400°C resulted in cracking in the following scheme:

tetralin ⟶ n-butylbenzene ⟶ ethyl benzene ⟶ toluene ⟶ benzene

2.6.3 Hydrogenation of Anthracene

9,10 dihydroanthracene is usually the main product in the hydrogenation of anthracene, but the yield varies considerably with conditions. With no catalyst, Penninger[77] found that excessive coke formation occurred at 485°C, 80 bar. Friedman[70], however, found that a 99% conversion was obtained using a $Co_2(CO)_8$ catalyst at 135°C, 200 bar but with a cobalt-molybdenum catalyst at 540°C, 42 bar, Krichko[78] obtained only a 14.4% yield of hydroanthracenes. Other products which Krichko obtained were 7.7% C_{12}-C_{14} alkylnaphthalenes, 2.9% methylnaphthalenes, 1.3% naphthalene, 0.9% tetralin, 34.8% coke and 15.9% gaseous hydrocarbons. This illustrates that hydrogenation products even of a simple feed can be complex. In Blom's hydrogenation of anthracene[79] at 385°C, 200 bar using a Sn/NH_4Cl catalyst, the products included 19.6% benzene, 32.7% toluene, and 14.5% ethyl benzene indicating that a high degree of hydrocracking had occurred.

2.6.4 Hydrogenation of Phenanthrene

The conversion of phenanthrene has been found in general to be a quarter that of anthracene[78]. Maiorov[76] found that the hydrogenation was almost zero order with respect to phenanthrene and first order with respect to hydrogen, but Qader[80] and Haynes[81] obtained first order kinetics.

In the absence of a catalyst, Penninger[77] found the main products to be 1,2,3,4-tetrahydrophenanthrene and 9,10-dihydrophenanthrene at 80 bar and 475 to 495°C. Cracking only occurred at 495°C or greater. Using a cobalt-molybdenum catalyst at 540°C, 42 bar, Krichco[78] obtained a product distribution of 3.7% hydrophenanthrenes, 0.7% methylnaphthalenes, 0.3% naphthalene, 1.4% biphenyl, 0.5% coke and 6.9% gaseous hydrocarbons. With a platinum catalyst at a higher pressure (157 bar), Frye's product[72] was a mixture of 5% dihydro-, 15% tetrahydro-, 23% octahydro- and 46%

perhydrophenanthrene.

Wu[82] suggested that the major reaction path in phenanthrene hydrogenation was saturation and cleavage of the terminal rings as shown by the presence of butyl tetralin and butylbenzene intermediates. Cracking at the saturated middle ring was a minor reaction only. The hydrogenation of anthracene proceeded similarly.

2.7 Thermal Decomposition of Coal

The geologically younger and less metamorphosed coals, such as brown coals and lignites, begin to break down more quickly with increasing temperature than the older coals. The greater ease of disintegration is probably related to the proportions of cellulosic and resinous constituents, the younger coals yielding a larger proportion of carbon dioxide and water at lower temperatures[83].

Coals undergo three main endothermic reactions on heating[84]; water removal, primary degasification and secondary degasification. The behaviour depends not only on the type of coal but also on the method of heating[85].

Water is generally removed at about 150°C[85].

Some gas is evolved from coal at temperatures below the decomposition point. This originates from the expulsion of occluded gas in the coal. Each type of coal, however, has a definite decomposition temperature marked by a rapid increase in gas evolution. This temperature is usually around 250°C[86], when hydrogen sulphide, ethylene and higher olefins[87] begin to be formed. Primary degasification continues with a rapid increase in the evolution of carbon monoxide, hydrogen, hydrocarbon gas and ammonia at 300-350°C. The rate of gas evolution then

steadily increases with temperature, but the rate of evolution of light gaseous hydrocarbons has been observed to go through a maximum[86]. Tarry liquids are also produced at about 300°C.

At 500°C, secondary degasification begins and the evolution of hydrogen, methane and carbon dioxide increases rapidly. This corresponds to a rapid decrease in the yield of tarry liquids with the formation of coke.

At 900°C, practically the whole of the volatile constituents of some bituminous coals are expelled.

Some kinetics of the thermal decomposition of coal have been studied.

Fitzgerald[88] found that the production of methane and hydrogen up to about 500°C took place as first order reactions. Above 500°C, structural changes in the coke made the interpretation of the kinetics difficult.

Yellow[89] found the overall reaction to be first order throughout. In the pyrolysis of bituminous coal, between 410 and 500°C, however, Wiser[90] found the order to decrease from second order initially through 1st order to zero order after 375 minutes. He obtained activation energies of 36.6 and 5.36 kcal $mole^{-1}$ for the 2nd and 1st order regions respectively.

2.8 Hydrogenation of Coal

The physical disadvantages of coal relative to petroleum are that coal is a solid and has a high ash content. The fundamental chemical problem in the manufacture of chemicals and gasoline from coal is the need to add hydrogen. The hydrogen content of coal is about 5% (w/w) while for gasoline it is about 14%. Technically it is possible to make high quality chemicals and gasoline from coal but currently, the economics

are unfavourable. In general, processes must be developed to reduce investment and operating costs for the hydrogenation of coal to liquids.

2.8.1 Methods of Coal Hydrogenation

2.8.1.1 In-situ Hydrogenation

Feasibility studies have been carried out into a number of in-situ coal extraction processes[91,92], but these assume that hydrogenation would be carried out as a surface operation. However, Pevere[93] has patented a process in which a seam of coal is hydrogenated at about 400°C and 70 bar hydrogen. Apparent advantages of the method would be the elimination or reduction of mining, coal preparation and high-pressure equipment costs. It is likely, however, that hydrogen losses would be high and control of the reaction would be extremely difficult.

2.8.1.2 Hydrogenation of Coal alone

In the laboratory, hydrogenation of coal alone has been attempted [94,95], but liquid yields have been low - 27% at a maximum. Using a cobalt-molybdenum catalyst, it has been shown[95] that hydrogenating coal in the absence of a solvent produced half as much asphaltenes in the product as hydrogenation using a slurry medium. The yield of material boiling below 300°C was found to be higher when no slurry medium was used. Schroeder[96] has found that sweet crude could be produced from coal with a fast reaction rate by solid-phase hydrogenation.

Some work has been done on the hydrogenation of coal in a fluidised state with the aim of producing low boiling liquids[97-101]. The usual conditions employed for this were 600°C and 1500 psi or lower. Batch and continuous systems have been examined, but the latter have not been successful because most coals agglomerated during hydrogenation and the systems became inoperable. However, the Standard Oil Company[101] claimed that agglomeration was prevented by the addition of a nonplasticizing

material such as clay, sand or solid residue from the process.

The low pressure required in the process favours the economics, but the high yields of gas obtained offset this.

2.8.1.3 Hydrogenation of Coal/Oil Mixtures

The hydrogenation of coal is usually carried out in the presence of a solvent to improve the ease of operation. In the production of low boiling liquid hydrocarbons, two stages are normally used. In the first stage, coal/oil slurry or coal extract is reacted in the liquid phase with hydrogen at 400-450°C and 200-400 bar in the presence of a fixed bed catalyst in a trickle bed reactor. Most of the heteroatoms and ash is removed and a distillable oil product results. The second stage is then carried out in the liquid or vapour phase with active catalysts to produce refined liquid fuels or chemical feedstocks.

Other processes have been patented[102,103] in which coal/oil mixtures are atomized into a stream of hot hydrogen, thus increasing the surface area of the feed and accelerating the rate of hydrogenation. It is claimed that higher liquid and lower gas yields were obtained by this process.

Also patented[104,105] is a process in which coal/oil/hydrogen mixtures are injected into a molten metal bath. The metal acts both as a catalyst and as a means of controlling the reaction temperature. It is claimed that a higher rate of hydrogenation was obtained by the use of this process.

2.8.1.4 The Use of Atomic Hydrogen

Numerous methods of coal hydrogenation have been patented where it is claimed that the production of atomic hydrogen in the reaction mixture increased the rate of reaction. However Letort[106] found that the main products were gaseous hydrocarbons when 20-50% atomic hydrogen was used.

2.8.1.5 The Use of Carbon Monoxide and Water

Atomic hydrogen is also thought to be formed during the hydrogenation of coal using carbon monoxide and water. This method of hydrogenation was first reported in 1921 by Fisher[107] who obtained higher yields of ether-soluble material than when molecular hydrogen was used.

The method has been studied more recently by Appell[108-110], Handwerk[111] and Fu[112]. The principal advantages of the CO/H_2O process over using molecular hydrogen are (1) low cost, (2) increased liquefaction, (3) reaction of carbon monoxide with oxygen which normally consumes hydrogen.

2.8.2 Product Distribution

The products obtained in the hydrogenation of coal depend on the starting materials and the reaction conditions. For example, in work carried out by the Fuel Research Station[113] it was found that without vehicle oil or catalyst, no significant reaction occurred below 400°C at 100 bar and the temperature had to be raised above 440°C for any noticeable reaction to occur. In the presence of vehicle oil and catalyst, the product distribution varied greatly with catalyst type and conditions employed.

In 1931, Gordon[114] found a relationship between product distribution and the rate of cracking of coal. If the rate of cracking were too fast, an excess concentration of aromatic compounds occurred. If cracking were too slow, a low yield of light products with excess concentration of naphthenic compounds occurred. The cracking rate was dependent upon temperature. Gordon also found that coke and gas formation were reduced by the use of excess hydrogen.

2.8.3 Mechanism and Kinetics of Coal Hydrogenation

2.8.3.1 Mechanistic Models

The mechanisms involved in heterogeneous catalysts are well known, but the rate-determining step is governed by the choice of reaction conditions. In 1924, Lush[115] proposed that three steps were important in the hydrogenation of vegetable oils at low temperatures and pressures using a metal catalyst. (i) The dissolution of hydrogen and its diffusion to the catalyst surface. (ii) The condensation of hydrogen on the catalyst and its appearance at, or its evaporation from, the surface as atomic hydrogen. If the latter condition were the limiting factor, then the reaction velocity $\propto \sqrt{H_2 \text{ pressure}}$. (iii) The reaction of atomic hydrogen with ethylene linkages of the unsaturated oil where the reaction velocity was independent of pressure.

Storch[116], in the hydrogenation of coal slurry between 300 and 450°C at 70 bar using a stannous sulphide catalyst, found that the diffusion of hydrogen through a liquid film surrounding the catalyst surface was the rate-controlling factor, while Anderson[117] suggested that the chemi-sorption of coal molecules on the molybdenum trioxide catalyst surface was rate-determining in the hydrogenation of low temperature coal tar in a batch autoclave at 475°C, 210 bar. Qader, however, found that hydrocracking reactions involving breakage of carbon-carbon and carbon-heteratom bonds on the catalyst surface were rate-determining both in trickle bed reactors[118] and in batch autoclaves[119]. The conditions used were 400-500°C and 70-210 bar.

2.8.3.2 Kinetic Models

Most authors agree that coal hydrogenation proceeds through two distinct kinetic stages, both first order with respect to coal remaining but with the first stage having a faster rate. For example, Pelipetz[120], Ishii[121] and Yoshida[122] in batch autoclave work suggested that the

scheme is:

coal ⟶ asphaltene ⟶ oil

Pelipetz[123] has studied the coal ⟶ asphaltene reaction and Weller[124] the conversion of asphaltene and both were found to be first order. Brooks[125] suggested a different two step process:

Coal ⟶ preasphaltenes ⟶ asphaltenes + oil

where the first step was non-catalytic. The overall reaction was thought to be first order.

However, Mukherjee[126] claimed that the reaction order varied as the overall process proceeded through three kinetic changes dependent upon the reaction temperature where the first stage was fractional or near first order and the other two stages were of second order with different rate constants. Gun[127] stated that the reaction proceeded in four steps, each of different kinetic order.

Struck's model[128] assumed that only three species were present in a tetralin coal extract: an unconvertible fraction, a fraction which converts rapidly and a fraction which converts slowly. Both the rapid and slow reactions were thought to be first order with different rate constants.

Several authors have made studies on fractions of the hydrogenated coal product. For example House[129] has worked on the 200-370°C fraction, Janardanarao[130] on the 250-350°C fraction and Peters[131] on the IBP-180°C, 180-340°C and 340-450°C fractions. The hydrogenations of all the fractions tested were found to follow first order kinetics.

Due to the chemical complexity of hydrogenated coal products, the kinetics have been simplified by studying the production of material in various boiling ranges. For example, Kuganov[132] used three fractions

(IBP-160°C, 160-350°C and >350°C) in his model as did Gagarin[133] (raw material, gasoline and gas), while Shah[134] used four fractions: gas, IBP-204°C, 204-343°C and >343°C. Considerable work has been carried out[135-140] in producing models for the hydrocracking of gas oil. In most of the studies, three fractions were used which were roughly equivalent to gas, IBP-200°C and 200-350°C.

Strangeland[141] has developed a mathematical model describing the production of material in any given boiling range and clearly the choice of boiling ranges for kinetic study can be governed by the requirements of the process.

2.8.3.3 Reaction mechanisms

The initial cleavage of the coal structure is thought to occur by the elimination of oxygen[120]. This began at 120°C according to Suzaki[142] and reached a maximum between 350 and 390°C[142,143]. Suzaki suggested CO_2 formation and breakdown of aldehydes and ketones as evidence for the deoxygenation reactions.

Hydrogenation begins at around 250°C[142,144] on the basis of water formation while Suzaki claimed that oil-forming reactions began at 340°C, although the reactions were slow below 400°C[113].

There is some disagreement in the literature as to when hydrocracking begins. Storch[145] and Qader[146] suggested that cracking started at around 370°C, Suzaki[142] and Mitsui[143] stated the temperature to be about 400°C while Maekawa[147] quoted 450°C.

Storch[116] also found that thermal decomposition predominated at temperatures over 415°C and coking occurred above 440°C even in the presence of 200 bar hydrogen.

Several authors have postulated a free radical mechanism for coal hydrogenation. Guin[42] stated that the initial breakdown of coal was thermally initiated but the net rate of hydrogenation depended on the nature of the solvent and its effectiveness in stabilising free radicals. Anderson[117] gave the following mechanism for the hydrogenation of a low temperature coal tar:

(1) $H_2 \rightleftharpoons H\cdot + H\cdot$

(2) $R_1 - R_2 \longrightarrow R_1\cdot + R_2\cdot$

(3) $R_3H_2C - QR_4 \longrightarrow R_3H_2C\cdot + R_4Q\cdot$

(4) $R_1\cdot + H\cdot \longrightarrow R_1H$

(5) $R_2\cdot + H\cdot \longrightarrow R_2H$

(6) $R_3H_2C\cdot + H\cdot \longrightarrow R_3CH_3$

(7) $R_4Q\cdot + 2H\cdot \longrightarrow R_4H + HQ$

where R represented a hydrocarbon radical or hydrogen atom and Q represented a heteroatom.

2.8.4 Kinetics of Heteroatom Removal

To produce clean fuels and chemical feedstocks from coal it is desirable to remove sulphur, nitrogen and oxygen during processing. Some work has been carried out on the kinetics of these processes. It is generally thought that heteroatom removal follows first order kinetics with respect to the heteroatoms removed and Qader[146,148] confirmed this in his work on low temperature coal tar. However, Heck[149] claimed that the heteroatom removal from a 170-420°C fraction from coal hydrogenation was a second order reaction.

Both Wilson[150] and Janardanarao[130] noted that the removal of nitrogen and sulphur was proportional to hydrogen partial pressure, although Wilson's results for sulphur removal were somewhat scattered.

Storch suggested that ammonia production was slow at first, increasing after two hours reaction time[145] and this indicated that C-C bonds had to be broken before C-N bonds could be attacked.

Sulphur occurs in coal in three forms according to Yergey[23]:

(1) In organic chemical combinations (mostly removed at 300°C).

(2) As pyrites and/or marcasites (removed at 400-600°C).

(3) As sulphates, usually of calcium and iron (removed at 500°C).

The relative proportions of these forms vary with the type of coal.

Qader[146] has comprehensively listed some of the typical reactions which may be involved during the hydro-removal of sulphur, nitrogen and oxygen from a low temperature coal tar.

2.8.5 Effect of Temperature

The hydrogenation of coal in well-stirred batch reactors is generally highly temperature dependent in the range 400-500°C. Reactions in poorly-stirred batch reactors or trickle-bed reactors are usually less dependent on temperature because of diffusion control, and lower activation energies are obtained.

The activation energy will also be affected by the nature of the catalyst, a more active catalyst tending to lower the energy of activation, and by any other temperature dependent factors in the system.

The following is a list of some of the activation energies obtained in the hydrogenation of various feedstocks.

TABLE LR2

Activation Energies Ea for various Feedstocks

Reaction	Ea (kcal $mole^{-1}$)	Reactor Type	Reaction Conditions		Catalyst	Reference
Anthracene ⟶ alkylbenzenes	16.5	Batch	400-500°C	120 bar	W	151
Phenanthrene ⟶ alkylbenzenes	20.8	Batch	400-500°C	120 bar	W	80/151
Phenanthrene hydrogenation	40	Flow	315-540°C	100-170 bar	Co/Mo	152
Quinoline denitrogenation	30	Batch	350-400°C	25-100 bar	Ni/W	153
Quinoline denitrogenation	20	Batch	300-350°C	70 bar	Ni/Mo	154
Thiophene hydrogenation	21.6	Batch	300-400°C	100 bar	Co/Mo	155
Coal dissolution in coal derived solvents	18.7	Batch	425-470°C	150 bar	none	156
Hydrogen absorption in coal derived solvent	29.5	Batch	450-465°C	150 bar	✓	156
Hydrogen absorption in coal derived solvent	20.2	Batch	450-465°C	150 bar	none	156
Coal slurry ⟶ alkylbenzenes	17.5	Batch	400-500°C	120 bar	W	151
Coal extract (tetralin) conversion	35	Batch	370-425°C	100-240 bar	$ZnO/ZnCl_2$	128
Low temp. coal tar ⟶ gasoline	17.6	Batch	450°C	200 bar	Ni/W	148
Low temp. coal tar ⟶ gasoline	11.5	Batch	475°C	200 bar	MoO_3	117
Solvent refined lignite ⟶ matl. b. <500°C	8.1	Batch	450°C	70-170 bar	Ni/W	157
Asphaltene conversion	35.8	Batch	430-440°C	170 bar	✓	124
Coal oil conversion	15.5	Flow	450°C	140 bar	Ni/W	118
Coal oil conversion	16.2	Flow	480°C	140 bar	✓	158
Coal oil ⟶ alkylbenzenes	19.1	Batch	400-500°C	120 bar	W	151
Gas oil conversion	14.3	Flow	450°C	140 bar	Ni/W	118
200-370°C fraction (unhydrofined) conversion	26.6	Batch	200-400°C	100 bar	✓	129
200-370°C fraction (hydrofined) conversion	37.4	Batch	200-400°C	100 bar	✓	129
Denitrogenation of low temp. coal tar	15.9	Batch	450°C	200 bar	Ni/W	148
Denitrogenation of low temp. coal tar	10	Batch	475°C	200 bar	MoO_3	117
Denitrogenation of low temp. coal tar	10	Batch	300-400°C	200 bar	W	159
Denitrogenation of naphtha	20.1	Flow	370°C	11 bar	Co/Mo	150
Desulphurization of coal slurry	33.0	Batch	360-420°C	200 bar	✓	160
Desulphurization of low temp. coal tar	14.5	Batch	450°C	200 bar	Ni/W	148
Desulphurization of naphtha	3.8	Flow	370°C	11 bar	Co/Mo	150

Use has been made of Eyring's equation:

$$\ln \frac{k}{T} = \ln \frac{k_B}{h} + \frac{\Delta S}{R} - \frac{\Delta H}{RT}$$

(where k_B and h are Boltzmann's and Planck's constants respectively) principally by Qader[117,148] in work on low temperature coal tar in a batch reactor at 450°C, 200 bar. His values for ΔH and ΔS were as follows.

Reaction	Catalyst	ΔH (kcal mole^{-1})	$-\Delta S$ (e.u.)
Conversion to gasoline	MoO_3	10.5	57.8
Conversion to gasoline	Ni/W	16.2	43.5
Desulphurization	Ni/W	12.2	44.9
Denitrogenation	Ni/W	14.9	45.9

TABLE LR3. ΔH & ΔS values from Eyring's Equation

Slotboom[59] noted that his stainless steel autoclave exhibited a "temperature history" effect - an increase in conversion occurred if the temperature of the previous run was higher, and vice versa.

2.8.6 Effect of Pressure

It is well known that an increase in pressure leads to an increase in reaction rate due to the increased partial pressure of hydrogen. Anderson[117] has observed that up to 100 bar, increased pressure had little effect on the cracking of low temperature coal tar in a batch autoclave. Between 140 and 170 bar, however, partial hydrogenation of aromatics to hydroaromatics occurred followed by cracking of the latter and at greater pressures complete hydrogenation to naphthenes occurred.

Qader[161] stated that 140 bar was the optimum pressure for maximum conversion of coal slurries in a flow reactor using a cobalt-molybdenum

catalyst. In studies on a 200-370°C distillate, House[129] reported that increased pressure doubled the rate of cracking of raw feed and trebled that of hydrofined feed.

Although the production of low boiling liquids increased with pressure, Mukherjee[162] found that the yield of gaseous hydrocarbons decreased. This was not, however confirmed by other workers and indeed Mima[163] found that the main product was gas at very high pressures.

Wilson[150] showed that hydrogen partial pressure was proportional to the rate of nitrogen removal from a naphtha feedstock.

In the hydrogenation scheme

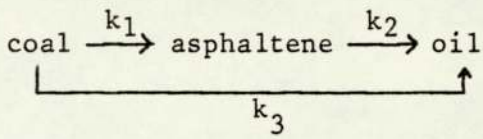

both Pelipetz[123] and Maekawa[164] found that k_1 increased linearly with pressure in a batch autoclave at 400°C but Maekawa found that k_3 remained essentially constant with increasing pressure.

At constant hydrogen partial pressure, Hoog[165] found that the addition of inert gas (nitrogen) suppressed the reaction velocity because of competition between hydrogen and nitrogen molecules for adsorption on the catalyst surface. The effect was small because hydrogen was adsorbed much more strongly than nitrogen.

2.8.7 Effect of Catalyst Loading

In batch reactors with cobalt molybdenum catalysts, the rate of hydrogenation has been found to increase markedly with catalyst loadings up to about 1% w/w feed[166]. On increasing the loading beyond 1%, however, Rapoport[41], Brooks[125] and Low[157] found that the rate increased much less sharply. Feldman[167] also obtained similar

results, and he suggested that at high catalyst loadings the reaction rate was controlled by the rate at which hydrogen could diffuse from the gas bubble to the liquid phase.

Ruether[168] predicted that if the hydrogenation of coal to oil proceeded by a solely catalytic reaction, the logarithm of the rate should be proportional to the logarithm of the catalyst loading. However his results did not show this proportionality and he attributed this to the non-catalytic reaction coal $\longrightarrow$ asphaltene.

Newman[169], Horton[170] and Bertolacini[171] found that in the presence of some metal oxides, less conversion of coal to low boiling liquids was achieved than with no catalyst at all. These catalysts included the oxides of aluminium, calcium, magnesium, bismuth, nickel and titanium.

Guin[56] and Sherwood[172] have observed a "memory" effect, where catalyst was adsorbed on the reactor walls giving a higher rate of reaction than expected in subsequent experiments.

CHAPTER 3

EXPERIMENTAL DESIGN

3.1 Reactor Type

Most of the experiments in this work were carried out in a semi-continuous stirred tank reactor with a batch charge of coal-derived feedstock and a continuous flow of hydrogen.

Stirred tank reactors have certain advantages over tubular-flow reactors because of the uniform temperature, pressure and composition attained as a result of mixing. Stirred tank reactors provide long residence times and can be operated isothermally at the optimum temperature for the reaction. Denbigh[173] has discussed the advantages and disadvantages of continuous stirred tank reactors in comparison with batch tank reactors.

Clark[174] has discussed the advantages and disadvantages of semi-continuously operated tank reactors. This type of operation has been little used for coal hydrogenation in tank reactors with slurried catalyst, although several authors[125,167,175,176,177] have carried out experiments in semi-continuous tank reactors with fixed beds of catalyst in baskets.

A stirred tank reactor with a slurried catalyst was chosen for this work because this is an efficient system for bringing hydrogen and liquids to the surface of a solid catalyst, which is a requirement for the effective hydrogenation of oils. The use of this type of reactor is well documented; for example, Calderbank[187] has described its use in the Fischer-Tropsch reaction between hydrogen and carbon monoxide, where these gases were dissolved in a slurry of hydrocarbon oil and catalyst particles.

Semi-continuous operation with continuous hydrogen flow was chosen for two main reasons: (1) An almost constant, high partial pressure of hydrogen can be maintained in the reactor giving higher reaction rates and less polymerization. (2) Reaction products may be removed from the reactor in the gas stream which increases the forward rate of reversible reactions and also eliminates any further, undesirable reaction of the products. In addition, the continuous flow of one of the reactants permits a measure of control of the concentration of the reaction mixture and hence the rate of reaction.

3.2 Experimental Programme

The experimental programme was designed in three parts, preliminary experiments, detailed study of selected parameters and experiments to elucidate mechanisms.

3.2.1 Preliminary Experiments

Preliminary experiments were carried out in the one litre autoclave system with a view to

(i) Establishing reproducibility of results.

(ii) Determining which parameters were important in the hydrogenation of coal extract solution and worthy of more detailed study.

(iii) Investigating and comparing potential catalysts for the reaction and selecting one for all future experiments.

(iv) Developing a standard procedure in terms of operation of the autoclave system and analysis of the products.

3.2.2 Detailed Study of Selected Parameters

Of the parameters investigated in the preliminary experiments, the following were thought of sufficient importance to warrant further, more detailed, scrutiny:

Reaction time

Reaction temperature

Pressure

Although not studied in the preliminary experiments, it was thought that both catalyst loading and initial coal concentration should also be investigated fully.

3.2.2.1 Reaction Time

A large range of conversion is required in order to distinguish unambiguously between zero, first and second order reactions, and so the reaction should be taken as closely as possible to completion. In order to achieve this, the reaction time was varied between 0 and 4 hours. The reaction time was also varied at different temperatures in order to investigate whether the reaction mechanism was influenced by a change in temperature.

3.2.2.2 Reaction Temperature

The reaction temperature was varied in order to obtain the overall activation energy for the reaction and to study changes in product composition. The range of temperature considered suitable was 420 to 460°C, since below 420°C little reaction occurred, while above 460°C excessive gas production was likely to occur. 460°C was also the maximum allowable operating temperature of the one-litre autoclave.

3.2.2.3 Pressure

Since hydrogen was one of the reactants, it was considered important to perform experiments in which its concentration (hydrogen partial pressure) was varied. In addition to determining the effect of pressure on the rate of hydrogenation, the results could be used to obtain an estimate of the solubility of hydrogen in the reactants (see section 5.2.6). This is important since it was thought that the rate of dissolution of hydrogen might control the overall rate of reaction.

The range of hydrogen partial pressure chosen for study was 85-340 bar. Below 85 bar, little reaction occurred and coking (polymerization reactions) was likely to cause practical and theoretical problems. 340 bar was the upper limit for operation in the one-litre autoclave.

3.2.2.4 Catalyst Loading

The effect of catalyst loading on the rate of hydrogenation was investigated to provide information concerning the rate-determining step of the reaction in terms of transport resistances and chemical reaction in the three phase system.

The range of catalyst loading used was based on the following considerations:-

(a) A large range of catalyst loading should be used, since the rate determining step may change with loading.

(b) Some very small loadings should be included as these often produce a large increase in conversion. A range between 0 and 25% w/w feed was considered suitable.

3.2.2.5 Coal Concentration

It was considered important to determine the effect on hydrogenation of varying the coal content of the coal extract solution. However, because of the complex nature of the solvent and the practical problems involved in isolating a solvent-free extract, it was difficult to prepare a series of coal extracts with different coal contents which were otherwise identical. For example, in a range of extracts prepared by solvent evaporation of a coal solution, the solvent portion of each extract would have a different composition.

Instead, it was considered preferable to regard the 50% coal extract solution as the basic solute and to vary its concentration by

dilution with the anthracene oil solvent.

The coal extract content in the mixtures thus prepared was in the range 0-100%.

3.2.3 Experiments to Elucidate Reaction Mechanisms

Although some data was obtained from the experiments described in section 3.2.2 for the elucidation of reaction mechanisms, it was necessary to perform further experiments on the suspected intermediates of the reaction. Two such intermediates were chosen for this study; the 355-420°C and 300-355°C distillation fractions of the hydrogenated product. Data was obtained at different times, from 0 to 4 hours, during the secondary hydrogenation of these fractions. From this data, a more accurate mechanism could be postulated and the rate constants for each step calculated.

CHAPTER 4

EXPERIMENTAL TECHNIQUES

4.1 Description of Apparatus

4.1.1 One Litre Autoclave

Most of the experiments performed were carried out in a stirred autoclave manufactured by Pressure Products Industries (P.P.I.), a division of the Duriron Company of the U.S.A.

Diagrams of the autoclave and of the complete reactor system are shown in Figures 1 and 2 respectively. The description given is that of the current status of this equipment. Since its installation there have been several modifications to the original design to help overcome problems or to provide additional facilities.

The autoclave has a capacity of one litre and was fitted with a variable speed stirrer. The stirrer was driven by an air motor through a magnetic coupling (Permanent Magnetic Drive Unit) and could achieve speeds of up to 2000 r.p.m. Indication of the rotational speed of the stirrer was by a tachometer connected directly to the stirrer shaft.

The choice, design and positioning of the stirrer head and baffles in the autoclave has been the subject of a report by Davis[179]. In it, he has examined the influence of stirrer head type, position, size and speed of rotation and baffle number, position and size on gas-liquid-solid mixing in a glass model of the autoclave. The recommendations of the investigation are shown in Table 1 and have been adopted in the autoclave in this work.

There were seven ports in the autoclave (one at the bottom and six at the top) some of which were used for the addition or removal of feed

and products, liquid sampling and the connection of lines to the bursting disc, pressure gauge and emergency vent.

The main closure seal of the autoclave was of the hoop ring type, details of which can be found in Appendix 1.

The autoclave was capable of operation at up to 460°C and 340 bar. Heat was supplied by a 3 kW furnace spot-welded to the outside of the autoclave. Temperature measurement was by a chromel-alumel thermocouple positioned just above the stirrer blades. Hydrogen was pressurized by a P.P.I. diaphragm compressor and the pressure in the autoclave was indicated by a 0-700 bar Astra gauge.

4.1.2 300 ml Autoclave

Some experiments, when the amount of feedstock was limited, were carried out in a smaller rocking-type autoclave of 300 ml capacity manufactured by Charles Cook and Sons Ltd. A diagram of the reactor system is given in Figure 3.

The maximum operating conditions for this autoclave were 450°C and 210 bar. The autoclave was clamped into a 1½ kW furnace and a thermowell in the head enabled the temperature of the contents to be measured. Hydrogen pressurization was by a Hofer diaphragm compressor and the pressure in the autoclave was indicated by a 0-1000 bar Budenberg gauge.

The autoclave was oscillated by an electric motor through 60° about the horizontal at approximately one cycle per second, to agitate the contents.

4.2 Construction of One Litre Autoclave System

The material of construction of the autoclave and of all pipework valves and fittings subjected to high pressure was Type 316 stainless steel. This is a steel containing nickel, titanium and chromium, the

latter improving the resistance of the steel to hydrogen embrittlement. This steel is suitable for high pressure operation at up to 500°C.

Either "cone and thread" or compression fittings were used in all high pressure connections. Both coning and threading was carried out using hand-operated tools. The components of this type of fitting and the theory involved are covered in Appendix 1. Specially designed and manufactured adapters were required to connect between the two types of fitting.

The autoclave was situated in a safety cell built with reinforced concrete blocks, ¼" mild steel doors and a blow-off roof. Valve handles protruded through a ¼" mild steel panel for operation outside the cell. All electrical connections were flameproof. A Seiger gas-leak detection system installed in the cell triggered an alarm if the concentration of hydrogen exceeded 10% of its lower explosion limit. The autoclave was fitted with a bursting disc which ruptured if the maximum operating pressure was exceeded by more than 5%, allowing the reactor contents to be dumped into a large tank outside the safety cell.

4.3 Operation

4.3.1 One-Litre Autoclave

The autoclave was operated as a stirred catalyst-slurry reactor in which there was a continuous flow of hydrogen through a batch charge of feed material mixed with powdered catalyst.

After the required weights of feed and catalyst had been loaded and the autoclave sealed, it was purged twice with 210 bar nitrogen. The reactor contents were then heated at a rate of approximately $3\frac{1}{2}$-$4\frac{1}{2}$°C/min.

Temperature control was effected by a Eurotherm three term thyristor controller and Eurotherm over-ride controller. The liquid temperature provided the signal to the thyristor controller so that it was the temp-

erature of the reactor contents which was controlled. The over-ride control ensured that the autoclave outside-wall temperature did not exceed the design specification of 515°C at pressure. In this way, the liquid temperature could be controlled to ± 1°C after an initial "overshoot" of about 5°C.

However the internal thermocouple tended to move out of the liquid region because of the stirring action, so recording a different temperature. This movement was minimized by strengthening the thermocouple with a ¼" stainless steel sheath.

At a furnace temperature of 320°C, hydrogen was introduced through the bottom of the autoclave and at 400°C, the stirrer was switched on.

The inlet pressure to the autoclave was controlled to ± 4 bar automatically by the compressor. The gas flowrate was controlled by the pressure let-down valve - a Platon Research Control Valve with P9 trim giving a valve coefficient of flow, Cv*, of 0.00008. The flowrate was indicated by a G.E.C. - Elliott 3-36 $1min^{-1}$ rotameter calibrated for hydrogen duty. For other duties, recalibration was necessary and this is detailed in Appendix 2.

The light products generated by the process were carried over in the gas stream from which they were separated by a knock-out pot on the high pressure side, and by condenser traps and by passing through a bed of active carbon on the low pressure side of the let-down valve. The true volume of the remaining gases was then measured by passage through a Parkinson Cowan dry gas meter, after which the gases were vented to the atmosphere.

*Cv = The volume of water, in U.S. gallons per minute at room temperature, which will flow through the valve, with the stem fully open, with a pressure drop of 1 psi across the valve.

At the end of each experiment, the reactor contents were cooled at a rate of about 4°C/min. Nitrogen was re-introduced when the temperature reached 250°C, and at 150°C the pressure was let down to atmospheric. The reactor contents were then removed (usually by running out of the bottom of the autoclave directly into a distillation vessel) and combined with the condenser liquids. Water in the condensate was removed by gravity separation. The light products trapped by the active carbon were recovered by steam distillation and the liquid obtained was added to the main product. The remaining material trapped by the active carbon was assumed to consist of gaseous products.

4.3.2 300 ml Autoclave

This autoclave was operated as a batch reactor, with no flow of feed or gas, except for the purpose of adjusting the reactor pressure.

After the required weights of feed and powdered catalyst had been loaded and the autoclave sealed, it was purged once with 75 bar nitrogen and three times with 210 bar hydrogen. The hydrogen pressure was finally set to 150 bar before the furnace and rocking motor were switched on.

A "mini-Ether" controller was used in conjunction with a T_1/T_2 thermocouple to control the temperature of the reactor contents. When this had risen to the required value, the hydrogen pressure was adjusted to 210 bar and held constant.

At the end of each experiment, after cooling to 60°C, the autoclave was depressurized by passing the gases slowly through a U.G.I. dry gas meter and venting to the atmosphere. The reactor contents were then removed.

4.4 Sampling and Analysis of Products from 1 l. Autoclave

4.4.1 In-run sampling

There were facilities in the autoclave system for in-run sampling of reactor contents, condensate and gas. Reactor contents samples (each of about 1 g) were removed when required through a dip-tube which incorporated a 40 μm stainless steel mesh filter to eliminate the catalyst. This system worked well with lower boiling feedstocks, but with more viscous liquids, frequent line blockages occurred.

Condensate was collected from the high pressure knock-out pot, the water condenser trap and the cold trap during each experiment and sampled as required.

Gas samples, each of 250 cm^3 volume at N.T.P., were collected from a point upstream of the active carbon trap during each experiment. A continuous stream of product gas flowed through the gas sample bottle, which was removed when required and replaced by another bottle for the next sample.

4.4.2 Post-run sampling

At the end of each experiment a small sample of the total condensate (including the light ends from the active carbon trap) was collected. After the catalyst had settled, a small sample of reactor contents liquid was also taken. The sample size in each case was approximately 3 g.

When required, a portion of the spent catalyst was recovered by Soxhlet extraction with tetrahydrofuran.

4.4.3 Sample Analysis

Liquid samples were analysed by Gas Liquid Chromatography using a 3.7 m OVI (a dimethyl silicone gum) packed column, temperature programmed from 60 to 250°C at a rate of 4°C/min. A 2m column packed with alumina and operated isothermally at 130°C was used for gas analysis.

The samples of condensate and reactor contents (catalyst free) taken after each experiment were analysed for carbon, hydrogen, oxygen, nitrogen, sulphur and ash using British Standard method BS 1016 pt.6*. By the same method, spent catalyst samples were analysed for carbon and hydrogen*. In addition, the surface area of some spent catalysts were measured by the B.E.T. method.+

4.4.4 Distillation

All the liquid products recovered from the autoclave after each run (including the spent catalyst, but excluding the various samples that were taken) were mixed together and distilled. Two methods of distillation analysis were employed. In the first, the product was fractionated using a 10" x 1" diameter column packed with Dixon gauze rings. The fraction boiling up to 170°C was distilled at atmospheric pressure, while the higher boiling fractions were distilled under vacuum (<2 torr) to prevent the possibility of thermal cracking. The temperatures recorded during vacuum distillation were converted to the equivalent at atmospheric pressure by the use of a conversion chart drawn up by the Anglo-Iranian Oil Co. for petroleum fractions. A series of fractions boiling below 420°C and a residue (boiling above 420°C) were obtained in this way, as follows:

Initial boiling point (IBP) - 170°C
170 - 250°C
250 - 300°C
300 - 355°C
355 - 420°C
>420°C (residue)

* These analyses carried out by C.R.E. Chemistry Department.
+ These analyses carried out by M.C.A. Services.

These were the nominal boiling ranges of each fraction, since in practice there was some overlap due to imperfect fractionation.

In the second distillation method, a straight vacuum distillation of the product was carried out giving a single fraction boiling below 290°C at 50 mm (equivalent to about 450°C at 760 mm. pressure). By a subsequent G.L.C. examination of the distillate it was possible to obtain a simulated distillation analysis of the total product in terms of a series of fractions with the above boiling ranges. This method of distillation analysis eliminated the overlap in boiling ranges that was encountered in using the first method.

Details of the choice of boiling range of each fraction can be found in Appendix 3.

4.4.5 Analysis of Distillates*

More detailed G.L.C. analyses of some of the low boiling (IBP-170°C) fractions obtained by fractional distillation were performed using a 50 m squalane capillary column, temperature programmed from 50 to 100°C at a rate of 2°C/min. after an isothermal period of 15 minutes. This enabled some of the individual components to be identified.

In addition, PNA analysis was carried out on some of these fractions giving the percentage of paraffins, naphthenes and aromatics present.

4.5 Analysis of Products from 300 ml Autoclave

Analysis of gaseous products was carried out as described in section 4.4.3.

The total liquid product from the autoclave was removed and a simulated distillation analysis was carried out by G.L.C. as described

* These analyses carried out by C.R.E. Chemistry Department.

in section 4.4.4.

4.6 Experimental Error

The precision of the various instruments and analyses used in the experiments is given in Table 2. Where possible, the precision of instruments is quoted from manufacturers specifications. With one exception, the precision of all the instruments and analyses was 3.5% or better. The exception was the analysis of products by fractional vacuum distillation, where the precision of the method was impaired by the uncertainty of the calibration. This calibration was used to convert measured temperatures under vacuum to the equivalent temperatures at atmospheric pressure and was drawn up for petroleum fractions.

It was found that the precision of analysis by fractional distillation deviated from that of GLC analysis mainly in the middle boiling range (170-350°C) with the maximum deviation occurring for components boiling around 300°C. For components boiling below 170°C and above 350°C, the precision was similar for both analyses.

The reproducibility of analyses is also shown in Table 2. Again, analysis by GLC showed better reproducibility than fractional distillation analysis. The relatively poor reproducibility of GLC analysis (compared to elemental analysis) was probably due to slight variations in the retention time of components in the chromatographic column causing differences in the amount of material in each boiling range.

In theory, the maximum experimental error associated with GLC and fractional distillation analyses was 6 and 14% respectively (i.e. precision + reproducibility errors).

4.7 Materials

4.7.1 Coal Extract Solution

Coal solutions were prepared by solvent extraction of the appropriate coal with solvent oil (see section 4.7.2) at 400°C followed by filtration to remove ash and undissolved coal. Solvent evaporation was then carried out to produce an extract solution containing approximately 50% original coal material, as characterized by its softening point.

Two coal extract solutions were used. The first (code number EP52FD10) was prepared from low rank Annesley coal and EP51D oil, and the second (code number E83) from high rank Beynon coal and EP20D1 oil. The extract solutions were added to the autoclave in powdered form (particle diameter less than 2.36 mm).

Analyses of both extract solutions are given in Table 3 and their boiling point distributions are shown in Figure 4. Although the extract solutions contained nominally 50% coal substance and most of the components in anthracene oil boiled below 420°C, Figure 4 shows that over 80% of the extract solutions boiled above this temperature. This is because the extract solution was prepared by solvent evaporation so that the small amount of material boiling above 420°C originally present in the oil was concentrated and made a significant contribution to the total amount of material boiling above this temperature.

Softening point determinations were carried out using the Ring and Ball (R&B) method[180]. Molecular weight determinations were carried out on the tetrahydrofuran-soluble fraction of each extract solution and from these a number average molecular weight was estimated for the whole of each extract solution.

4.7.2 Solvent Oil

Some experiments were carried out on the original solvent used to prepare the low rank coal extract solution. This was anthracene

oil, a by-product in the manufacture of coke. The code number of the oil was EP51D and analyses are shown in Table 3. Molecular weight determinations were carried out by the method described in section 4.7.1.

The oil used to prepare the high rank coal extract solution was slightly different to that used in the preparation of the low rank extract solution. An analysis of this oil, code numbered EP20D1; is also given in Table 3.

4.7.3 Distillate Fractions of Hydrogenated Product used as Feed

Later experiments were performed on distillation fractions of the hydrogenated product used as the feed. Two fractions were used, one boiling between 355 and 420°C, the other between 300 and 355°C. Because of the relatively large quantities required, the fractions were obtained from two sources. First, from the hydrocracking of a 20% coal extract solution in a continuous, trickle bed pilot plant and second, by bulking together all the appropriate fractions from the experiments performed in the one litre autoclave. Analyses of these feeds are shown in Table 3.

4.7.4 Mixtures of Coal Extract Solution and Anthracene Oil as Feed

Some experiments were performed on mixtures of low rank coal extract solution (EP52FD10) and anthracene oil (EP51D). Table 4 shows the boiling ranges and elemental composition of these mixtures which were calculated from the analyses of the respective pure components of the mixture (Table 3).

4.7.5 Catalyst

A commercial catalyst, Harshaw 0402T, was used in all the kinetics experiments. This was chosen because of its high activity and proven success in other coal conversion processes. It is a cobalt-molybdenum catalyst on a silica-stabilized alumina support. Data for the proprietary

form of the catalyst ($\frac{1}{8}$" pellets) is given in Table 5. The catalyst was ground through the sieve of a Glen Creston Hammer-Mill which produced a wide particle size distribution, as shown in Table 6.

The pore size distribution for the ground catalyst is shown in Figure 5. These results* were obtained using the B.E.T. multipoint method.

4.8 Commissioning of the One-Litre Autoclave System

4.8.1 Mechanical Commissioning

The one-litre autoclave was commissioned in a series of 10 tests to monitor and improve the performance of different parts of the system.

The tests involved pressurizing and heating the autoclave in stages up to its maximum operating limits. Pressurization was with nitrogen or hydrogen and the autoclave either contained no liquid or was charged with anthracene oil or coal extract solution. The leak rate of gas from the autoclave and its rate of heating were determined at each stage, the former by the rate of decay of pressure in the autoclave when isolated. The following table shows the order in which the tests were carried out.

	Auto. Empty	Auto. charged with anth. oil	Auto. charged with extract
N_2 pressure	1	-	-
Heat	2	6	-
N_2 pressure + heat	3	7	9
H_2 pressure	4	-	-
H_2 pressure + heat	5	8	10

TABLE E.T.1. Sequence of Performing Mechanical Commissioning Tests

In addition to the pressure and heat tests, the gas compressor, process lines and heaters, valves, cooling water lines and thermocouples

* This analysis carried out by M.C.A. Services.

were also thoroughly tested during commissioning.

4.8.2 Process Commissioning

Experiments were carried out in the autoclave using coal extract solution and catalyst with a view to:

(i) Solving the problems inherent in the start-up of a new system.

(ii) Determining the amount of feed material to be added to the autoclave.

(iii) Testing the efficiency of the gas-liquid separation system.

(iv) Comparing a fixed catalyst bed to a catalyst slurry and choosing one of the systems for future work.

CHAPTER 5

CALCULATIONS AND THEORETICAL ASPECTS

5.1 Calculations

5.1.1 Gas Yields

In the calculation of gas yields the concentration of each gaseous hydrocarbon (obtained by chromatographic analysis) was plotted as a function of time and, by graphical integration, a time-average concentration was determined. Using these values and the total metered gas volume, the total yield of each hydrocarbon was calculated.

5.1.2 Yields of Distillation Fractions

The weight of material, x, in each fraction of the total recovered product was calculated as follows:

Weight of individual distillate fraction = A

Weight of residue (material boiling above 420°C) from distillation = B

Weight of total recovered product = C

Weight of material to be distilled = D

Weight of catalyst feed = E

For fractions boiling below 420°C, x_b,

$$x_b = A\left(\frac{C-E}{D-E}\right)$$

For the residue (material boiling above 420°C), x_a,

$$x_a = (B-E)\left(\frac{C-E}{D-E}\right)$$

When simulated distillations were carried out using G.L.C., x_b was determined as above, but the calculation of x_a was slightly different.

Weight residue from distillation (material boiling above 450°C) = F

Weight residue from G.L.C. (material boiling between 420 and 450°C) = G

Now, $x_a = (F + G - E)\left(\frac{C-E}{D-E}\right)$

The final weight of the fractions should be corrected by dividing each fraction by the total percentage mass balance.

5.1.3 Heteroatom Removal and Hydrogen Consumption

Example: Run JK34

Total weight recovered reactor contents (excluding catalyst feed) = 285.4 g

Total weight recovered condensate (excluding water) = 130.8 g

Total weight gaseous hydrocarbons = 47.6 g

Weight coal extract solution feed = 496.8 g

Weight catalyst feed = 122.4 g

From the elemental analyses of feedstock, reactor contents and condensate, a material balance for carbon, hydrogen, oxygen, nitrogen and sulphur was calculated:-

	Liquid in g.	Reactor contents out g.	Condensate out g.	Total liquid out g.	Gaseous hydrocarbons out g.
C	444.1	258.8	113.4	372.2	37.6
H	24.7	21.5	13.4	34.9	10.0
O	15.2	2.7	3.3	6.0	NIL
N	9.7	1.8	0.7	2.5	NIL
S	3.1	0.6	NIL	0.6	NIL
TOTAL	496.8	285.4	130.8	416.2	47.6

TABLE C.1 Elemental Mass Balances

Thus the yields of water, ammonia and hydrogen sulphide were calculated assuming O, N and S were not removed as any other compound. The hydrogen consumption for the formation of each compound was also calculated.

(i) Water

Oxygen in feed = 15.2 g.

Oxygen in products = 6.0 g.

∴ Balance converted to water = 9.2 g.

∴ Water produced = 10.4 g.

Hydrogen consumed to produce water = 10.4 - 9.2 = 1.2 g.

(ii) Ammonia

Nitrogen in feed = 9.7 g.

Nitrogen in products = 2.5 g.

∴ Balance converted to ammonia = 7.2 g.

∴ Ammonia produced = 8.7 g.

Hydrogen consumed to produce ammonia = 8.7 - 7.2 = 1.5 g.

(iii) Hydrogen sulphide

Sulphur in feed = 3.1 g.

Sulphur in products = 0.6 g.

∴ Balance converted to hydrogen sulphide = 2.5 g.

∴ Hydrogen sulphide produced = 2.7 g.

Hydrogen consumed to produce sulphur = 2.7 - 2.5 = 0.2 g.

There is now sufficient data to calculate the overall hydrogen consumption.

	H_2 IN g.	H_2 OUT g.
Hydrogen in feed	24.7	
Hydrogen in total liquid product		34.9
Hydrogen in gaseous hydrocarbons		10.0
Hydrogen in water		1.2
Hydrogen in ammonia		1.5
Hydrogen in hydrogen sulphide		0.2
TOTAL	24.7	47.8

TABLE C.2 Hydrogen Mass Balance

Thus total hydrogen consumption = 47.8 - 24.7 g. = 23.1 g.

Thus, the product yields are:

	Yield (g)	Yield (% w/w feed)
Liquid product	416.2	83.8
Gaseous hydrocarbons	47.6	9.6
Water	10.4	2.1
Ammonia	8.7	1.7
Hydrogen sulphide	2.7	0.5
Total	485.6	97.7

TABLE C.3 Product Yields

The final weight of products should be corrected by dividing each component by the total percentage mass balance, i.e. 97.7 - hydrogen consumption (=4.6)/100 = 0.931.

5.1.4 Conversion

The calculation of conversion was based on the amount of product which boiled above 420°C in the feed (A_o) and the product (A), so that

$$\% \text{ Conversion} = \frac{A_o - A/M}{A_o} \times 100 \qquad (5\text{-}1)$$

where M is the % mass balance and A, A_o are expressed as % w/w feed. The value of 420°C was chosen as the cut-off point because most of the components in anthracene oil boil below this temperature and all unreacted coal and/or coal-derived material in the extract solution is assumed to boil above 420°C.

5.2 Treatment of Results

5.2.1 Removal of Material from the Autoclave

The volume of material removed from the autoclave during each experiment, R, was given by the sum of the condensate (including light

ends in the active carbon trap) and hydrocarbon and heteroatom gases less the amount of hydrogen consumed by the reactor contents. Thus:

$$V_o - R = V$$

Here, V_o and V refer to the volume of reactor contents initially and at time, t, respectively, and were thought to be related by the equation

$$V = V_o e^{-at} \qquad (5\text{-}2)$$

where a is a constant. Plots of $\ln {}^{V_o}/_{V}$ against t at each reaction temperature (shown in Figure 6) are straight lines which confirms the relationship shown in equation 5-2.

5.2.2 Physical Resistances to the Reaction Rate

In a heterogeneous reaction, the overall rate will include the effects of mass and energy transfer processes from fluid to solid surface and within the solid particle. In two-phase reactors and slurry reactors, energy transfer resistances are usually negligible because the large surface area and turbulence prevent significant temperature variations. However, expressions for the overall rate must be formulated in terms of mass transfer and this is effected by considering each step in the process. The sequence of steps in a gas-liquid-solid catalyst system is:

(i) Mass transfer from bulk concentration in gas bubble to bubble-liquid interface.

(ii) Mass-transfer from the bubble interface to the bulk-liquid phase.

(iii) Mixing and diffusion in the bulk liquid.

(iv) Mass-transfer to external surface of catalyst particles.

(v) Intraparticle transport of reactants into catalyst particle.

(vi) Adsorption of reactants at interior sites of catalyst particle.

(vii) Chemical reaction of adsorbed reactants to adsorbed products.

(viii) Desorption of adsorbed products.

(ix) Transport of products from interior sites to outer surface of catalyst particle.

(x) Transport of products from liquid-solid interface into bulk liquid phase.

In slurry reactors, agitation is usually sufficient to achieve uniform conditions in the bulk liquid (as shown by Kolbel[181] and Siemes[182]) and intraparticle diffusion resistance is small because of the small size of the catalyst particles. Furusawa[183] found that pore diffusional effects were only significant in particles larger than 200 μm. Thus the resistances of steps (iii) and (v) can be assumed to be negligible.

5.2.3 Resistance due to adsorption and desorption

The adsorption, reaction, desorption steps, (vi), (vii), (viii), can be described by the model of Langmuir[184] who based the model on a series of assumptions. Although some of these assumptions are not strictly correct, the general treatment is valid.

Rate of adsorption, $r_a = KaP\ (1-\theta)$

and rate of desorption, $r_d = k_d\ \theta$

where P is the pressure of the adsorbing gas. At equilibrium, $r_a = r_d$ so that

$$\theta = \frac{K_a P}{k_d + K_a P}$$

Rate of surface reaction, $r = k_s N_s \theta$

where N_s is the number of surface sites available for adsorption.

$$\therefore\ r = \frac{K_a k_s N_s P}{K_d + K_a P} \qquad (5\text{-}3)$$

5.2.4 Resistance due to external transport processes

Now the effect of external transport resistances on the rate, i.e. steps (i), (ii), (iv) and (vii) in the sequence given in section 5.2.2, are considered.

Assuming a first-order, irreversible catalytic reaction, the overall rate per unit volume of bubble-free slurry with respect to hydrogen, r_v, is given by:

$$r_v = K_s a_c C_s \qquad (5\text{-}4)$$

where a_c = external area of catalyst particles per unit volume bubble-free slurry.

C_s = concentration of hydrogen at outer surface of catalyst particle.

Alternatively, the overall rate may be expressed in terms of the rates of the three mass-transfer processes:

$$r_v = k_g a_g (C_g - C_{ig}) \quad \text{gas to bubble interface} \qquad (5\text{-}5)$$

$$r_v = k_l a_g (C_{il} - C_l) \quad \text{bubble interface to bulk liquid} \qquad (5\text{-}6)$$

$$r_v = k_c a_c (C_l - C_s) \quad \text{bulk liquid to catalyst surface} \qquad (5\text{-}7)$$

where a_g = gas bubble-liquid interfacial area per unit volume bubble-free slurry.

If equilibrium exists at the bubble-liquid interface, by Henry's law:

$$C_{ig} = k_H C_{il} \qquad (5\text{-}8)$$

Combining equations 5.4-5.8 gives the rate solely in terms of the concentration of reactant in the gas at equilibrium:

$$r_v = k_o a_c C_g \qquad (5\text{-}9)$$

where $$\frac{1}{k_o} = \frac{a_c}{a_g}\frac{1}{kg} + \frac{a_c}{a_g}\frac{k_H}{k_l} + k_H\left(\frac{1}{k_e} + \frac{1}{k_s}\right)$$

With pure hydrogen or even mixtures with other components, kg appears to be much larger than $\frac{k_l}{k_H}$ (185) and there is little resistance to diffusion from bulk gas to bubble-liquid interface. Thus, $Cg = C_{ig}$ and

$$\frac{1}{k_o k_H} = \frac{a_c}{a_g}\frac{1}{k_1} + \frac{1}{k_c} + \frac{1}{k_s} \quad ,$$

Thus: $$r_v = \frac{a_c a_g k_1 k_c k_s . C_g}{a_c k_c k_s + a_g k_1 k_s + a_g k_1 k_c} \qquad (5\text{-}10)$$

5.2.5 Derivation of Overall Rate Expression

Defining the overall rate, r, in terms of the liquid-phase concentration of hydrogen in equilibrium with Cg ([H]) and the concentration of liquid hydrocarbon reactant ([A], the concentration of material boiling above 420°C), from equation 5-10:

$$r = \frac{a_c a_g k_1 k_c k_s [H]}{a_c k_c k_s + a_g k_1 k_s + a_g k_1 k_c} [A] \qquad (5\text{-}11)$$

where square brackets denote concentrations.

Although the solubility of hydrogen increases with decreasing molecular weight[49,50], the low molecular weight compounds produced during the reaction were removed from the autoclave as soon as they were formed. It is assumed, therefore, that the molecular weight of the liquid reactor contents (and therefore [H]) remained constant throughout each experiment, at constant temperature, pressure and stirrer speed.

Thus, with these conditions constant, it can be assumed that all the terms other than [A] in equation 5-11 are constant, so that

$$r = k_1[A]$$

where $$k_1 = \frac{a_c a_g k_1 k_c k_s [H]}{a_c k_c k_s + a_g k_1 k_s + a_g k_1 k_c}$$

For a tank reactor with uniform concentrations and temperature:

$$r = -\frac{1}{V}\frac{dN}{dt}$$

where V is the total volume and N = the number of moles of reactant.

Since

$$N = [A]\ V$$

then $$r = -\frac{1}{v}\frac{d[A]V}{dt} = k_1[A]$$

$$\therefore \frac{d[A]}{dt} = -\frac{[A]}{V}\frac{dV}{dt} - k_1[A]$$

From equation 5-2:

$$v = v_o e^{-at}$$

$$\therefore \frac{dv}{dt} = -aV_o e^{-at}$$

$$\therefore \frac{d[A]}{[A]} = (a - k_1)dt$$

Integrating:

$$\ln[A] = at - k_1 t + I$$

where I is the integration constant.

When $t = o$, $[A] = [A_o]$,

$$I = \ln [A_o]$$

Also, $at = \ln {}^{V_o}/_{v}$ (from equation 5-2)

$$\therefore \ln {}^{A}/_{A_o} = -k_1 t \qquad (5\text{-}12)$$

5.2.6 Modification of Rate Expression for Experiments Performed at Different Pressures

Equation 5-12 may be re-written:

$$\ln {}^{A}/_{A_o} = -k'[H]\ t \qquad (5\text{-}13)$$

where $$k' = \frac{a_c a_g k_1 k_c k_s}{a_c k_c k_s + a_g k_1 k_s + a_g k_1 k_c}$$

and $$k' = \frac{k_1}{[H]}$$

Henry's Law states that

$$P = k_H X_B$$

where X_B is the mole fraction of hydrogen in solution and K_H is Henry's Law constant. It is assumed that this law is obeyed over the pressure range studied. Several authors[49,50,51] have reported that the solubility of hydrogen in high molecular weight material followed Henry's Law over a wide range of pressure.

The mole fraction of hydrogen in solution is given by:

$$X_B = \frac{[H]/M_H}{[A']/M_A + [H]/M_H}$$

where the units of $[A']$ and $[H]$ are gcm^{-3} and M_A and M_H are the molecular weights of the liquid hydrocarbon reactant and hydrogen respectively.

Thus, assuming hydrogen is present in solution as H_2:

$$P = k_H \frac{\frac{1}{2}[H]}{[A']/M_A + \frac{1}{2}[H]}$$

$$\therefore [H] = \frac{P[A']/M_A}{\frac{1}{2}(k_H - P)} \qquad (5\text{-}14)$$

$$\therefore \frac{1}{[H]} = \frac{k_H M_A}{2[A']} \cdot \frac{1}{P} - \frac{M_A}{2[A']}$$

Therefore, substituting in equation 5-13:

$$\frac{t}{\ln A/A_o} = -\frac{k_H M_A}{2k'[A']} \frac{1}{P} + \frac{M_A}{2k'[A']} \qquad (5\text{-}15)$$

CHAPTER 6

RESULTS AND DISCUSSION OF COMMISSIONING AND PRELIMINARY EXPERIMENTS

6.1 Mechanical Commissioning of the One Litre Autoclave System

A programme of mechanical commissioning of the one litre autoclave system was carried out to test all the newly assembled equipment. In particular pressurization technique and leakage and heating rates were investigated.

6.1.1 Autoclave and Line Pressurization

The minimum inlet pressure to the compressor required to achieve a reactor pressure of 210 bar was found to be about 34 bar. For higher reactor pressures, correspondingly higher inlet pressures were needed. For example, to achieve reactor pressures of 270 and 340 bar, inlet pressures to the compressor of 41 and 48 bar respectively were required.

In mechanical commissioning, the average leakage rate of hydrogen from the autoclave was found to be about 0.2 bar/min. at reactor conditions of 210 bar and 450°C. This was thought to be acceptable from the point of view of safety and material loss. The source of leakage was principally from the main closure seal.

The high pressure lines into and out of the autoclave were found to be leak-free.

6.1.2 Autoclave and Line Heating

The heating rate of 450g of E83 high rank coal extract solution and 100 g. catalyst was found to be about $3^{\circ}\ min^{-1}$ at 50% furnace power and about $4\frac{1}{2}^{\circ}\ min^{-1}$ at 60% power. Higher heating rates were not used because it was thought that the increased temperature differential across the thick autoclave wall could give rise to excessive stresses.

The Eurotherm temperature controller gave good control after maximum initial overshoot of about 5°C.

It was found that the lines from the autoclave to the gas-liquid separation systems had to be heated in order to alleviate blocking by the products. It was also found that the temperature of these lines had an effect in the yield of condensate, a higher temperature giving a higher condensate yield. For this reason, a constant line temperature of 110°C was chosen as standard for future experiments.

6.2 Process Commissioning of the One Litre Autoclave System

Process commissioning was carried out in order to solve some of the practical problems inherent in the start up of a new system. For this purpose, short experiments were performed using toluene, anthracene oil and coal extract solution respectively as feed materials. The main problems to be solved were the estimation of the weight of feed required, the maximization of the efficiency of the gas-liquid separation system and the choice of fixed-bed or slurried catalyst.

6.2.1 Estimation of Required Feed Weight

In the early process commissioning experiments, it was apparent that there was a certain minimum amount of feed material that must be added to the autoclave at the start of an experiment. The explanation of this is as follows.

As products were removed during the run the liquid level in the reactor fell and, if insufficient feed had been used, the level fell below the bottom of the thermocouple, which then recorded a lower temperature. The furnace temperature controller then compensated for the apparent decrease in temperature with the result that the liquid temperature was raised by 10°C or more.

It was found that in order to prevent the occurrence of this effect, a minimum of 450 g of total feed (coal extract solution + catalyst) was required for most runs, rising to 625 g. for runs of long duration.

6.2.2 Efficiency of Gas-Liquid Separation System

Tests to determine the efficiency of gas-liquid separation system resulted in the installation of a high pressure knock-out pot which was capable of trapping most of the liquids carried over from the autoclave. On the low pressure side, collection of the remaining liquid product was effected by a water condenser, a cold trap and a bed of active carbon. Some of the products were frozen in the cold trap when an acetone/dry-ice mixture was used and this caused blocking. Dry-ice alone was subsequently found to be adequate.

6.2.3 Fixed-Bed v. Slurried Catalyst

Initially, the autoclave was operated with a fixed catalyst bed in order to eliminate the difficulties of catalyst separation and recovery in a slurry system. However, preliminary experiments using a catalyst basket showed that only a small degree of hydrogenation was achieved as indicated by:

(i) The low hydrogen to carbon atomic ratio of the product, which was similar to that of the feed.

(ii) The small amount of product boiling under 200°C.

Other workers[175,186] have also obtained low yields when using catalyst baskets in batch autoclaves and only a spinning basket system[176, 177] seems capable of producing yields comparable to those obtained in a slurry reactor.

Thus, for kinetic studies, the fixed catalyst basket system was abandoned in favour of catalyst slurries, since the latter were found

to give much better results due to increased contact between the catalyst particles and the feed and to the smaller particle size that could be employed in slurries.

Subsequent separation of the slurried catalyst was carried out by distillation.

6.3 Preliminary Experiments in the One-Litre Autoclave

Preliminary experiments were carried out in the one litre autoclave using coal extract solution feed and slurried catalyst with a view to:

(i) Establishing reproducibility of results.

(ii) Determining and making a preliminary investigation of the important parameters in coal extract solution hydrogenation.

(iii) Comparing different catalysts.

(iv) Developing a standard procedure in terms of operation and analysis for future experiments.

The reaction time was defined as the period during which the reactor contents were held at the required temperature for the experiment, while the hydrogen flow time referred to the time during which hydrogen was admitted to the autoclave. The rate of flow of permanent gases out of the autoclave was termed the gas flowrate.

A 25% (w/w extract feed) loading of powdered Harshaw 0402T catalyst was used in all the preliminary experiments.

6.3.1 Reproducibility of Results

Initially, four experiments were performed using similar conditions in order to establish that reproducible results could be obtained. The conditions used were:

Coal extract solution feed	E83 High Rank
Reaction time	2 hrs.
Reaction temperature	450°C

Pressure	210 bar
Gas flowrate	10 $lmin^{-1}$
Average catalyst particle size	173 μm
Stirrer speed	850 r.p.m.

Product yields and hydrogen to carbon atomic ratios are shown in Table 7 for each experiment along with the mean ($\bar{x}$) and standard deviation (s), over the four experiments. The latter was calculated from the equation

$$s = \sqrt{\frac{\Sigma (x-\bar{x})^2}{n-1}}$$

where n was the number of experiments performed.

It can be seen that the standard deviations were quite low and that the yields, conversions and H/C ratios could be reproduced to within about 5% of their mean values.

In other series of experiments, many repeats were carried out to monitor reproducibility and these will be discussed later.

6.3.2 Effect of Reaction Time on Hydrogenation of Coal Extract Solution

Several experiments were carried out for reaction times between 0 and 3 hours. Zero reaction time was equivalent to the sum of the heating and cooling periods i.e. heating of the reactor ceased as soon as the reaction temperature was reached. Other conditions were:

Coal extract solution feed	E83 High Rank
Reaction Temperature	450°C
Pressure	210 bar
Gas flowrate	10 l min^{-1}
Average catalyst particle size	173 μm
Stirrer speed	850 r.p.m.

The results are shown in Table 8 in which it can be seen that the yields of gaseous hydrocarbons and liquids boiling below 350°C increased with reaction time, while the yield of residue, A, (material boiling above 350°C) decreased. Very little gas or low-boiling liquids were produced at zero reaction time.

A plot of $\ln {}^{A}/_{A_o}$ versus hydrogen flow time is shown in Figure 7. This is a straight line of slope 5.8×10^{-3} min^{-1}. This indicates that the overall reaction is of first order with respect to coal material remaining, with the slope equal to the overall first order rate constant.

The H/C ratio in the condensate (predominantly material boiling below 300°C) increased with time, although the effect was less pronounced at the longer reaction times. The H/C ratio of the reactor contents, however, remained approximately constant. This indicates that hydrogen was added to the material in the reactor contents at a similar rate to that of its removal in the form of low boiling components in the condensate.

6.3.3 Effect of Temperature on Hydrogenation of Coal Extract Solution

Two experiments were carried out at different reaction temperatures, 430 and 450°C. The other conditions were:

Coal extract solution feed	EP52FD10 Low Rank
Reaction time	1 hour
Pressure	210 bar
Gas flowrate	10 l min^{-1}
Average catalyst particle size	173 μm
Stirrer speed	850 r.p.m.

The results are shown in Table 9 from which it can be seen that the yields of gas and liquids boiling below 350°C increased quite sharply with reaction temperature and the yield of residue decreased by nearly 14% w/w feed when the temperature was raised by only 20°C.

An approximate apparent activation energy, E_a, for the conversion to material boiling below 350°C was calculated from the results using the equation

$$E_a = -R \frac{\ln k_1 - \ln k_2}{1/T_1 - 1/T_2}$$

where R is the gas constant and k was calculated from

$$k = \frac{\ln A/A_o}{t}$$

The value of the activation energy was found to be 30.3 kcal $mole^{-1}$. This indicates that the predominant rate determining step in the reaction was probably one which showed a high temperature dependence.

6.3.4 Effect of Pressure on Hydrogenation of Coal Extract Solution

A pair of experiments were carried out at different total pressures, 210 and 240 bar. The other conditions used were:

Coal extract solution feed	E83 High Rank
Reaction time	2 hrs.
Reaction temperature	450°C
Gas flowrate	10 l min^{-1}
Average catalyst particle size	173 μm
Stirrer speed	850 rpm

The results in Table 10 show that at the higher pressure there was relatively more gas produced than low-boiling liquids. This is indicative of increased hydrocracking of the lower boiling liquids at higher pressures. There was little change in yield of heavier liquids.

In general, the change in yields was small and only a 6% increase in conversion resulted from a 14% increase in pressure.

6.3.5 Effect of Gas Flowrate on Hydrogenation of Coal Extract Solution

To determine the effect on hydrogenation of a change in gas flowrate, two experiments were performed at gas flowrates of 10 and 20 l min^{-1} respectively and the other conditions were:

Coal extract solution feed	E83 High Rank
Reaction time	1 hr.
Reaction temperature	450°C
Pressure	210 bar
Average catalyst particle size	173 μm
Stirrer speed	850 rpm

The results are shown in Table 11. Although twice the amount of condensate was produced when the flowrate was doubled, analysis of the total product revealed that little overall change in the yields of gaseous hydrocarbons and liquid fractions had occurred.

The H/C ratio of the condensate also remained the same after runs at different flowrates, as did the reactor contents H/C ratio.

An increase in gas flowrate might be expected to produce an increase in the amount of hydrogen dissolved in the reactant (and thus an increase in reaction rate) due to the greater availability of fresh hydrogen and to improved mixing due to the increased turbulence of the gas in the liquid. However the fact that the gas flowrate had little effect on the hydrogenation of coal extract solution indicates that either the solubility of hydrogen may have reached saturation or that gas flowrate did not affect the rate of mass transfer of hydrogen from the gas to the liquid phase.

In a glass-model of the 1 l. autoclave, it was found[179] that the gas flowrate had little effect on the degree of mixing. Calderbank[185,187] found that gas flowrate had no effect on the rate of mass transfer of hydrogen from the gas to the liquid phase either with or without agitation.

A constant gas flowrate of 10 $lmin^{-1}$ was used in all subsequent experiments.

6.3.6 Effect of Catalyst Particle Size on Hydrogenation of Coal Extract Solution

Experiments were conducted with the catalyst ground and sieved to two different average particle sizes, 80 and 173 μm. Other conditions used were:

Coal extract solution feed	E83 High Rank
Reaction time	2 hrs.
Reaction temperature	450°C
Pressure	210 bar
Gas flowrate	10 $lmin^{-1}$
Stirrer speed	850 r.p.m.

Table 12 shows the results. It can be seen that the gas and higher-boiling liquid yields increased slightly with reduced catalyst particle size, while the yield of low-boiling liquids decreased. However no significant change in overall conversion to material boiling below 420°C was found when catalyst of smaller particle size was used.

Neither the H/C ratio of the condensate nor that of the reactor contents was affected in runs with smaller catalyst particles.

The results indicate that the product distribution was altered slightly by a change in catalyst particle size, probably due to increased hydrocracking of lower-boiling material. However, that the overall conversion

was unaffected may indicate that intraparticle diffusion resistance was not a rate limiting factor. This is in agreement with Furusawa,[183] who found that pore diffusional effects were only significant for particles larger than 200 μm.

It was decided to use catalyst of the same average particle size (173 μm) in all future experiments.

6.3.7 Effect of Stirrer Speed on Hydrogenation of Coal Extract Solution

Experiments were performed at two different stirrer speeds of revolution (850 and 1200 r.p.m.), the other conditions being as follows:

Coal extract solution feed	EP52FD10 Low Rank
Reaction time	1 hr.
Reaction temperature	450°C
Pressure	210 bar
Gas flowrate	10 $lmin^{-1}$
Average catalyst particle size	173 μm

The results shown in Table 13 indicate that only a small increase in the yields of gaseous hydrocarbons and low-boiling liquids occurred at higher stirrer speed.

These results indicate that the stirrer speed was high enough to avoid any serious rate limitations due to external diffusion resistances. Davis[179] confirmed that there was little improvement in mixing in a glass model of the one-litre autoclave with stirrer speeds in excess of about 750 r.p.m. and Brooks[125] obtained less than a 3% increase in conversion of a coal slurry when the stirrer speed was raised from 1200 to 1800 r.p.m.

A stirrer speed of 850 rpm was chosen for all future experiments, since practical problems were encountered at higher speeds.

6.3.8 Comparison of Harshaw 0402T with Other Catalysts

Some experiments were carried out in order to compare Harshaw 0402T with other hydrocracking catalysts. The conditions used in the investigation were:

Coal extract solution feed	EP52FD10 Low Rank
Reaction time	2 hrs.
Reaction temperature	450°C
Pressure	210 bar
Gas flowrate	10 $lmin^{-1}$
Average catalyst particle size	173 μm
Stirrer speed	850 r.p.m.

The results are presented in Table 14. In general it was found that, with respect to the total conversion to products boiling below 350°C, the activity of the catalysts fell in the order Co-Mo > Ni-Mo > Ni-W. The activity of Harshaw 0402T (Co-Mo) was found to be quite high, although not as great as either Comox 471 or Aero HDS 16A catalysts (both Co-Mo based).

Much work has been carried out at C.R.E. using Comox 471 and, since the availability of Aero HDS 16A was limited, Harshaw 0402T was chosen for future experiments. This catalyst has been used in other coal conversion processes, e.g. the Synthoil Process in the U.S.A.

6.4 Commissioning and Preliminary Experiments in the 300 ml. Autoclave

No commissioning or preliminary experiments were carried out in the 300 ml. autoclave, as this facility was already fully operational.

CHAPTER 7

EXPERIMENTAL RESULTS

The reaction time was defined as the period during which the reactor contents were held at the required temperature for the experiment, while the hydrogen flow time referred to the time during which hydrogen was admitted to the autoclave. The gas flowrate referred to the rate of flow of permanent gases out of the autoclave.

Powdered Harshaw 0402T catalyst was used in all the experiments. The same gas flowrate, average catalyst particle size and stirrer speed were used throughout, the values of which were 10 $lmin^{-1}$, 173 μm and 850 r.p.m. respectively.

When not themselves subject to investigation, the reaction temperature and pressure were held constant at 450°C and 210 bar respectively.

7.1 Effect of Reaction Time on Hydrogenation of Coal Extract Solution

Experiments were carried out at reaction times up to four hours at different reaction temperatures. Low rank coal extract solution (EP52FD10) was used as feed and the catalyst loading was held at 25% w/w feed.

Product yields, hydrogen consumption, mass balance and conversion data are presented in Tables 15 to 18 for both the reaction time and reaction temperature series of experiments. The results showing the effect of reaction time on hydrogenation are described in this section, and those showing the effect of reaction temperature in section 7.2.

7.1.1 Formation of Individual Gaseous Hydrocarbons

Saturated C_1 - C_4 hydrocarbons were the main constituents of the gaseous hydrocarbons product from coal extract solution hydrogenation.

Unsaturated gases such as ethene and propene were also formed, mainly at longer reaction times, but their yields were generally below 0.05% w/w extract. Neither butene nor ethyne were detected. All the gases were adsorbed to a certain extent (total of about 2% w/w feed) in the active carbon trap, but no preferential adsorption of individual gaseous hydrocarbons was observed.

Tables 15 to 18 show the total yield of each gas produced during each experiment. The yields decreased in the order methane > ethane > propane > butane and all increased with reaction time.

Because there were relatively few components in the gaseous product and because the latter was removed continuously from the autoclave, it was possible to follow the change in gas yields with time during each experiment. Thus, the volumetric fraction of each gaseous hydrocarbon in the gas stream was plotted as a function of hydrogen flow time throughout each experiment. The shape of the curves was essentially the same in all the experiments and a typical example is shown in Figure 8 for a four-hour run at a reaction temperature of 460°C.

It can be seen from this figure that the concentration of methane increased very sharply to a maximum, after which it fell more slowly. Ethane, propane and butane behaved similarly except that the time taken to reach their maximum concentration, and the peak width, increased steadily with the molecular weight of the gas. In Figure 8 the times of maximum methane, ethane, propane and butane concentrations were 113, 126, 146 and 159 minutes, respectively. The time taken for the reactor contents to reach 460°C was 107 minutes, and the maximum temperature (due to slight overshoot) was reached after 112 minutes. These times were of the same order in other experiments.

7.1.2 Hydrocarbon Product Yields

The overall yields of gases and liquid hydrocarbon fractions of the product and the yield of the residue, A, (boiling above 420°C) are given in Tables 15 to 18. The yields of the individual fractions boiling below 300°C all increased with time while the yield of residue decreased. The yield of the 300-355°C fraction tended towards a constant value at long reaction times, or even showed a broad maximum at some reaction temperatures. The yield of the 355-420°C fraction possibly reached a maximum at the beginning of the reaction after which it decreased steadily with time. The rate of production of the 250-300°C fraction was slow at first, especially at the higher temperatures. In general, the change in yields of the fractions with time was similar at different reaction temperatures and the results are shown graphically in Figures 9-12.

The first order rate expression (equation 5-12) was derived in Section 5.2.5. Similar equations can be derived for other orders and Figure 13 shows plots of A, lnA and $^1/_A$ versus hydrogen flow time at the same temperature. These correspond to zero, first and second order equations respectively. It can be seen that while the plots of A and $^1/_A$ against t are curves, lnA versus t is a straight line indicating that the overall reaction was first order with respect to material boiling above 420°C. Figure 14 shows further first order plots of $\ln A/A_o$ versus hydrogen flow time at the different reaction temperatures. These are straight lines, the slopes of which are equal to the overall rate constants, k_1, which are given in Table 19.

The graphs in Figure 14 were extrapolated to $\ln A/A_o = 0$, when t_o was equal to an average of about 57 minutes. This was taken as the hydrogen flow time at which A began to react to produce lower boiling products.

7.1.3 Hydrofining

Tables 15 to 18 show that the removal of nitrogen as ammonia increased with reaction time. Graphs of $\ln {}^{N}/_{N_o}$ against hydrogen flow time were plotted at the different reaction temperatures (Figure 15) and were straight lines. The slopes (which are equal to the rate constants for nitrogen removal) are given in Table 19. On extrapolation of the graphs, t_o was found to be about 80 minutes which was taken to be the hydrogen flow time at which nitrogen removal began. Most of the small amount of sulphur present in the feed was removed as hydrogen sulphide even at low temperatures and no attempt was made to derive kinetic data.

The determination of oxygen content in the product was not always reliable because it was difficult to ensure that all of the water had been removed from the liquid products. No kinetic data have been derived.

7.1.4 Composition of IBP-170^{o}C Fraction

Analysis of the IBP-170^{o}C distillation fraction revealed that the main constituents present were benzene, cyclohexane, toluene, methyl cyclohexane, ethyl benzene, ethyl cyclohexane, propyl benzene, propyl cyclohexane and xylene.

Although the concentrations of benzene, toluene, ethylbenzene, propyl benzene and m and p xylenes did not appear to change regularly with reaction time, their ratio to the corresponding naphthenes generally increased with time as shown in Table 20. This is further illustrated by the paraffin (P), naphthene (N) and aromatic (A) content of some of the fractions from experiments performed at the same temperature.

7.1.5 Deposition of Carbon on the Catalyst

The amount of carbon deposition on some spent catalysts is shown in Table 21. Carbon deposition was in the range 9.3 - 12.7% and increased

slightly with reaction time.

Surface area determinations were carried out on three spent catalysts from experiments at different reaction times, and the results are shown in Table 22 along with those for fresh catalyst (ground and pelletted). The surface area of the ground catalyst varied from 156 to 96 m^2g^{-1} as the reaction time increased.

7.2 Effect of Reaction Temperature on Hydrogenation of Coal Extract Solution

Experiments were performed at reaction temperatures between 420 and 460°C at different reaction times, as discussed in section 7.1.

7.2.1 Hydrocarbon Product Yields

The composition of the gaseous hydrocarbons product was discussed in section 7.1.1. The yield of each individual gas increased with reaction temperature. Over 20% of the feed was converted to gaseous hydrocarbons at the highest temperature.

The yields of liquid product fractions boiling below 300°C all increased with temperature while the yield of residue decreased. The yields of the 300-355°C and 355-420°C fractions were relatively unaffected by a change in temperature.

The overall rate constant for the reaction, k_1 (see Table 19), increased with temperature. From the Arrhenius equation

$$k_1 = Ae^{-E/RT}$$

a graph of $\ln k_1$ against $^1/_T$ is shown in Figure 16. This is a straight line of slope 13.12×10^3 °K.

7.2.2 Hydrofining

Tables 15 to 18 show that the removal of nitrogen as ammonia increased with temperature. A plot of the Arrhenius equation (Figure 16) gave a straight line of slope 7.54×10^3 °K.

The removal of sulphur as hydrogen sulphide appeared to increase slightly with temperature, although most of the sulphur present in the feed was removed even at the lower temperatures.

Although the removal of oxygen from the feed appeared to increase with temperature, the results were scattered due to the difficulty of eliminating water from the product before oxygen determination.

7.2.3 Composition of IBP-170°C Fraction

The main constituents of the IBP-170°C fractions were listed in section 7.1.4.

The individual components in the fraction did not change regularly with temperature. However Table 20 shows that the ratios of benzene, toluene, ethyl benzene, propyl benzene and m and p xylenes to their corresponding naphthenes increased with temperature. This was confirmed by PNA analysis, where the A:N ratio in the whole fraction also increased with temperature.

7.2.4 Deposition of Carbon on the Catalyst

Table 21 shows the amount of carbon deposited on the catalyst after experiments at different reaction temperatures. The carbon deposition was of the order of 10%, but no significant change in deposition was observed at different temperatures.

7.3 Effect of Pressure on Hydrogenation of Coal Extract Solution

Experiments were carried out at total pressures between 138 and 339 bar and at hydrogen concentrations between 40 and 100% by volume. Nitrogen and argon were used as inert diluents. High rank coal extract solution (E83) was used as feed, the reaction time was held at 1 hour and the catalyst loading was 15% w/w feed.

Because of the difference in density of hydrogen and nitrogen, the gas flowrate was adjusted, in runs where 100% hydrogen was used, to

6 $lmin^{-1}$, which was equivalent to 10 l min^{-1} of hydrogen/nitrogen mixture. Calibration curves are shown in Appendix 2.

The results are shown in Table 23 which gives product yields, hydrogen consumption, mass balance and conversion data.

7.3.1 Hydrocarbon Product Yields

The yields of all the products increased with hydrogen pressure, except for the 355-420°C fraction, which remained essentially constant throughout the range of pressure studied, and the material boiling above 420°C, which decreased.

The rate decreased slightly when the partial pressure of inert gas was raised while the hydrogen partial pressure was kept constant, as shown in Figure 17.

It can also be seen that there was no significant difference in product yields, hydrogen consumption or conversion when different types of inert diluents were used at the same hydrogen partial pressure.

The modified rate expression for use when the pressure was varied in successive experiments (equation 5-15) was derived in section 5.2.6. Figure 18 shows a plot of $\frac{t}{\ln A/A_o}$ against the reciprocal of the hydrogen pressure. Here the values of $\ln A/A_o$ have been corrected for the effect of the different concentrations of inert gas present by the use of the following correction factor and Figure 17:

$$\frac{(\ln A/A_o)_o}{(\ln A/A_o)_x}$$

i.e. the value of $\ln A/A_o$ at 0% inert gas pressure divided by the value at a given % inert gas.

From Figure 18, which is a straight line, the value of Henry's Law constant was calculated as 564 bar. From equation 5-14, the solubility

of hydrogen in the reactants was calculated as 24 cm^3/g reactant at 210 bar.

7.3.2 Hydrofining

The removal of nitrogen and sulphur from the feed as ammonia and hydrogen sulphide increased with pressure. At the highest pressure, 70% of the sulphur and 60% of the nitrogen was removed.

The results obtained for the removal of oxygen were subject to considerable scatter due to the presence of water dissolved or suspended in the product.

7.3.3 Composition of IBP-170°C Fraction

The main components present in the IBP-170°C product fractions are shown in Table 24. From this it can be seen that at low hydrogen partial pressures 20% toluene and 20% xylenes were produced. At the higher hydrogen partial pressures, over 35% cyclohexane and methyl cyclohexane was present in the fraction.

The ratios of benzene, toluene, propyl benzene and m and p xylenes to their corresponding naphthenes are shown in Table 25 and were found to decrease markedly with increasing hydrogen partial pressure. This is further illustrated by the PNA analyses of the whole fraction which are also shown in Table 25. It can be seen that the paraffins and naphthenes increased with hydrogen partial pressure while the aromatics content decreased.

7.4 Effect of Catalyst Loading on Hydrogenation of Coal Extract Solution

A series of experiments was carried out to determine the effect on coal extract solution hydrogenation of varying the catalyst loading in the range 0-25% w/w feed.

In order to maintain the same contact mass in the reactor during each experiment and so retain similar dynamic conditions and total volume, catalyst and inert powder were mixed to give a constant weight of charge. Alumina, powdered to the same particle size as the catalyst, was used as the inert as this material has been found to have little catalytic effect on coal hydrogenation.

Low rank coal extract solution (EP52FD10) was used as feed in these experiments, and the reaction time was held at 2 hours.

Product yields, hydrogen consumption, mass balance and conversion data are presented in Table 26.

7.4.1 Hydrocarbon Product Yields

As the catalyst loading increased, the amount of material boiling below 355°C increased and the amount of residue(material boiling above 420°C) decreased by large amounts at first, then by less as the loading was raised above 10%.

Figure 19 shows how the rate changes with catalyst loading. It can be seen that the rate increased rapidly on the addition of only a small amount of catalyst, but at higher loadings the increase was much less. However a constant rate was not reached in the range of catalyst loading studied.

In experiments performed in the absence of active catalyst, 5% less conversion was obtained with a 25% loading of alumina than with no alumina at all. In the latter case, the conversion figure was 27.6%. Over 60% conversion was achieved with a 25% loading of active catalyst.

7.4.2 Hydrofining

As with the yields of the hydrocarbon products, the calculated yields of ammonia, hydrogen sulphide and water were strongly dependent upon catalyst loading up to about 5-10%, but as the loading was raised beyond this, the dependency became smaller.

7.4.3 Composition of IBP-170°C Fraction

The main constituents present in the IBP-170°C fraction were similar to those reported in section 7.1.4 except that with zero catalyst loadings, appreciable quantities of ethyl toluene and mesitylene were also produced.

Ratios of individual aromatic to naphthenic compounds are given in Table 27. In general, this ratio fell with increased catalyst loading, although the ratio of benzene to cyclohexane remained essentially constant other than at zero loading. These results are further illustrated in the PNA analyses of the whole fraction, where the A:N ratio fell with increased catalyst loading.

7.5 Effect of Initial Concentration of Coal Extract Solution on Hydrogenation

Experiments were carried out using feeds with different quantities of low rank coal extract solution (EP52FD10) dissolved in anthracene oil (EP51D). The solvent was the same as that used in the preparation of the extract solution itself. The proportion of extract solution ranged from 0 to 100%. The reaction time and catalyst loading were held at 1 hour and 15% w/w feed respectively.

7.5.1 Hydrocarbon Product Yields

Table 28 shows the product yields obtained from the hydrogenation of the coal extract solutions. While the yield of gaseous hydrocarbons increased from 3.6 to 9.0% w/w feed as the initial concentration of coal extract solution was raised, the yield of the IBP-170°C fraction decreased.

Figure 20 shows a plot of $\ln A$ against $\ln A_o$ (where A and A_o refer to the amount of material boiling above 420°C in product and feed respectively). This was a straight line of slope 1.19. This was greater than the slope which is expected from the rate expression (equation 5-12)

which is 1.00. Greater departure of the experimental from the expected line occurred at lower coal extract solution concentrations.

Also shown in the figure is the line obtained after the results had been corrected for the effect of hydrogen solubility, which increased with the concentration of anthracene oil in the feed. This graph was, in fact, a plot of equation 5-13, where H ranged from 1 for pure anthracene oil to 2 for pure coal extract solution (the solubility of hydrogen in anthracene oil is thought to be twice that in coal extract solution).

7.5.2 Hydrofining

The calculated yields of water, ammonia and hydrogen sulphide appeared to be relatively unaffected by the initial concentration of coal extract solution.

7.6 Secondary Hydrogenation of Product Distillation Fractions

Experiments were carried out on two product distillation fractions obtained from the hydrogenation of coal extract solution. These were nominally the 355-420°C fraction (B) and the 300-355°C fraction (C). These fractions were chosen for further study because it was thought that they were the main intermediates in the overall reaction.

Two series of experiments were performed on the fractions. First, experiments where samples were taken at different reaction times giving reaction rate information and second, experiments where the catalyst loading was varied in different runs.

7.6.1 Rate of Hydrogenation of 355-420°C Fraction

Since the amount of feedstock available was limited, only one run was carried out in the 1 litre autoclave and samples of the total product (gas, condensate and reactor contents) were collected at times between

0 and 4 hours. Little or no hydrogenation took place during the cooling period since the samples were quenched immediately on withdrawal. A 25% catalyst loading was used.

Table 29 shows product yields, hydrogen consumptions, mass balances and conversions at different times during the experiment. It can be seen that the yields of hydrocarbon gas and the fractions boiling below 300°C all increased with time, while the yield of the 355-420°C fraction decreased. However, the yield of both the 300-355°C fraction and material boiling over 420°C reached a maximum value before decreasing. The changes in yields with time are shown in Figure 21.

There was a large range in the amount of material boiling above 355°C in the feed that was converted to material boiling below 355°C in the product, 80% being converted after 4 hours.

The yields of water and ammonia tended towards constant values at longer times.

7.6.2 Effect of Catalyst Loading on Hydrogenation of 355-420°C Fraction

The experiments were carried out in the 300 ml autoclave so that as many runs as possible could be performed using the limited quantity of feedstock available. The catalyst loading was varied between 0 and 10% w/w feed.

The results are given in Table 30 and show that the yield of material boiling below 300°C increased by a large amount as the catalyst loading was raised at low loadings, but by lower amounts at higher loadings.

Little gas was produced in the absence of catalyst, but the gas yield increased with catalyst loading.

The yield of material boiling above 420°C remained virtually constant as the catalyst loading was raised.

7.6.3 Rate of Hydrogenation of 300-355°C Fraction

Since the amount of feedstock available was limited, only one run was carried out in the 1 litre autoclave and samples of the total product were collected at times between 0 and 4 hours. Little or no hydrogenation occurred during the cooling period since the samples were immediately quenched on withdrawal. The catalyst loading in the experiment was 25% w/w feed.

Table 31 shows product yields, hydrogen consumptions, mass balances and conversions at different times during the experiment. The yields of gaseous hydrocarbons and the IBP-170°C and 170-250°C fractions increased with time while the yields of the 300-355°C and 355-420°C fractions decreased. However, the yield of both the 250-300°C fraction and of material boiling over 420°C went through a maximum. The amount of material produced which boiled over 420°C was very small. The changes in yields with time are shown in Figure 22.

There was a very large range in the amount of material boiling above 300°C in the feed that was converted to material boiling below 300°C in the product, 88% being converted after 4 hours.

The amount of water produced in the reaction appeared to increase with time, while ammonia production reached a constant value at longer times.

7.6.4 Effect of Catalyst Loading on Hydrogenation of 300-355°C Fraction

These experiments, where the catalyst loading was varied between 0 and 10% w/w feed, were carried out in the 300 ml autoclave, so that as many runs as possible could be performed using the limited quantity of feedstock available.

The results are shown in Table 32 from which it can be seen that at small catalyst loadings, the yield of material boiling below 300°C increased sharply with loading, but at higher loadings smaller increases were observed.

Very little gas was produced in the absence of catalyst, but the gas yield increased with catalyst loading.

7.7 Hydrogen Consumption

In the experiments performed, the hydrogen consumption ranged from 1.5 to 7.8% w/w feed.

Graphs of conversion against calculated hydrogen consumption for all the experiments using low and high rank coal extract solutions as feed are shown in Figures 23 and 24 respectively. In the figures, the hydrogen consumption has been corrected to take into account the different mass balance of each experiment.

The graphs were both straight lines, although there was considerable scatter in the results. By extrapolation of the graphs, it appeared that, for the low rank extract solutions, some hydrogen was consumed before the extract was converted to material boiling under 420°C, while for the high rank extract solutions, some conversion occurred before any hydrogen was consumed.

7.8 Mass Balances

In the experiments on the hydrogenation of coal extract solutions, mass balances were on average about 96%. No correlation was found between the mass balance and any of the reaction conditions employed. However in the experiments involving the secondary hydrogenation of primary product fractions, mass balances (which were in the range 97-100%) decreased with time.

7.9 Reproducibility

Many of the experiments performed were repeated under identical conditions as a test of reproducibility. Table 33 shows the mean, standard deviation and percentage error of product yields, hydrogen consumption and conversion for the experiments which were repeated at least 3 times.

In general, the results could be reproduced to within about 10% of their mean value. However the yields of the IBP-170^{o}C and 170-250^{o}C fractions showed a departure of more than 10% from the mean, while the yields of total liquid product and the conversion could be reproduced to within 5%.

CHAPTER 8

DISCUSSION OF RESULTS

8.1 Effect of Reaction Time on Hydrogenation of Coal Extract Solution

8.1.1 Formation of Individual Gaseous Hydrocarbons

Gaseous hydrocarbons are in general a product of cracking reactions, the nature of the gas produced depending on the particular carbon-carbon bonds in the reactant that are broken. For example, in the hydrocracking of octahydro-phenanthrene,

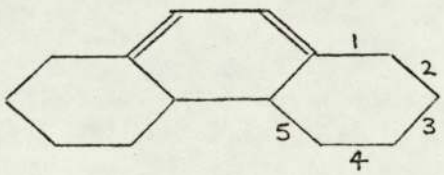

if bonds 1 and 2 are broken, methane will be produced while the breaking of 1 and 3 produces ethane; 1 and 4, propane and 1 and 5, butane. The hydrocracking of other compounds may be selective in the gas produced; for example with fluorene,

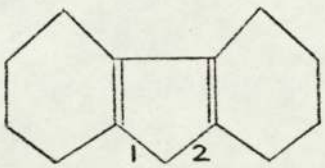

cleavage of C-C bonds at 1 and 2 will only yield methane.

In the hydrogenation of coal extract solution, little unsaturated gas was detected, indicating that hydrocracking proceeded mainly by the splitting of saturated rings.

The total amount of saturated gases generally decreased from methane to butane. This may be explained by considering again the hydrocracking of octahydro-phenanthrene. Methane can be produced by cleavage of bonds 1 and 2, 2 and 3, 3 and 4 or 4 and 5 and so has a

greater chance of being produced than that of, for example, propane where only bonds 1 and 4 or 2 and 5 must be broken.

It is also possible that $CH_3\cdot$ and $C_2H_5\cdot$ radicals were produced during hydrocracking and that these combined not only with hydrogen but also with themselves to form the higher molecular weight hydrocarbons; for example, by the following mechanisms:

$$CH_3\cdot + CH_3\cdot \longrightarrow C_2H_6$$

$$CH_3\cdot + C_2H_5\cdot \longrightarrow C_3H_8$$

$$C_2H_5\cdot + C_2H_5\cdot \longrightarrow C_4H_{10}$$

It appears unlikely that any significant amount of $C_3H_8\cdot$ or higher molecular weight radicals were formed since only small quantities of pentane, hexane, etc. were detected.

However, it is probable that two types of cracking occurred simultaneously in the catalytic hydrogenation of coal extract solution: thermal and catalytic. The maximum rate of production of methane occurred at almost exactly the same time as the maximum reaction temperature was reached irrespective of whether or not active catalyst was used (see Figure 8). This indicates that much of the methane was produced by thermal cracking. Subsequently, the rate fell more slowly in runs where active catalyst was present indicating a greater amount of catalytic cracking.

Little gas was produced during the experiments on the 355-420°C and 300-355°C product fractions in the absence of a catalyst (see Tables 30 and 32), indicating that little thermal cracking of these fractions occurred. Thus gas produced by thermal cracking originated almost exclusively from the fraction boiling above 420°C. This was confirmed in the experiments where the initial concentration of coal extract solution in the feed was varied by dilution in anthracene oil

(see section 8.5). Here, the gas yields increased with the concentration of coal extract solution, indicating that more gas was produced from the coal portion than the anthracene oil (which boiled predominantly below 420°C). This effect has also been observed by Shah[134] in the hydrogenation of a 40% and a 20% coal slurry.

The time taken to reach maximum gas production increased with the molecular weight of the gas. This was probably due to the fact that thermal cracking gave a different gas product distribution than catalytic cracking. This was in part confirmed in experiments performed without catalyst (see section 8.4) where proportionally more methane was produced, (see Table 26). In addition, as the peak width also increased with the molecular weight of the hydrocarbon gas it was thought that less higher molecular weight hydrocarbons were produced from thermal cracking and more from catalytic cracking reactions. This was confirmed in the catalytic experiments on the 355-420°C and 300-355°C product fractions (see Tables 29 and 31), where catalytic cracking only took place. Here, the yields of ethane, propane and butane were generally greater than that of methane.

8.1.2 Kinetic Order of the Overall Reaction

A vast number of products were obtained from the hydrogenation of coal extract solution (see, for example, Figure A3-1 which shows an analysis of a typical product). In order to describe the kinetics and mechanism of the reaction, therefore, a simplification of the reaction products was required.

There are at least three possible ways of simplifying the reaction products. First, some of the main chemical constituents of the product could be selected and their change in concentration followed during the course of the reaction. Such compounds could include anthracene,

phenanthrene, tetralin, naphthalene, benzene and cyclohexane, for example. Second, the products could be characterised by their solubility in various solvents such as quinoline, pyridine, benzene or hexane, for example. The third category, which was that adopted in this work, involved splitting the product into groups characterised by their boiling ranges, each of which broadly represented a class of compounds.

The advantages of this method of simplification are: (i) There is little ambiguity as to the nature of the product. (ii) The method accounts for all the products formed. (iii) The characterised products are those which are commercially important. (iv) The method of characterisation is the most convenient. The main disadvantage of the method is that since the boiling ranges are chosen on a fairly arbitrary basis, there is a possibility of reactions occurring within each fraction. This is especially evident in the fraction boiling above 420°C.

The boiling ranges chosen (see Appendix 3) were:

A Material boiling over 420°C

B " " 355-420°C

C " " 300-355°C

D " " 250-300°C

E " " 170-250°C

F Liquids " up to 170°C

G Gases.

Using the above nomenclature, the overall reaction coal $\longrightarrow$ products can be represented by

$$A \longrightarrow B + C + D + E + F + G$$

This reaction was found to be first order with respect to the amount of A remaining, which was in agreement with most of the work found in the literature.

The rate constant calculated for the overall reaction was 4.7 x 10^{-3} min^{-1} for the experiments carried out at a reaction temperature of 450°C using low rank coal extract solution as feed. This was of the same order as the rate constant calculated from preliminary experiments (see section 6.3.2) which was 5.8 x 10^{-3} min^{-1}. The discrepancy between the two values was due to the fact that in the preliminary experiments "reactant" was taken as material boiling above 350°C, and thus contained more lower boiling material which reacted at a faster rate.

The calculated rate constant, however, was an overall value and included not only the rate constant for the chemical reaction on the surface of the catalyst but also all the effects of internal and external resistances as detailed in section 5.2.4. The magnitude of the overall rate constant, therefore, was more a function of the system than of the reaction itself.

8.1.3 Chemical Composition of Fractions

Although each fraction contained many different compounds, the majority of components in any one fraction contained the same number of cyclic rings in their structure. Thus, in general, fraction A contained compounds with four or more cyclic rings in their structure, B contained compounds with predominately four rings, C, three rings, D and E two rings and F, one ring. To illustrate this, some typical compounds present in each fraction are listed with their boiling points in Appendix 4.

8.1.4 Development of Kinetic Model

In section 8.1.2, the overall reaction was represented as:

$$A \longrightarrow B + C + D + E + F + G$$

However, from the shapes of the curves in Figures 9-12, it is evident that some of the products in the scheme were themselves taking part in further reactions. Although not clearly defined, the yields of B and C possibly showed maxima during the hydrogenation of coal extract solutions, especially at the higher temperatures, indicating their breakdown to other products. Thus B and C were thought to be the main intermediates in the reaction. This was confirmed in the experiments on B and C alone. Both reacted to yield large amounts of lower boiling products and C showed a clear maximum during the hydrogenation of B (see Figures 21 and 22). Thus:

$$A \longrightarrow B \longrightarrow C \longrightarrow D + E + F + G$$

During the $A \longrightarrow B$ and $B \longrightarrow C$ reactions above, other lower boiling products must also have been formed simultaneously, i.e.:

$$A \longrightarrow B + C \text{ or } D \text{ or } E \text{ or } F \text{ or } G$$

(depending on the size of the molecule in A that reacted) and

$$B \longrightarrow C + F \text{ or } G$$

(i.e. Here, a four-ringed structure (B) reacts to produce a three-ringed species (C) and either a one-ringed species (F) or a paraffin (G)). Thus:

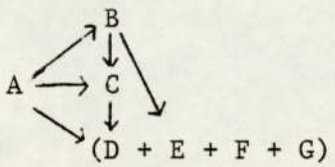

It can also be seen in Figures 9-12 that the initial rate of production of D was slower than that of E, F or G. This indicates that the rate of formation of D from A was less significant than that of E, F or G from A, relative to the production from other species.

In the experiments performed on C alone, a maximum was observed in the yield of D after a considerable reaction time. This indicates that D too was an intermediate. This maximum was not observed in other experiments, and the reason for this is as follows. The secondary hydrogenations of B and C represent progressively later stages of the overall reaction of coal extract solution. Earlier in the reaction (i.e. during the hydrogenation of large initial amounts of A) the yield of D was still increasing towards its maximum value and the reaction was not sufficiently complete for the maximum to be observed under the conditions employed. It was only during the later stages of the overall reaction studied in the experiments on C alone, when the amount of A was very small and the amount of C was decreasing rapidly, that the reaction had progressed far enough for the maximum in D to be observed.

Assuming the absence of a reverse reaction, the maximum in the production of D must have been due to the formation of E, F and/or G. No evidence was found, however, to suggest that E, F or G broke down to any appreciable extent under the conditions employed in these experiments. Indeed it has been found[188] that a temperature of over 500°C is required before E reacts to give significant yields of lower-boiling products. Thus E, F and G were assumed to constitute the final products in the overall reaction and the final kinetic model proposed is:

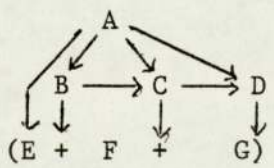

Several other authors have proposed kinetic models for the hydrogenation of coal or oil-derived feedstocks.

Shah[134] has developed a model using product distillate fractions for the hydrogenation of a coal slurry. He used boiling ranges which were slightly different to those used in this work, but his model is equivalent to the following:

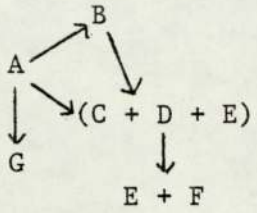

The main differences between Shah's model and that developed here are the absence of C and D as separate intermediates and the lack of any reactions producing G other than from A.

Kuganov[132] also did not observe C and D as separate intermediates in his model for the hydrocracking of crude oil distillates, which was equivalent to:

$$A + B \longrightarrow (C + D + E) \longrightarrow F$$

However Gagarin[133] found that C + D + E was converted to gas as well as to low boiling liquids:

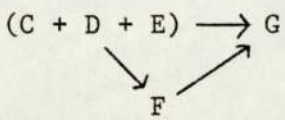

where the feed in this case was a distillation fraction from the hydrogenation of coal.

8.1.5 Calculation of Rate Constants

Assuming that all the reactions considered are first order, if the amounts of the seven components A to G at time t are denoted by M_i (i = 1-7), then:

$$\frac{dM_i}{dt} = \sum_{j=1}^{7} k_{ij} M_j$$

or in matrix notation: $\frac{dM}{dt} = kM$

where k_{ij} are the reaction rates. This equation was used to determine the rate constants of the reactions involving the breakdown of components A, B and C in the simplified model:

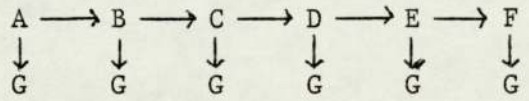

Assuming that E, F and G constituted the final products of the reaction, the rates of reaction of A, B and C to E, F and G were then calculated from the experimental data and the rates of reaction of D to E, F and G were arbitrarily chosen to be one third of the D $\longrightarrow$ E + F + G rate. On comparing the predicted results with the experimental (see section 8.1.7), it was found that species C and D were under-predicted. This was corrected by including the A $\longrightarrow$ C and A $\longrightarrow$ D reactions and fixing their rates by trial and error. The scheme of reactions is now the same as that in the kinetic model proposed in section 8.1.4.

The rate constants for all seventeen reactions considered in the model are given in Table 34.

It can be seen that the rate constant for the overall A $\longrightarrow$ products reaction as calculated from the model (4.3×10^{-3} min^{-1}) differed slightly from that calculated in section 8.1.2 (4.7×10^{-3} min^{-1}). This is because the latter was calculated from the experiments on A only while the former was calculated from the experiments on A, B and C. The rate constant obtained from the model is likely to be the more accurate since it was calculated from a greater amount of data, although the discrepancy between the two values lies within the limits of experimental error.

8.1.6 Consequences of the Model

From Table 34, it can be seen that the reaction with the slowest rate was B $\longrightarrow$ E + F + G. However, the rate of production of E, F and G was not limited by this reaction since the rates of the B $\longrightarrow$ C and C $\longrightarrow$ E + F + G reactions were much faster, and it is evident that there was no one reaction step that entirely determined the rate of production of the final products.

The major reaction path appeared to be through the intermediates B and C, as suggested above, ie:

$$A \longrightarrow B \longrightarrow C \longrightarrow E + F + G$$

Here, the A $\longrightarrow$ B reaction was the slowest step, although the production of the final products directly from A proceeded at a similar rate.

The rate of disappearance of both B and C was faster than that of A, which is to be expected because of the relative chemical complexity of the latter. Thus the rate of the overall reaction was limited more by the rate of initial breakdown of coal material than by the rates of the subsequent reactions.

While A, B and C reacted at a faster rate than they were formed, the rate of production of D was five times faster than its rate of reaction, so that an accumulation of this species occurred in the reaction mixture. This would be undesirable in a commercial process, since D (the 250-300^{o}C fraction) is not as valuable as either E or F. However, D could be recycled as a coal solvent which would be advantageous as it would be relatively inert at the processing conditions employed. Alternatively, the fraction could be re-processed under more rigorous operating conditions using a more active catalyst to increase its rate of reaction.

8.1.7 Comparison of Predicted and Experimental Results

The model can be used to predict product yields from the hydrogenation of low rank coal extract solutions at any reaction time, given the initial composition of the feed. The predictions at time t and initial composition M_o were calculated using the solution to the differential equations:

$$M = M_o e^{kt} \quad \text{(matrix notation)}$$

A special computer programme was written to evaluate this, since it was not practicable to take the exponent of a seven by seven matrix by hand.

The observed and predicted yields of the various species are shown in Table 35 and compared graphically in Figures 25 and 26.

The fit of the experimental results with the model is good for components A, B, C, D and F with a maximum error of about 10%. However the experimental yields for components E and G were higher than predicted, the maximum errors being about 50% and 25% respectively. The former error is improved if E and F are taken together. The bulking of these two fractions may in fact be desirable because of the uncertainty of the 170°C cut-point, when atmospheric distillation finishes and vacuum distillation begins.

8.1.8 Application of the Model to other Reactor Systems

The rate of reaction will vary with the type of reactor system due to the different rate controlling regimes that are in operation. However, the reaction path should be similar in different reactors when the same type of feedstock is used.

This can be illustrated with reference to two types of reactor systems in operation at C.R.E. The first is a two litre autoclave where

the conditions were similar to those in this work, except that $\frac{1}{8}$" catalyst pellets were used and contained in a spinning basket attached to the stirrer. In this reactor system, unlike a slurry reactor, it was likely that mass transfer to the surface of the catalyst was one of the rate controlling factors because of the large particle size and the relative inaccessability of the catalyst in the centre of the bed. Thus, the reaction rate was lower than that in the one-litre autoclave. However, the yield v. time curves (shown in Figure 27 for the two-litre reactor) are similar in shape to those from the one-litre autoclave, except for the gas yields, with observable maxima in the yields of C and D. This indicates that a similar reaction path is followed in both reactors.

The second reactor system is a continuous trickle-bed reactor. Here, the main rate controlling mechanism was mass transfer to the catalyst surface because of the large catalyst particle size and lack of turbulence in the catalyst bed. Again the yield v. space time* curves (Figure 28) show a strong resemblance to those found in this work, except for the gas yields, with a maximum being observed in the production of C.

Figures 27 and 28 show that the gas yields were much lower than in the experiments performed in the one-litre autoclave. This was because since the feedstocks contained much less material boiling above 420°C, much less thermal cracking occurred (see section 8.1.1).

8.1.9 Limitations of the Model

The reaction scheme developed above is applicable for the catalytic hydrogenation of coal extract solutions not only in well-

*space time = $\frac{1}{\text{LHSV}}$, where LHSV = Liquid hourly space velocity

$= \frac{\text{liquid feedrate}}{\text{vol. of catalyst}}$

stirred tank reactors, but probably in other reactor systems also (see section 8.1.8). However, the rate constants associated with each individual step will only be applicable to the hydrogenation of low rank coal extract solutions at the specific conditions employed in this work.

Despite the good fit of the model, the calculated rate constants cannot be claimed to be accurate because of the large number of parameters (seventeen) involved in the fit and the relatively small amount of data. They will, however, be accurate to within an order of magnitude.

It is also apparent that the model is an empirical one, since it is based on the weights rather than the number of moles of reacting species. For B, C, D, E, F and G it would be possible to make a reasonably accurate estimate of the average molecular weight, based on the composition of each fraction (see section 8.1.3), and thus the number of moles in each fraction. However, molecular weight estimates for A are much more uncertain and since A breaks down to all the other fractions, a moles-based model would be very inaccurate.

There are several reactions which are not included in the model, namely:

$$B \longrightarrow D$$

$$E \longrightarrow F$$

$$E \longrightarrow G$$

$$F \longrightarrow G$$

There was no evidence to suggest any breakdown of E or F (as discussed in section 8.1.4), but it was possible that this and the $B \longrightarrow D$ reaction occurred at a low rate. In any event, an adequate fit to the data can be found without these reactions.

Nor were any reversible reactions included in the model, although evidence for one such reaction was found. In the hydrogenation of B it was found that a small, but significant amount of A was produced initially which suggested that the A $\longrightarrow$ B reaction was to some extent reversible, with B undergoing polymerization reactions to form A. Very small amounts of A were also produced in the hydrogenation of C, and probably originated from the small quantity of B which was present initially. It appeared that the effect was catalytic, since no B $\longrightarrow$ A reaction was evident in experiments performed in the absence of catalyst (see section 8.4.2). Again, an adequate fit of the model to the data can be found without the use of this or any other reversible reaction.

Heterogases (H_2O, NH_3, H_2S) were not included in the model since their yields were small and they were an undesirable product from a commercial viewpoint.

8.1.10 Hydrofining

It is desirable to remove oxygen, nitrogen and sulphur from coal during processing for two reasons. First, in the production of liquid fuels from coal, environmental considerations require low levels of heteroatom contamination. Second, in secondary refining processes, highly active catalysts are used which would be easily poisoned by the presence of heteroatoms - especially nitrogen and sulphur.

The removal of nitrogen as ammonia was found to be first order with respect to the amount of nitrogen remaining in the feed. This is in agreement with the work of Qader[146,148].

The rate constant calculated for denitrogenation was 10.3×10^{-3} min^{-1} for the experiments carried out at a reaction temperature of 450°C. This indicates that denitrogenation reactions proceeded at a faster

rate than the overall hydrogenation reaction, whose rate constant was 4.3×10^{-3} min^{-1} at the same temperature, and this was due to the fact that C-N bonds are more readily broken than are C-C bonds.

Although no kinetic data were derived for the removal of sulphur and oxygen in the hydrogenation of coal extract solution, some general trends are worthy of mention. Most of the sulphur in the feed was removed as hydrogen sulphide after only 1-2 hours, but the remaining 15-20% appeared to be difficult to eliminate. There are three forms of sulphur present in coal, organic chemical combinations, pyrites and sulphates. The former, according to Yergey[23], is removed at 300°C during hydrodesulphurization while the other forms are removed only at temperatures between 400 and 600°C. Thus the 15-20% sulphur which was difficult to eliminate in the hydrogenation of coal extract solution might have been present as pyrites and/or sulphates. The quantity involved would be about 0.1% w/w feed and this amount could pass through the filtration stage during the preparation of the extract as does a similar amount of ash. A higher temperature than that employed in these experiments would be required for complete sulphur removal.

No sulphur was detected in any of the product fractions which boiled below 420°C and it was assumed that residual sulphur remained in the fraction boiling above 420°C. This indicated that all the organic sulphur present had in fact been removed.

Less oxygen removal was accomplished than either nitrogen or sulphur, although this interpretation may be erroneous due to the presence of water dissolved or suspended in the hydrogenation product.

Initially (up to 2 hours reaction time), the rate of heteroatom removal decreased in the order S>N>O. During the later stages of the

reaction, however, when most of the sulphur had been removed, the rate of nitrogen removal was fastest and N>S>O. Qader[146,148] found that the rate of sulphur removal was consistently faster than that of nitrogen. His feedstock, however, was low temperature coal tar which contained very little nitrogen.

8.1.11 Composition of IBP-170°C Fraction

To achieve the maximum potential value of the naphtha (IBP-170°C) fraction as an aromatic feedstock, the naphthenic + aromatic (N+A) yield should be maximised and an increase in A yield relative to N is also desirable[189]. Most oil-derived commercial naphthas have an N+A content of 20-50%. In comparison, the product from hydrogenation of this coal extract solution had an N+A content of over 80%.

However, the N+A content did not increase significantly at longer reaction times. The ratio A:N did rise slightly with time either because of an increase in the amount of aromatic compounds or because of a decrease in naphthenics. The PNA analysis at the 450°C reaction temperature in Table 20 suggests that naphthenes may have broken down to paraffins while the aromatics remained approximately constant.

8.1.12 Catalyst Deactivation

Carbon deposition is undoubtedly a cause of catalyst deactivation as indicated, for example, in the work of Weisser[62], Kang[66] and McColgan[67].

Carbon deposition was found to increase only slightly with reaction time during the hydrogenation of coal extract solution, although over 9% deposition was found after zero reaction time. Thus catalyst deactivation by carbon deposition was thought to have occurred largely on contact with the extract solution before the hydrocracking reactions had begun.

Further evidence for this was provided by catalyst surface area measurements. There was a large drop in surface area when fresh catalyst was contacted with liquid coal extract solution, but only a small further decrease as hydrogenation proceeded, (see Table 22). This indicates that catalyst deactivation might also have been due to blocking of catalyst pores by the large molecules initially present in the reaction mixture. This is similar to Kovach's suggestion that deactivation can be attributed to the blocking of pores by, amongst other things, large porphyrin-type molecules[65].

The large molecules initially present in the feed are also the most susceptible to polymerization reactions which produce coke, and the B $\longrightarrow$ A reverse reaction mentioned in section 8.1.9 may be a factor in catalyst deactivation.

Catalyst deactivation was not taken into account in the rate expression derived in section 5.2.5 since its effect was to decrease the rate by only a small amount during the reaction. Also, this decrease was to a large extent cancelled out by a small increase in rate due to the apparent increase in catalyst loading with time. This occurred because of the decrease in volume of the reactor contents during each experiment.

8.2 Effect of Reaction Temperature on Hydrogenation of Coal Extract Solution

8.2.1 Hydrocarbon Product Yields

It can be seen that the general shape of the yield v. time curves shown in Figures 9-12 remained similar at different reaction temperatures. This indicates that the reaction network developed in the kinetic model at the 450°C reaction temperature (section 8.1.4) was probably unaffected by the reaction temperature.

The yields of material boiling below 300°C increased quite sharply with temperature but at the highest temperature (460°C) over 20% gaseous hydrocarbons were produced which were not a desired product for the production of liquid fuels and chemical feedstocks.

Even at the highest temperature, the rate of production of material boiling in the range IBP-250°C showed little sign of reaching a minimum value and this fraction and the gaseous products were considered to be the end products of the reaction under the conditions employed.

Due to there being insufficient data, it was not possible to fit rate constants to the yield data at different reaction temperatures in a similar way to that used in the development of the kinetic model at 450°C in section 8.1.5. However, a trial and error method was carried out as follows.

First the rates of the A $\longrightarrow$ products reactions at the different temperatures were determined directly from the experimental data using equation 5-12 (see Figure 14 and Table 19). Then the rates of the B $\longrightarrow$ products, C $\longrightarrow$ products and D $\longrightarrow$ products reactions at the different temperatures (k_T) were chosen by trial and error until the best fit of the predicted yields (obtained by the method described in section 8.1.7) to the experimental yields was obtained. The rates of reaction of A, B, C and D to the individual products were obtained from the corresponding rates in the 450°C model (see Table 34) changed by the ratio $\frac{k_T}{k_{450}}$, where k_{450} is the rate of reaction of A, B, C or D to all products at 450°C.

The estimated rate constants for all seventeen reactions involved in the model at the three reaction temperatures are shown in Table 36.

The method described above produced fits which were reasonable and the observed and predicted yields of the various species are shown in Tables 37, 38 and 39 for the three reaction temperatures. The error between the observed and predicted yields was generally less than 20%, except for the gas yields at the 460°C reaction temperature, which consistently showed a larger error. Thus more gas was produced during the reaction than was predicted by the model.

8.2.2 Apparent Activation Energy

Essentially, the true activation energy is the energy that must be acquired by the reacting molecules in order to reach their activated state. Clearly, in a complex system, the influence of temperature on the rate of reaction must include many factors so that the activation energy is a composite quantity, known as the apparent activation energy, E_a. Factors which were temperature-dependent in the system studied included hydrogen solubility, internal and external mass transfer, adsorption and desorption, and the surface reaction (which gives rise to the true activation energy). If any one of these factors were to control the overall rate of reaction, its temperature dependence would greatly influence the magnitude of the apparent activation energy.

In general, the rates of chemical processes show a much higher temperature dependence that the rates of physical processes. For example, mass transfer is a function of $\sqrt{T}$ while chemical reaction is a function of $e^{-1/T}$.

8.2.3 Apparent Activation Energy for A $\longrightarrow$ products Reaction

A high apparent activation energy for the overall reaction in the hydrogenation of coal extract solution (A $\longrightarrow$ products) was expected since a value of 30.3 kcal $mole^{-1}$ was obtained from the preliminary

experiments (section 6.3.3). The value calculated from the subsequent experiments was 26.1 kcal $mole^{-1}$. The difference in the two values occurred because the first value was calculated from the yields of A at two reaction temperatures, while the second was calculated from the rate constants at four different temperatures. The second value was therefore much more reliable because of the larger amount of data used to calculate the result.

The relatively high apparent activation energy rules out the possibility of any significant diffusional control on the rate of the overall reaction and indicates that the latter may have been limited by the rate of the surface reaction.

However, hydrogen solubility has been found to be quite strongly temperature dependent, the solubility increasing with temperature [38,39,42,43]. Han[156] has quoted an activation energy of 29.5 kcal $mole^{-1}$ for the absorption of hydrogen in coal derived solvent in a batch autoclave at 450-465°C. Thus hydrogen solubility could also be a rate-limiting process.

High activation energies have also been quoted in the literature for coal hydrogenation. Some of these may be misleading since different systems are likely to give rise to different rate controlling mechanisms. Both the rate controlling mechanism and the type of catalyst used have a profound effect on the apparent activation energy. However, most of the values quoted are relatively high, for example 35.0 kcal $mole^{-1}$ was obtained for the hydrogenation of a tetralin coal extract[128] and 35.8 kcal $mole^{-1}$ for the hydrogenation of asphaltene[124] obtained from coal.

From the high activation energy, it appears that a high temperature would be required for the coal hydrogenation process. However, as

mentioned in section 8.2.1, temperatures higher than about 450°C result in excessive gas production which is commercially undesirable. A reaction temperature of 450°C, therefore, would appear to be an acceptable compromise.

8.2.4 Temperature Dependence of Rate Constants of B, C and D ⟶ products Reactions

The rate constants for the overall reactions

B ⟶ products

C ⟶ products

and D ⟶ products

at three reaction temperatures (420,440,460°C) have been estimated (see section 8.2.1) and the corresponding rate constants at 450°C calculated (see section 8.1.5). Thus, it is now possible to draw up Arrhenius plots for the three species, and these are shown in Figure 29 along with the plot for species A as a comparison.

While species A showed an Arrhenius temperature dependence, as discussed in section 8.2.3, the plots for the other species curved upwards at high temperatures. This curvature could have been due to the occurrence of two processes of widely different activation energy. If the two processes occurred in series, the observed rate would have been that of the slower rate at a particular temperature and the Arrhenius plot would have curved downwards. If the two processes were competing in parallel, however, the faster rate would have been the one observed and this would have led to an upward curvature of the Arrhenius plot.

There were several parallel processes which may have been in operation during the overall reaction. First, there were the reactions in the liquid and vapour phases. Obviously the amount of material present in the vapour phase increased with temperature, but was probably small at the high pressures employed. It is also uncertain

whether the reaction in the vapour phase would have proceeded at a faster rate than in the liquid phase.

The second pair of processes was the homogeneous (non-catalytic) and heterogeneous reactions. Clearly, the homogeneous reaction played a significant role in the overall reaction since quite large conversions were obtained in the absence of catalyst at a temperature of 450°C (see Table 26). Since the activation energy for the homogeneous path would have been higher than for the heterogeneous route, then the rate of the former may have been the larger at high temperatures.

The other explanation of the anti-Arrhenius behaviour lies in the rates of the hydrocracking and hydrogen addition reactions. At low temperatures, these two reactions occurred in series, but at high temperatures it is thought that hydrocracking could have proceeded without prior hydrogen addition so that the two reactions competed in parallel. Thermodynamic considerations indicate that less hydrogen addition occurred as the temperature was raised[190] (see section 8.2.6) and hydrocracking may have had a higher activation energy than hydrogen addition. Thus an upward curvature of the Arrhenius plot would be observed. Increased hydrocracking at high temperatures is in fact indicated by the large experimental gas yields obtained, which were greater than those predicted by the model.

It has also been found that the hydrocracking of species A has a lower activation energy than for the hydrocracking of lower-boiling species[188] which may explain why a true Arrhenius dependence was obtained for species A.

8.2.5 Hydrofining

The removal of oxygen, nitrogen and sulphur from the feed increased with reaction temperature. Nitrogen removal showed an Arrhenius

temperature dependence and the apparent activation energy was calculated as 15.0 kcal $mole^{-1}$. This indicates that the removal of nitrogen was easier than the overall hydrogenation reaction and this was due to the fact that C-N bonds are weaker than C-C bonds and are broken at lower temperatures.

The value of E_a for denitrogenation is in agreement with those found in the literature, which generally were in the range 10-20 kcal $mole^{-1}$.(117,148,150,159)

8.2.6 Composition of IBP-170°C Fraction

Little change in the yield of naphthenics + aromatics (N+A) with reaction temperature occurred in the IBP-170°C fraction, but the N+A yield was over 80% at all temperatures studied.

There was, however, quite a large increase in the ratio of aromatic to naphthenic compounds with temperature. This can be explained from the standpoint of thermodynamics. The following reactions can be taken as examples of typical hydrogen addition and hydrocracking processes respectively occurring during the hydrogenation of coal extract solution:

$$C_6H_6 + 3H_2 \rightleftharpoons C_6H_{12}$$

benzene cyclohexane

$$C_{10}H_8 + 4H_2 \rightleftharpoons C_6H_6 + C_4H_{10}$$

naphthalene benzene butane

Sweeney(190) gives thermodynamic data for these reactions and this shows that an increase in temperature pushes the equilibria to the left. In the hydrocracking reaction, the hydrocracked products predominate to such an extent under the conditions employed that the equilibrium shift due to temperature increase is negligible. (The equilibrium constants at 200 bar, and 410 and 460°C are about 10^8 and 10^7 respectively).

In the hydrogen addition reaction, however, the respective equilibrium constants are only about 500 and 70 so that although the naphthenic product predominates, the increase in the A:N ratio with temperature is significant.

8.2.7 Deposition of Carbon on the Catalyst

No significant change in the amount of carbon deposited on the catalyst with temperature was detected. However, since the average deposition amounted to about 10%, this must have been deposited at temperatures lower than 420°C. Polymerization reactions probably accounted for most of the carbon deposition. Although these reactions are thermodynamically favourable at higher temperatures, they are likely to occur to an appreciable extent only at lower temperatures when hydrocracking reaction rates are slow.

8.3 Effect of Pressure on Hydrogenation of Coal Extract Solution

8.3.1 Hydrocarbon Product Yields

It was found that an increase in hydrogen partial pressure invariably resulted in an increase in conversion. This was expected because of the solubility of hydrogen in coal extract solution, which increased with pressure.

The product distribution was similar at all pressures except the highest, when the gaseous hydrocarbons yield was higher than expected. This indicates that the reactions were proceeding by the same mechanism except at high pressure, when a greater degree of hydrocracking, especially of the 300-355°C fraction, occurred. Increased gas production at high pressures has also been observed by various authors in the literature, especially Mima[163], and in the preliminary experiments (section 6.3.4).

A small decrease in conversion occurred when the partial pressure of inert gas was raised at constant hydrogen partial pressure. This indicated that there was some competition between hydrogen and the inert gas (nitrogen) in one or more of the reaction steps. The solubility of nitrogen in the reactants was lower than that of hydrogen, but was significant at higher nitrogen partial pressures. Under these conditions, there may have been competition for solution with a lowering of the amount of hydrogen dissolved and thus a drop in the rate of reaction. Alternatively, since the rate of adsorption on to the catalyst surface is proportional to the pressure of the adsorbing species (section 5.2.3), increased adsorption of nitrogen occurred at higher nitrogen partial pressures resulting in a reduction in the amount of hydrogen adsorbed and thus a reduction in reaction rate.

Although both the above effects may have occurred, it is probable that the former was mainly responsible for the decrease in conversion since hydrogen solubility was more likely to be a rate limiting factor than adsorption (see section 8.4.1). Hoog[165] also observed a small reduction in conversion with increased inert gas partial pressure, although he attributed this to competition for adsorption rather than for solution.

This result is important in processes where the product gas stream is recycled causing a drop in hydrogen partial pressure. Restoring the original hydrogen partial pressure by increasing the total pressure would not restore the original conversion because of the effect of the inert gas. To recover the original conversion, a further increase in total pressure would be required. However, if the hydrogen partial pressure were to drop below about 75% the

required total pressure to retain the original conversion would be beyond the design specification of most commercial plants.

The formation of ammonia from the hydrogen-nitrogen mixtures used in these experiments was considered a possibility. The conditions of temperature and pressure were favourable and it was thought that cobalt-molybdenum might catalyse the reaction to some extent. However due to the comparatively low solubility of nitrogen in the reactants, little reaction was thought possible either in the liquid phase (except at high nitrogen partial pressures), or in the gaseous phase, where contact with the catalyst was poor. Any ammonia that was formed did not appear to affect the rate of the hydrogenation reaction since an experiment using argon as the inert gas produced no significant difference in the product yields.

8.3.2 Estimation of Hydrogen Solubility

Henry's Law constant was calculated as 564 bar, although this was an average value over a range of pressure. Thus Henry's Law could not be tested using the results obtained in these experiments. However, it has been reported[49,50,51] that the Law is obeyed over a wide range of pressure.

The calculated hydrogen solubility, 24 cm^3/ g reactant (i.e. the reactor contents - generally boiling >300°C) at 210 bar, was of the right order of magnitude. Prather[43] obtained a value of 31.4 cm^3/g for the solubility of hydrogen in creosote oil (which has a similar composition to anthracene oil) under similar conditions while Rapoport[41] quoted a value of 10.5 cm^3/g in the product from coal hydrogenation. From other experiments carried out at C.R.E., it was estimated that at 450°C and 210 bar the solubility of hydrogen in anthracene oil and in coal extract solution was about 30 cm^3/g and 15 cm^3/g respectively.

Although the value of hydrogen solubility calculated in these experiments was in general agreement with other work, it can only be taken as an order of magnitude value because of the assumptions made in the calculations. These were as follows: (1) Henry's Law was obeyed at the conditions employed, (2) the molecular weight of the liquid reactor contents remained constant throughout each experiment. Although the average molecular weight of E83 coal extract solution was estimated at 710, the average molecular of the reactor contents after experiments at different conditions was found to be in the range 340 to 500. Thus, it was thought that after an initial decrease in molecular weight, the value remained approximately constant throughout an experiment.

However, other determinations of hydrogen solubility are subject to errors due to uncertainties in the measurement of vapour pressures, sample weights and dissolved gas volumes.

A knowledge of hydrogen solubility is important for design purposes and it also gives a value to one of the constants, $[H]$, incorporated in the overall rate constant (see sections 5.2.4 and 5.2.5).

8.3.3 Hydrofining

In experiments carried out at 85 bar and 337 bar hydrogen pressure, the calculated yield of ammonia doubled while that of hydrogen sulphide trebled. Thus a higher pressure favoured the removal of nitrogen and sulphur from the feed due to increased hydrocracking. Both Wilson[150] and Janardanarao[130] found that the removal of nitrogen and sulphur was proportional to the hydrogen partial pressure.

8.3.4 Composition of IBP-170°C Fraction

In Section 8.3.1 it was observed that the product distribution

with respect to the different fractions remained virtually unchanged with increased pressure. The change in chemical composition within the IBP-170°C fraction, however, was very striking. Large amounts of aromatic compounds were present in the fraction after experiments at lower pressures, while at high pressures, naphthenic compounds predominated. This can be explained by considering again the model hydrogen addition and hydrocracking reactions used in Section 8.2.6:

$$C_6H_6 + 3H_2 \rightleftharpoons C_6H_{12}$$

benzene — cyclohexane

$$C_{10}H_8 + 4H_2 \rightleftharpoons C_6H_6 + C_4H_{10}$$

naphthalene — benzene + butane

It can be seen that an increase in hydrogen pressure pushes the equilibrium to the right favouring the naphthenic and also paraffinic products (although the equilibrium is already far to the right in the case of the hydrocracking reaction). Low pressures, however, favour the production of aromatics.

Thus it would be possible to obtain the required product by a suitable choice of hydrogen pressure. For example, for aromatics production, a low pressure would be desirable but if the requirement were a feedstock for ethylene production, a high pressure would be needed favouring the paraffinic and naphthenic products.

8.4 Effect of Catalyst Loading on Hydrogenation of Coal Extract Solution

8.4.1 Effect on the Overall Rate of Reaction

These results appeared to be a little more scattered than for other series of experiments and this was possibly due to the existence of a "memory" effect where catalyst from the previous experiment was adsorbed on to the autoclave wall. This effect has also been observed by Guin[56] and Sherwood[171].

As the catalyst loading increased, the yields of all the individual fractions boiling below 350°C increased in roughly the same proportion. The rate of increase, however, varied drastically with the amount of catalyst present.

From Figure 19 it can be seen that at low catalyst loadings (less than about 1% w/w feed), the rate of the overall reaction was very strongly dependent upon the loading. This is in agreement with the work of Schlesinger[166].

In equation 5-11 (section 5.2.5), if the external surface area of the catalyst particles, a_c, (which is proportional to the catalyst loading) is small then the $a_c k_c k_s$ term can be considered negligible in comparison to either $a_g k_l k_s$ or $a_g k_l k_c$ and the equation reduces to:

$$r = \frac{a_c k_c k_s [H] [A]}{k_s + k_c}$$

Thus, as found experimentally, the rate is dependent upon a_c and the possible rate controlling mechanisms are adsorption (k_a) and desorption (k_d) (which also depend on a_c), reaction on the catalyst surface (k_s) and mass transfer to the external surface of the catalyst particles (k_c). The latter is likely to be quite rapid due to agitation producing quite a high relative velocity between the particles and the liquid. Calderbank[191] has found that the effect of agitation is pronounced for particles of 210 μm or larger and the average particle size used in these experiments (173 μm) was not much smaller than this. Adsorption and desorption were also thought to be rapid due to the high pressures employed. Thus at low catalyst loadings, the rate of the overall reaction was probably controlled by the rate of the surface reaction, i.e. there was little physical resistance to the rate at low catalyst loadings.

As the catalyst loading was raised beyond 1%, however, the rate was found to be progressively less dependent on the loading and under these conditions there was competition between catalyst particles for reactant. Other authors[41,125,157,167] have also observed this effect.

When the catalyst loading (and thus a_c) becomes very large, the $a_g k_l k_s$ and $a_g k_l k_c$ terms in equation 5-11 can be considered negligible in comparison to $a_c k_c k_s$ and

$$r = a_g k_l [H][A]$$

Under these conditions, the rate is independent of a_c and the rate controlling mechanism is the mass transfer of hydrogen from the bubble interface into the bulk liquid (k_l). This situation was approached experimentally but not achieved at the conditions employed, since even at 25% loading the rate was still increasing.

Thus, in the region of 15-25% catalyst loading (which was the amount of catalyst used in most of the experiments in this work) it is considered that all the terms in equation 5-11 may have been important, although k_a, k_d, k_c (as discussed above) and k_g (as discussed in section 5.2.4) were quite large. Thus, in this range of catalyst loading the rate of the surface reaction and the rate of mass transfer of hydrogen in to the bulk liquid (i.e. the rate of dissolution of hydrogen) predominantly determined the rate of the overall reaction.

Since both the rate of the surface reaction and the rate of mass transfer of hydrogen are highly temperature dependent and also control the rate of the overall reaction to an appreciable extent, the apparent activation energy for the overall reaction could be expected to be high. This was in fact the case, as discussed in section 8.2.3.

8.4.2 Effect of Alumina on the Rate of Reaction

The cobalt-molybdenum catalyst used in all the kinetics experiments was supported by γ-alumina. In experiments using γ-alumina alone, it was observed that lower conversions were obtained than in the absence of any added catalyst material. This effect was probably due to the catalysis of the B ⟶ A (polymerization) reaction by alumina, which tended to lower the overall conversion, since greater yields of A and smaller yields of B were obtained in these experiments. In the secondary hydrogenation of B, no A appeared to be produced in the absence of catalyst (see Table 30), but as the (cobalt-molybdenum) catalyst loading was raised, the yield of A remained virtually constant indicating the possibility of an equilibrium between A and B.

The effect has also been observed in other work, notably that by Newman[168], Horton[169] and Bertolacini[170] but no explanation was offered.

It is thought that the B ⟶ A reaction observed in the experiments using cobalt-molybdenum catalyst (see section 8.1.9) may have been entirely due to the presence of the alumina support.

8.4.3 Hydrofining

The effect of catalyst loading on the removal of oxygen, nitrogen and sulphur was similar to the effect on the yields of hydrocarbon products. This suggested that the heterocyclic compounds present in the coal extract solution were subject to the same rate controlling mechanisms as those encountered in the hydrogenation of the poly-aromatic material.

8.4.4 Composition of IBP-170°C Fraction

Thermal hydrogenation of coal extract solution (in the presence of alumina) produced a more aromatic product than catalytic hydrogenation

but although this may be desirable commercially, the product yields obtained in the absence of catalyst were low.

Relatively, the amount of catalyst present above 1% did not significantly affect the aromaticity of the product.

8.5 Effect of Initial Concentration of Coal Extract Solution on Hydrogenation

8.5.1 Hydrocarbon Product Yields

An attempt was made to predict product yields for the hydrogenation of mixtures of coal extract solution and anthracene oil from the yields obtained from the hydrogenation of the individual components. The predictions are compared to the actual product yields in Table 40. However, the predictions are not good and the explanation for this lies in the different solubility of hydrogen in the two components.

Hydrogen is more soluble in anthracene oil than in coal extract solution. When a mixture of the components is hydrogenated, the rate of hydrogenation of the extract portion is increased while that of the oil portion is decreased relative to the rates of hydrogenation of the pure components. Basically, the reacting species in the mixture are A and some B for the extract portion and B and C for the oil portion. Thus, at low extract concentrations, less A, slightly more B and more C would be expected in the product compared to the predicted yields. At high extract concentrations, slightly less A and more B and C would be expected compared to the prediction. Table 40 shows that this is, in fact, the case.

The effect of hydrogen solubility on the rate of hydrogenation of these mixtures is further illustrated by the graph of lnA versus $\ln A_o$ (Figure 20). This is a straight line as expected from rearrangement

of equation 5-12 into the form:

$$\ln A = \ln A_o - k_1 t$$

However, the slope of the line expected from this equation is 1.00, but the experimental value was 1.19. Greater departure of the experimental from the calculated line occurred at lower initial coal extract solution concentrations, and it was thought that this was due to increased hydrogen solubility.

It has been estimated that at 450°C and 210 bar, the solubility of hydrogen in anthracene oil and in coal extract solution is 30 cm^3/g and 15 cm^3/g, (see section 8.3.2) and Derbyshire[192] has found by experiment that the values at about 280°C and 140 bar were about 10.2 cm^3/g and 5.5 cm^3/g respectively. Thus the solubility of hydrogen in anthracene oil is approximately twice that in coal extract solution.

Using this relationship, the plot of $\ln A$ versus $\ln A_o$ can be corrected (see equation 5-13) to take into account the increased hydrogen solubility in the experiments at reduced initial coal extract solution concentrations and the corrected line is also shown in Figure 20. This has a slope of 0.97 which is insignificantly different from the expected slope of 1.00. This confirms that the different solubility of hydrogen in oil and extract solution was responsible for the discrepancy between experimental and predicted product yields.

8.5.2 Hydrofining

Taking into account the elemental composition of each feed, the removal of oxygen, nitrogen and sulphur was relatively unaffected by the initial concentration of coal extract solution, although the calculated ammonia yield appeared to decrease slightly as the extract solution concentration was raised. These results indicate that the

rates of removal of heteroatoms from anthracene oil and coal extract solution were similar, and probably occurred by the same mechanisms.

8.6 Secondary Hydrogenation of Product Distillation Fractions

The secondary hydrogenations of the 355-420°C and 300-355°C product fractions have been discussed in relation to the kinetic model and the effect of catalyst loading on the hydrogenation of coal extract solution in Sections 8.1 and 8.4 respectively.

8.7 Hydrogen Consumption

The conversion to material boiling below 420°C was found to be dependent on the amount of hydrogen consumed. However, although the results showed a fair degree of scatter (see Figures 23 and 24), there appeared to be a difference in the behaviour of the two extract solutions studied.

For the high rank coal extract solution, a positive conversion was apparently obtained with zero hydrogen consumption. This was possibly due to the greater hydrogen-donating ability of the solvent used to prepare this extract solution. This solvent had a greater hydrogen to carbon atomic ratio than that of the solvent used to prepare the low rank extract solution (see Table 3).

For the low rank coal extract solution, however, hydrogen was consumed before any conversion was achieved and it was probable that, since low rank coal molecules are thought to be larger than those of high rank coal, some breakdown of the low rank coal molecules occurred yielding products whose boiling points remained above 420°C. This would not produce a change in the conversion as defined in section 5.1.4. A similar effect has been observed by Ruether[167].

8.8 Mass Balances

Mass balances of 100% were rarely achieved in any of the experiments, but the average was about 96%. Sources of material loss during each experiment were:

(1) On reactor walls.

(2) In pipelines.

(3) Entrainment of liquid into the gas stream during depressurization.

(4) Vapourization of the hot reactor contents on removal of autoclave head.

(5) Evaporation of the condensate during sampling.

(6) Leaks.

These losses were minimized and amounted to no more than 2% w/w feed.

The calculation of hydrocarbon gas yield also may have contributed to the reduced mass balances, since the analysis could only detect C_1-C_4 hydrocarbons. It is likely that C_5+ hydrocarbons were also present in the gas stream, since these compounds were detected in the analysis of the IBP-170^{o}C liquid fraction. However, lower mass balances were not observed at higher reaction temperatures when increased yields of gaseous hydrocarbons occurred.

No correlation was found between the mass balance and any of the process parameters in the experiments involving the hydrogenation of coal extract solution. It might be expected, however, that losses due to (5) and (6) above would increase with reaction time. Such a trend was not observed because of the randomness of the other losses, except in the secondary hydrogenation experiments. Here, because yield data was calculated from samples taken from the autoclave, losses from (1), (2) and (4) were eliminated and the mass balances were observed to decrease with time.

8.9 Reproducibility

In general, yields could be reproduced to within about 10% in repeated experiments. This was not as good as the reproducibility obtained in the preliminary experiments (Chapter 6). The reason for this was because, in the latter, the boiling range of the distillation cuts was wider and therefore there was more material present in each cut. This resulted in a reduction in the error associated with the determination of the yields.

The yields of the IBP-170°C and 170-250°C fractions, however, were difficult to reproduce to within 10%. This was probably due to two factors. First, the IBP-170°C fraction was very volatile and material may have been lost due to evaporation during condensate collection and analysis. Second, when fractional distillation was used to analyse the product, the IBP-170°C fraction was distilled at atmospheric pressure, while all other fractions were distilled under vacuum. Thus the changeover from atmospheric pressure to vacuum distillation may have resulted in an overlap of the IBP-170°C and 170-250°C fractions due to the uncertainties inherent in conversion chart used for vacuum distillation (see section 4.4.4).

Table 33 shows that the reproducibility of the IBP-250°C fraction yield was generally much better than that of the yields of the two fractions taken separately.

The main factors which had an adverse effect on reproducibility were heating rate and reaction temperature. The heating time varied due to the relatively insensitive power control of the autoclave furnace and also due to variations in the ambient temperature. Although the reactor contents temperature controller was good, only a small

change in temperature in the region of 450°C was needed to produce a significant change in reaction rate, as shown by the high apparent activation energy for the overall reaction (see section 8.2.3).

CHAPTER 9

CONCLUSIONS

The following conclusions have been drawn from a study of the chemical kinetics of the catalytic hydrogenation of coal extract solutions.

(1) The kinetics could be adequately described in terms of a series of distillation fractions of different boiling range. The most suitable boiling ranges were:

<IBP (initial boiling point)	(G)
IBP-170°C	(F)
170-250°C	(E)
250-300°C	(D)
300-355°C	(C)
355-420°C	(B)
>420°C	(A)

(2) Experiments could generally be reproduced to within 10%, or better, especially if fractions (E) and (F) were treated as a single fraction.

(3) The overall reaction was found to be first order with respect to (A) remaining and the rate constant at the conditions of 450°C, 210 bar and 25% catalyst loading was 4.3×10^{-3} min^{-1}. However, this was a composite value which included the effects of mass transfer, chemical reaction, catalyst surface area and the concentration of hydrogen in solution.

Heteroatom removal was also thought to be first order, but with a higher rate constant than the overall reaction. For example, the rate constant for nitrogen removal was 10.3×10^{-3} min^{-1} at the same conditions.

(4) The slowest steps of the overall reaction were the chemical reaction on the surface of the catalyst and the dissolution of hydrogen in the reactants, both of which proceeded at a similar rate under the conditions employed.

(5) The following scheme was proposed to describe the chemical reactions involved in the hydrogenation of low rank coal extract solution:

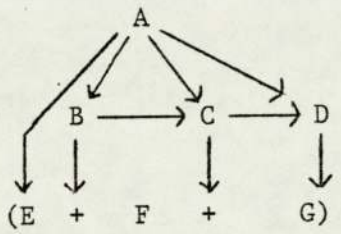

The scheme was thought to be similar at all the reaction temperatures studied and also in different types of reactor systems.

(6) Using this reaction scheme, mathematical models were developed so that the yields of products at each reaction temperature could be predicted. These predictions agreed quite well with the experimental results. From the calculated rate constants, the major reaction path was found to be:

$$A \longrightarrow B \longrightarrow C \longrightarrow (E + F + G)$$

(7) The rate of the overall reaction was found to be quite strongly temperature dependent and the apparent activation energy for low rank coal extract solution was 26.1 kcal $mole^{-1}$ in the range 420-460^{o}C at 210 bar and 25% catalyst loading.

The calculated rate constants (from the models) for the reactions of B, C and D to all products did not follow an Arrhenius temperature dependence, the rates being higher than expected at high temperatures. This was thought to be due to the occurrence of two processes competing in parallel with different activation energies.

The rate of removal of heteroatoms from the feed was less temperature dependent than the rate of the overall reaction; for example, the apparent activation energy for denitrogenation was 15.0 kcal $mole^{-1}$ at the same conditions.

(8) The rate of reaction of high rank coal extract solution increased with hydrogen pressure, but the addition of inert gas at constant hydrogen partial pressure produced a slight decrease in conversion. From the pressure experiments, the solubility of hydrogen was found to be about 24 cm^3/g reactant.

(9) The reaction rate was very strongly dependent upon the catalyst loading up to about 1% w/w feed, but was increasingly less dependent as the loading was raised further due to mass transfer limitations. Alumina was found to have an adverse effect on the overall rate.

(10) The rate of reaction increased with dilution of coal extract solutions with anthracene oil due to increased hydrogen solubility in the mixture. More gaseous hydrocarbons were produced during the hydrogenation of more concentrated coal extract solutions due to increased thermal cracking of the coal material.

(11) Heteroatom removal increased with pressure and temperature, but neither catalyst loadings above 1% nor the coal content of extract solutions had any significant effect.

(12) The aromatics/naphthenics ratio in the IBP-170^{o}C product fraction increased with temperature and the aromatics content increased at low pressures, while a high pressure favoured the production of naphthenic and paraffinic material.

(13) It was thought that catalyst deactivation by carbon deposition occurred on contact with liquid coal extract solution, with little further deactivation taking place during the reaction.

TABLE 1

RECOMMENDED STIRRER AND BAFFLE PARAMETERS FROM GLASS-MODEL INVESTIGATIONS[179]

Stirrer type	Disc and vane
Stirrer diameter	$1\frac{1}{2}$"
Stirrer position	$<1\frac{1}{2}$" above bottom of autoclave.
Stirrer speed	$\geq$750 r.p.m.
Baffle number	2
Baffle width	$\frac{1}{2}$"
Baffle position	Lower edge $<1\frac{1}{2}$" above bottom of autoclave.

TABLE 2

EXPERIMENTAL ERROR

Measurement/analysis	Component	% error
PRECISION		
Temperature	Thermocouple	0.5 @ 450°C
	Controller	1 @ 450°C
	Recorder	2 f.s.
Pressure	Controller	0.3 f.s.
	Indicator	3 @ 200 bar
Stirrer speed	Indicator	2 f.s.
Gas flowrate	Indicator	2 f.s.
G.L.C. analysis	Detector	1
	Integrator	1
	Calibration	2
Fractional dist-illation analysis	Temp. indicator	1 f.s.
	Pres. indicator	1 f.s.
	Column efficiency	1
	Calibration	6
REPRODUCIBILITY		
G.L.C. analysis		2
Distillation + GLC anal.		3
Fractional dist. analysis		5
Elemental analysis: C		0.5
H		0.2
O		0.3
N		0.1
S		0.1

f.s. : full-scale.

TABLE 3

ANALYSIS OF FEED MATERIALS

	Coal Extract Solution		Anthacene Oil EP51D	Anthacene Oil EP20D1	Nominal 355-420°C Product fraction		Nominal 300-355°C Product fraction	
	EP52FD10	E83			A	B	A	B
Softening point (°C)	185	235	N.A.	N.A.	N.A.	N.A.	N.A.	N.A.
Volatile matter (% w/w feed)	55.6	45.9	100.0	100.0	100.0	100.0	100.0	100.0
Ash (% w/w feed)	0.2	0.3	NIL	Nil	Nil	Nil	Nil	Nil
Carbon (% w/w d.a.f. feed)	89.3	90.7	90.4	89.7	90.9	91.4	89.4	90.6
Hydrogen (% w/w d.a.f. feed)	5.0	4.9	5.5	5.8	7.8	7.0	8.9	8.3
Oxygen (% w/w d.a.f. feed)	3.1	2.1	2.1	2.5	0.7	1.0	1.1	0.4
Nitrogen (% w/w d.a.f. feed)	2.0	1.5	1.1	1.1	0.6	0.5	0.6	0.5
Sulphur (% w/w d.a.f. feed)	0.6	0.8	0.9	0.9	<0.1	<0.1	<0.1	<0.1
Material boiling: (% w/w d.a.f. feed)								
IBP-170°C	Nil	Nil	Nil	0.3	Nil	Nil	Nil	0.4
170-250°C	Nil	Nil	5.6	14.3	0.1	Nil	0.6	Nil
250-300°C	Nil	Nil	7.3	11.5	0.3	Nil	3.0	0.3
300-355°C	Nil	Nil	38.5	36.4	10.0	1.3	79.6	72.5
355-420°C	12.8	15.2	34.5	33.2	75.7	78.3	16.7	26.7
>420°C	87.2	84.8	14.1	4.3	13.9	20.4	0.1	0.1
Average molecular weight	650	710	200	180	-	-	-	-

A - obtained from 1 l. autoclave

B - obtained from continuous plant

N.A. - not applicable

TABLE 4

CALCULATED BOILING RANGES AND ELEMENTAL COMPOSITIONS OF MIXTURES OF COAL EXTRACT SOLUTION AND ANTHRACENE OIL

% EP52FD10 Coal Extract Solution		0	20	40	60	80	100
% EP51D Anthracene Oil		100	80	60	40	20	0
IPB-170°C	% w/w total feed	Nil	Nil	Nil	Nil	Nil	Nil
170-250°C		5.6	4.5	3.4	2.3	1.1	Nil
250-300°C		7.3	5.8	4.4	2.9	1.5	Nil
300-355°C		38.5	30.8	23.0	15.5	7.9	Nil
355-420°C		34.5	30.2	25.8	21.5	17.2	12.8
>420 (residue)		14.1	28.7	43.4	57.8	72.3	87.2
Oxygen		2.1	2.3	2.5	2.7	2.9	3.1
Nitrogen		1.1	1.3	1.5	1.6	1.8	2.0
Sulphur		0.9	0.8	0.8	0.7	0.7	0.6

TABLE 5

DATA FOR HARSHAW 0402T CATALYST ($\frac{1}{8}$" PELLETS)

Cobalt oxide content (% w/w)	3
Molybdenum oxide content (% w/w)	9
Bulk density (kg m^{-3})	960
Pore volume (cm^3 g^{-1})	0.4
Surface area (m^2 kg^{-1})	0.16
Strength (kg)	11

TABLE 6

AVERAGE PARTICLE SIZE DISTRIBUTION OF GROUND CATALYST

Particle diameter range (micron)	B.S. Mesh size range	Average % w/w
>500	>32	5
500-355	32-42	6
355-212	42-72	8
212-150	72-100	15
150- 90	100-170	52
90- 63	170-250	10
<63	<250	4

TABLE 7

PRODUCT YIELDS AND H/C RATIOS FROM REPRODUCIBILITY EXPERIMENTS

		Run J18	Run J19	Run J23	Run J24	Mean	Standard deviation
H_2 flow time (min.)		262	241	253	252	252	9
Gaseous C_1-C_4 hydrocarbons	% w/w feed	9.9	9.0	9.1	9.5	9.4	0.4
Liquids boiling <200°C	% w/w feed	9.7	8.9	9.5	9.2	9.4	0.4
Liquids boiling 200-420°C	% w/w feed	27.4	25.9	27.0	25.7	26.5	0.8
Residue boiling >420°C	% w/w feed	44.2	46.5	46.1	46.2	45.8	1.0
% Conversion		47.9	45.2	45.6	45.5	46.1	1.2
H/C atomic ratio in condensate		1.31	1.31	1.32	1.32	1.32	0.01
H/C atomic ratio in reactor contents		0.87	0.86	0.91	0.94	0.90	0.04

TABLE 8

PRODUCT YIELDS AND H/C RATIOS FROM PRELIMINARY REACTION TIME EXPERIMENTS

Run number		J25	J26	J30	J31
Reaction time (hr.)		0	1	2	3
Hydrogen flow time (min.)	% w/w feed	139	200	259	322
Gaseous C_1 - C_4 hydrocarbons		0.4	5.4	10.9	14.3
Liquids boiling $<200^{o}C$		0.2	3.5	9.9	10.5
Liquids boiling $200-350^{o}C$		13.2	23.3	30.8	41.1
Residue boiling $>350^{o}C$		84.5	57.4	45.2	29.3
H/C Atomic ratio in condensate		1.17	1.30	1.32	1.35
H/C Atomic ratio in reactor contents		0.78	0.87	0.91	0.84

TABLE 9

PRODUCT YIELDS FROM PRELIMINARY REACTION TEMPERATURE EXPERIMENTS

Run number		J34	J32
Reaction temperature (^{o}C)		430	450
Gaseous C_1 - C_4 Hydrocarbons	% w/w feed	4.2	11.4
Liquids:			
IBP-$150^{o}C$		2.0	3.5
$150-235^{o}C$		3.5	6.0
$235-300^{o}C$		7.5	10.4
$300-350^{o}C$		11.0	13.4
Residue b. $>350^{o}C$		65.1	51.3
Total liquid + gas		93.3	96.0

TABLE 10

PRODUCT YIELDS FROM PRELIMINARY PRESSURE EXPERIMENTS

Experiment		Mean from Table 7	J21
Pressure (bar)		210	240
Gaseous C_1-C_4 hydrocarbons	% w/w feed	9.4	11.1
Liquids boiling <200°C	% w/w feed	9.4	10.5
Liquids boiling 200-420°C	% w/w feed	26.5	26.0
Residue boiling >420°C	% w/w feed	45.8	43.5
% conversion		46.1	48.7

TABLE 11

PRODUCT YIELDS AND H/C RATIOS FROM PRELIMINARY GAS FLOWRATE EXPERIMENTS

Run number		J26	J27
Gas flowrate (l min^{-1})		10	20
Gaseous C_1-C_4 hydrocarbons	% w/w feed	5.4	5.9
Liquids boiling <200°C	% w/w feed	3.5	2.2
Liquids boiling >200°C	% w/w feed	80.7	82.0
Total condensate	% w/w feed	10.6	20.9
H/C atomic ratio in condensate		1.30	1.26
H/C atomic ratio in reactor contents		0.87	0.86

TABLE 12

PRODUCT YIELDS AND H/C RATIOS FROM PRELIMINARY CATALYST PARTICLE SIZE EXPERIMENTS

Experiment		J20	Mean from Table 7
Average particle size of catalyst (micron)		80	173
Gaseous C_1-C_4 hydrocarbons	% w/w feed	11.6	9.4
Liquids boiling <200°C	% w/w feed	6.7	9.4
Liquids boiling 200-420°C	% w/w feed	29.4	26.5
Residue boiling >420°C	% w/w feed	45.0	45.8
% conversion		46.9	46.1
H/C Atomic ratio in condensate		1.32	1.32
H/C Atomic ratio in reactor contents		0.93	0.90

TABLE 13

PRODUCT YIELDS FROM PRELIMINARY STIRRER SPEED EXPERIMENTS

Run number		J32	J33
Stirrer speed (r.p.m.)		850	1200
Gaseous C_1-C_4 hydrocarbons	(% w/w feed)	11.4	12.1
Liquids:			
IBP-150°C		3.5	4.0
150-235°C		6.0	5.9
235-300°C		10.4	12.5
300-350°C		13.4	14.8
Residue b. >350°C		51.3	48.6
TOTAL liquid + gas (% w/w feed)		96.0	97.9

TABLE 14

PRODUCT YIELDS FROM CATALYST COMPARISON EXPERIMENTS

Catalyst	Yields (% w/w feed)			
	C_1-C_4 gaseous hydrocarbons	Liquid products		
		IBP-90°C	90-300°C	300-350°C
Harshaw 0402T Co-Mo	18.6	5.8	17.1	7.1
Comox 471 Co-Mo	13.5	6.5	20.4	11.6
Aero HDS 16A Co-Mo	14.5	5.3	17.1	12.8
Comox MD1 Co-Mo	13.9	4.7	13.9	8.1
Akzo 153S Ni-Mo	12.9	9.2	14.3	8.8
Harshaw HT 115E Ni-Mo	14.0	6.5	15.8	6.2
NCB E Ni-Mo	13.9	4.7	16.8	10.5
Aero HDS 86 Ni-W	13.0	4.3	15.5	8.8
Harshaw 4301E Ni-W	14.4	3.8	12.0	8.3

TABLE 15

YIELDS, MASS BALANCES AND CONVERSIONS FROM REACTION TIME EXPERIMENTS

REACTION TEMPERATURE: 420°C

	RUN NUMBER		JK31	JK33	JK36	JK37	JK5	JK10	JK25	JK56
	Reaction Time at Temperature (hr)		0	1	1	2	4	4	4	4
	Hydrogen Flow Time (min)		121	178	178	236	368	369	363	368
HYDROCARBON GAS	CH_4	YIELDS (% w/w FEED)	0.6	1.7	1.4	2.4	3.2	3.1	3.1	2.6
	C_2H_6		0.3	1.0	0.9	1.6	2.4	2.3	2.1	1.9
	C_3H_8		0.1	0.4	0.4	0.8	2.1	1.9	1.6	1.8
	C_4H_{10}		-	-	0.1	0.2	1.3	1.2	0.9	1.2
	Sub-total		1.0	3.1	2.8	5.0	9.0	8.5	7.7	7.5
LIQUID PRODUCTS	IBP - 170°C		0.5	5.7	2.4	3.0	2.7	3.5	6.2	8.9
	170 - 250°C		1.2	1.8	4.2	6.3	6.2	7.8	6.6	5.0
	250 - 300°C		2.4	3.2	7.2	8.3	10.3	9.2	8.3	8.6
	300 - 355°C		4.5	5.7	5.5	11.5	11.0	12.0	11.1	10.9
	355 - 420°C		9.2	9.5	9.6	8.7	8.0	6.4	7.0	7.5
	420°C +		76.3	65.0	67.2	57.2	42.8	38.3	45.1	40.5
	Sub-total		94.1	90.9	96.1	95.0	81.0	77.2	84.3	81.4
HETERO-GAS	H_2O		0.5	1.5	1.7	1.8	1.9	1.2	2.0	1.7
	NH_3		0.5	1.1	1.0	1.1	1.8	1.7	1.8	1.8
	H_2S		0.3	0.5	0.4	0.4	0.6	0.5	0.5	0.5
	Sub-total		1.3	3.1	3.1	3.3	4.3	3.4	4.3	4.0
	TOTAL		96.4	97.1	102.0	103.3	94.3	89.1	96.3	92.9
	HYDROGEN CONSUMPTION		1.5	2.7	2.7	3.6	4.1	3.3	4.1	4.4
	% MASS BALANCE		94.9	94.4	99.3	99.7	90.2	85.8	92.2	88.5
	% CONVERSION		7.8	21.0	22.4	34.2	45.6	48.8	43.9	47.5

TABLE 16

YIELDS, MASS BALANCES AND CONVERSIONS FROM REACTION TIME EXPERIMENTS

REACTION TEMPERATURE: 440°C

	RUN NUMBER		JK59	JK29	JK28	JK34	JK7	JK39	JK62
	Reaction Time at Temperature (hr)		0	1	2	2	4	4	4
	Hydrogen Flow Time (min)		132	195	251	252	383	374	376
HYDROCARBON GAS	CH_4	YIELDS (% w/w FEED)	0.6	2.6	3.5	3.7	5.7	4.3	5.0
	C_2H_6		0.7	1.7	2.6	3.0	4.1	3.7	4.3
	C_3H_8		0.2	1.2	2.0	2.3	3.3	4.3	4.8
	C_4H_{10}		-	0.4	0.4	0.4	1.8	2.2	2.5
	Sub-total		1.5	5.9	8.5	9.6	14.9	14.5	16.6
LIQUID PRODUCTS	IBP - 170°C		1.2	7.1	7.7	7.5	9.6	12.9	9.6
	170 - 250°C		3.1	2.3	7.0	6.0	12.9	9.7	11.8
	250 - 300°C		3.7	6.8	10.8	10.9	14.1	16.5	14.4
	300 - 355°C		7.0	10.5	10.8	8.5	11.3	10.5	11.4
	355 - 420°C		16.2	13.8	11.7	11.4	5.9	5.6	6.0
	420°C +		62.8	53.2	36.7	39.5	21.6	27.2	23.6
	Sub-total		94.0	93.7	84.7	83.8	75.4	82.4	76.8
HETERO-GAS	H_2O		0.8	0.6	1.8	2.1	2.1	1.3	1.8
	NH_3		0.8	1.5	1.8	1.7	2.0	2.1	2.0
	H_2S		0.3	0.5	0.6	0.5	0.5	0.5	0.4
	Sub-total		1.9	2.6	4.2	4.3	4.6	3.9	4.2
	TOTAL		97.4	102.2	97.4	97.7	94.9	100.8	97.6
	HYDROGEN CONSUMPTION		1.9	3.8	4.0	4.6	4.7	5.9	5.7
	% MASS BALANCE		95.5	98.4	93.4	93.1	90.2	94.9	91.9
	% CONVERSION		24.6	38.0	54.9	51.4	72.5	67.1	70.6

TABLE 17

YIELDS, MASS BALANCES AND CONVERSIONS FROM REACTION TIME EXPERIMENTS

REACTION TEMPERATURE: 450°C

	RUN NUMBER		JK58	JK63	JK20	JK61	JK8
	Reaction Time at Temperature (hr)		0	1	2	2	4
	Hydrogen Flow Time (min)		132	207	256	264	380
HYDROCARBON GAS	CH_4	YIELDS (% w/w FEED)	1.5	4.0	3.5	4.7	5.5
	C_2H_6		0.8	3.0	2.8	3.9	4.9
	C_3H_8		0.3	2.2	3.0	3.7	5.6
	C_4H_{10}		-	0.9	2.7	1.4	2.9
	Sub-total		2.6	10.1	12.0	13.7	18.9
LIQUID PRODUCTS	IBP - 170°C		1.5	5.2	6.4	6.6	11.3
	170 - 250°C		4.7	8.3	9.5	12.5	14.1
	250 - 300°C		4.1	7.9	10.1	13.2	18.0
	300 - 355°C		8.9	10.3	10.0	9.6	6.8
	355 - 420°C		15.0	11.0	11.1	10.2	4.4
	420°C +		59.3	38.9	32.4	31.4	18.0
	Sub-total		93.5	81.6	79.5	83.5	72.6
HETERO-GAS	H_2O		1.2	2.0	2.2	2.2	2.7
	NH_3		0.9	1.6	1.9	1.9	2.1
	H_2S		0.4	0.5	0.5	0.6	0.5
	Sub-total		2.5	4.1	4.6	4.7	5.3
	TOTAL		98.6	95.8	96.1	101.9	96.8
	HYDROGEN CONSUMPTION		2.4	4.3	4.8	5.0	5.4
	% MASS BALANCE		96.2	91.5	91.3	96.9	91.4
	% CONVERSION		29.3	51.3	59.3	62.8	77.4

TABLE 18

YIELDS, MASS BALANCES AND CONVERSIONS FROM REACTION TIME EXPERIMENTS

REACTION TEMPERATURE: 460°C

	RUN NUMBER		JK35	JK30	JK26	JK6	JK27	JK60
	Reaction Time at Temperature (hr)		0	1	2	4	4	4
	Hydrogen Flow Time (min)		144	208	263	378	385	390
HYDROCARBON GAS	CH_4	YIELDS (% w/w FEED)	2.4	3.7	5.1	4.9	6.0	6.6
	C_2H_6		1.5	3.2	4.5	5.2	5.5	6.1
	C_3H_8		0.7	3.0	4.9	6.2	6.8	7.3
	C_4H_{10}		0.1	1.5	1.8	5.5	4.3	4.2
	Sub-total		4.7	11.4	16.3	21.8	22.6	24.2
LIQUID PRODUCTS	IBP - 170°C		4.2	8.1	11.4	9.5	15.8	14.9
	170 - 250°C		1.3	10.6	9.2	20.8	15.8	15.0
	250 - 300°C		4.6	5.4	11.0	17.1	16.5	15.8
	300 - 355°C		4.5	10.6	9.5	10.6	10.0	10.9
	355 - 420°C		11.7	8.4	7.1	-	2.4	-
	420°C +		65.2	37.4	28.8	13.6	10.3	14.3
	Sub-total		91.5	80.5	77.0	71.8	70.8	70.9
HETERO-GAS	H_2O		1.3	1.5	2.1	1.2	1.6	0.8
	NH_3		1.0	1.8	1.8	2.1	2.1	2.1
	H_2S		0.4	0.6	0.6	0.5	0.5	0.5
	Sub-total		2.7	3.9	4.5	3.8	4.2	3.4
	TOTAL		98.9	95.8	97.8	97.4	97.6	98.5
	HYDROGEN CONSUMPTION		2.7	4.7	5.8	6.1	6.7	7.1
	% MASS BALANCE		96.2	91.1	92.0	91.3	90.9	91.4
	% CONVERSION		22.3	52.9	64.1	82.9	87.0	82.1

TABLE 19

CALCULATED RATE CONSTANTS FOR THE OVERALL REACTION AND FOR NITROGEN REMOVAL AT DIFFERENT TEMPERATURES

Reaction Temperature (^{o}C)	Overall Reaction Rate Constant (min^{-1})	Nitrogen Removal Rate Constant (min^{-1})
420	2.0×10^{-3}	6.3×10^{-3}
440	3.7×10^{-3}	8.8×10^{-3}
450	4.7×10^{-3}	10.3×10^{-3}
460	6.3×10^{-3}	11.5×10^{-3}

TABLE 20

PARAFFINS, NAPHTHENES AND AROMATICS IN IBP - 170°C PRODUCT FRACTION

FROM REACTION TIME AND TEMPERATURE EXPERIMENTS

Run Number	Reaction Time(hr)	Reaction Temp(°C)	Benzene: Cyclohexane (CH)	Toluene: Methyl-CH	Ethyl-Benzene: Ethyl-CH	Propyl-Benzene: Propyl-CH	m+p Xylene: 1,3+1,4 - Dimethyl-CH	Paraffins P (%)	Naphthenes N (%)	Aromatics A (%)	A : N
JK33	1	420	0.13	0.47	-	0.57	-	-	-	-	-
JK37	2	420	-	-	-	-	-	10.8	53.2	36.0	0.68
JK5	4	420	0.31	0.58	1.09	-	4.00	-	-	-	-
JK29	1	440	0.26	0.65	-	0.55	3.87	-	-	-	-
JK34	2	440	0.27	0.59	-	0.56	3.99	14.1	49.4	36.6	0.74
JK7	4	440	0.33	1.85	1.19	-	4.35	-	-	-	-
JK63	1	450	-	-	-	-	-	15.0	49.0	36.0	0.73
JK20	2	450	0.30	0.86	1.58	0.69	3.10	12.3	49.7	38.0	0.76
JK8	4	450	0.37	1.02	1.43	-	5.88	18.7	45.4	35.9	0.79
JK35	0	460	0.13	0.57	-	0.64	-	-	-	-	-
JK30	1	460	0.38	0.99	-	0.68	4.30	-	-	-	-
JK26	2	460	0.33	2.46	-	0.81	4.80	15.1	41.3	43.6	1.06
JK6	4	460	0.38	3.22	1.64	-	7.14	-	-	-	-

- : Not determined

TABLE 21

% CARBON DEPOSITION ON SPENT CATALYSTS

Reaction Time (hr)	Reaction Temp. (°C)	% Carbon Deposition
0	420	10.6
1	420	10.2
2	420	10.8
4	420	11.8
1	440	9.3
2	440	11.3
4	440	10.9
4	450	11.0
0	460	9.8
1	460	10.1
2	460	10.2
4	460	12.7

TABLE 22

SURFACE AREA DETERMINATIONS OF FRESH AND SPENT CATALYSTS

Catalyst State	Conditions of Treatment			Surface Area (m^2g^{-1})
	Hydrogen Flow Time (min)	Reaction Temp.(°C)	Pressure (bar)	
Fresh, pelleted	-	-	-	160
Fresh, ground	-	-	-	156
Spent, ground	NIL	250	210 (N_2)	119
Spent, ground	144	460	210 (H_2)	107
Spent, ground	385	460	210 (H_2)	96

TABLE 23

YIELDS, MASS BALANCES AND CONVERSIONS FROM PRESSURE EXPERIMENTS

	RUN NUMBER	JK74	JK66	JK67	JK71	JK89	JK65	JK75	JK91	JK78	JK79	JK88	JK87	JK72	JK90	JK77	JK86
	Total Pressure(bar)	212	211	212	211	138	211	211	211	272	306	307	339	211	210	271	337
	Hydrogen Partial Pressure (bar)	85	93	106	106	138	141	141	141	136	135	135	135	169	210	271	337
	Inert Gas Partial Pressure (bar)	127	118	106	105*	0	70	70	70	136	171	172	204	42	0	0	0
HYDROCARBON GAS	CH_4	2.9	3.4	3.2	3.9	3.6	3.3	3.2	3.4	3.2	3.1	3.1	2.6	3.4	3.8	3.6	6.0
	C_2H_6	1.3	1.1	1.5	1.5	2.3	1.3	1.8	1.8	1.8	1.4	1.6	1.3	1.8	2.1	2.2	4.0
	C_3H_8	0.6	-	0.2	-	1.0	0.9	0.7	0.7	0.7	0.4	0.5	0.6	1.2	1.1	1.4	2.2
	C_4H_{10}	0.1	-	-	-	-	0.2	0.1	-	-	0.1	-	0.1	0.6	0.1	0.4	0.2
	Sub-total	4.9	4.5	4.9	5.4	6.9	5.7	5.8	5.9	5.7	5.0	5.2	4.6	7.0	7.1	7.6	12.4
LIQUID PRODUCTS	IBP - 170°C	1.4	1.8	1.8	1.8	2.8	2.0	2.5	2.2	1.8	1.2	1.9	1.5	2.4	3.6	4.4	5.2
	170 - 250°C	2.8	3.1	3.5	3.2	4.4	4.1	4.5	4.1	3.6	3.6	3.5	3.3	5.0	4.9	6.4	6.6
	250 - 300°C	2.6	2.9	2.6	2.5	4.1	3.7	3.7	3.6	3.4	3.4	3.4	3.1	4.2	4.7	5.9	6.1
	300 - 355°C	5.2	5.8	6.2	6.6	7.8	7.3	7.6	7.4	6.7	6.6	6.7	6.4	8.8	9.1	10.9	11.1
	355 - 420°C	11.9	13.7	12.7	12.5	13.2	13.5	14.0	13.8	13.8	13.9	14.6	14.2	13.0	13.0	13.2	12.9
	420°C +	69.7	64.5	66.0	63.9	59.3	59.7	60.7	61.0	62.1	62.8	62.2	63.4	58.0	55.5	50.4	48.5
	Sub-total	93.6	91.8	92.8	90.5	91.6	90.3	93.0	92.1	91.4	91.5	92.3	91.9	91.4	90.8	91.2	90.4
HETERO-GAS	H_2O	-	0.2	0.4	0.5	0.2	0.6	0.8	0.9	0.1	-	-	-	0.9	1.0	0.9	0.2
	NH_3	0.5	0.5	0.5	0.2	0.6	0.5	0.6	0.5	0.3	0.3	0.3	0.4	0.7	0.9	1.1	1.1
	H_2S	0.2	0.5	0.5	0.3	0.5	0.4	0.5	0.4	0.5	0.5	0.3	0.4	0.5	0.6	0.6	0.6
	Sub-total	0.7	1.2	1.4	1.0	1.3	1.5	1.9	1.8	0.9	0.8	0.6	0.8	2.1	2.5	2.6	1.9
	TOTAL	99.2	97.5	99.1	96.9	99.8	97.5	100.7	99.8	98.0	97.3	98.1	97.3	100.5	100.4	101.4	104.7
	HYDROGEN CONSUMPTION	1.5	2.3	1.7	1.6	2.9	3.1	3.0	2.4	2.1	1.9	2.0	1.6	3.0	3.4	4.1	5.1
	% MASS BALANCE	97.7	95.2	97.4	95.3	96.9	94.4	97.7	97.4	95.9	95.4	96.1	95.7	97.5	97.0	97.3	99.6
	% CONVERSION	15.9	20.1	20.1	20.9	27.8	25.4	26.7	26.1	23.6	22.4	23.7	21.9	29.9	32.5	38.9	42.6

YIELDS (% w/w FEED)

* Inert gas was argon - otherwise nitrogen throughout.

TABLE 24

MAIN COMPONENTS FROM G.L.C. ANALYSIS OF IBP-170°C PRODUCT FRACTIONS FROM PRESSURE EXPERIMENTS

(Expressed as % of total fraction)

Run Number	JK74	JK89	JK87	JK90	JK86
Total Pressure (bar)	210	138	339	210	337
Hydrogen Partial Pressure (bar)	85	138	135	210	337
Yield IBP-170°C Fraction(%w/w feed)	1.4	2.8	1.5	3.6	5.2
Pentane	-	0.2	-	1.6	1.4
Hexane	0.3	0.5	0.8	3.5	3.0
Methyl cyclopentane	0.8	2.9	0.9	3.8	3.0
Benzene	5.5	4.5	6.4	4.5	3.1
Cyclohexane	4.5	16.9	7.2	23.0	20.8
Heptane	0.4	0.9	0.6	1.3	1.5
Methyl cyclohexane	4.6	11.5	7.9	15.1	16.3
Toluene	19.6	11.1	22.6	9.8	7.4
Ethyl benzene + ethyl cyclohexane	10.4	8.6	11.8	7.8	7.9
p-Xylene	3.7	2.0	3.3	1.3	1.1
m-Xylene	9.3	4.8	8.3	3.2	2.7
o-Xylene	10.3	5.2	8.7	3.0	2.6
n + iso-Propyl benzene	2.2	2.0	1.7	0.8	1.1
n + iso-Propyl cyclohexane	1.4	3.2	1.9	2.2	2.9
m-Ethyl toluene	6.6	4.3	3.8	1.5	2.0
p-Ethyl toluene	2.0	1.1	0.9	0.4	0.5
o-Ethyl toluene	3.2	1.9	1.5	0.7	0.7
Pseudocumene	4.4	3.0	2.0	0.6	1.0
Others	7.4	10.1	7.5	12.2	14.7
Unidentified	3.4	5.3	2.2	3.0	6.3

TABLE 25

PARAFFINS, NAPHTHENES AND AROMATICS IN IBP - 170°C PRODUCT FRACTION FROM PRESSURE EXPERIMENTS

Run Number	H_2 Partial Pressure (bar)	Total Pressure (bar)	Benzene: Cyclohexane (CH)	Toluene: Methyl-CH	Propyl-Benzene: Propyl-CH	m+p Xylene: 1,3 + 1,4-Dimethyl-CH	Paraffins P (%)	Naphthenes N (%)	Aromatics A (%)	A : N
JK74	85	210	1.22	4.26	1.57	14.44	3.8	17.5	78.7	4.50
JK87	135	339	0.89	2.86	0.89	7.65	-	-	-	-
JK89	138	138	0.27	0.96	0.63	4.03	6.3	31.8	61.9	1.95
JK90	210	210	0.20	0.65	0.36	1.93	11.4	55.7	32.9	0.59
JK86	337	337	0.15	0.45	0.38	1.43	12.5	57.0	30.5	0.54

TABLE 26

YIELDS, MASS BALANCES AND CONVERSIONS FROM CATALYST LOADING EXPERIMENTS

	RUN NUMBER	JK55	JK80	JK11	JK81	JK54	JK22	JK19	JK21	JK12	JK13	JK14	JK15	JK20	JK61
	Active Catalyst (% w/w extract feed)	0*	0*	0"	0"	0.2	0.9	2.3	2.3	4.6	9.4	14.0	18.8	23.1	23.5
HYDROCARBON GAS	CH_4	3.7	3.2	2.8	2.6	3.5	3.4	3.7	3.7	3.9	3.7	3.6	3.1	3.5	4.7
	C_2H_6	1.7	1.7	1.3	1.2	2.0	2.3	2.5	2.6	2.9	2.7	2.9	2.5	2.8	3.9
	C_3H_8	1.3	1.5	0.9	0.7	1.8	2.5	2.6	2.8	3.1	2.8	3.2	2.7	3.0	3.7
	C_4H_{10}	0.6	1.0	0.5	0.7	1.2	1.9	1.9	2.6	2.2	2.0	2.3	2.1	2.7	1.4
	Sub-total	7.3	7.4	5.5	5.2	8.5	10.1	10.7	11.7	12.1	11.2	12.0	10.4	12.0	13.7
LIQUID PRODUCTS	IBP - 170°C	3.1	3.4	3.5	3.0	4.1	3.3	6.0	4.6	4.2	7.9	8.2	8.2	6.4	6.6
	170 - 250°C	2.4	2.7	2.6	3.0	3.6	6.8	5.3	7.7	8.0	5.0	8.6	12.6	9.5	12.5
	250 - 300°C	3.9	3.1	2.6	2.3	7.3	8.1	9.9	8.5	12.3	12.1	14.2	8.8	10.1	13.2
	300 - 355°C	5.2	5.1	4.6	4.1	9.0	9.6	8.8	9.0	7.9	11.1	9.6	10.5	10.0	9.6
	355 - 420°C	12.8	13.4	10.6	11.9	12.5	13.4	11.4	12.4	10.3	10.6	10.3	10.7	11.1	10.2
	420°C +	60.5	61.8	64.6	66.0	53.7	41.2	35.8	37.5	36.0	31.4	33.8	30.5	32.4	31.4
	Sub-total	87.9	89.5	88.5	90.3	90.2	82.4	77.2	79.7	78.7	78.1	84.7	81.3	79.5	83.5
HETERO-GAS	H_2O	1.6	1.7	ND	1.5	1.2	1.9	2.3	1.9	2.5	2.7	2.3	2.8	2.2	2.2
	NH_3	0.6	0.7	ND	0.5	0.8	1.0	1.3	1.1	1.5	1.6	1.7	1.8	1.9	1.9
	H_2S	0.3	0.4	ND	0.4	0.3	0.5	0.5	0.5	0.5	0.6	0.5	0.5	0.5	0.6
	Sub-total	2.5	2.8	ND	2.4	2.3	3.4	4.1	3.5	4.5	4.9	4.5	5.2	4.6	4.7
YIELDS (% w/w FEED)	TOTAL	97.7	99.7	ND	97.9	101.0	95.9	92.0	94.9	95.3	94.2	101.2	96.9	96.1	101.9
	HYDROGEN CONSUMPTION	1.8	2.0	ND	1.7	2.3	3.4	3.2	4.1	3.9	4.0	5.0	4.3	4.8	5.0
	% MASS BALANCE	95.9	97.7	~95	96.2	98.7	92.5	88.8	90.8	91.4	90.2	96.2	92.6	91.3	96.9
	% CONVERSION	27.7	27.5	~22	21.3	37.6	48.9	53.8	52.6	54.8	60.1	59.7	62.2	59.3	62.8

* No active catalyst; no alumina.

" No active catalyst; 23.1% w/w extract feed of alumina.

ND Not determined.

TABLE 27

PARAFFINS, NAPHTHENES AND AROMATICS IN IBP - 170°C PRODUCT FRACTION FROM CATALYST LOADING EXPERIMENTS

Run Number	Catalyst Loading (%w/w feed)	Benzene: Cyclohexane (CH)	Toluene: Methyl-CH	Ethyl-Benzene: Ethyl-CH	Paraffins P (%)	Naphthenes N (%)	Aromatics A (%)	A : N
JK11/81	0	0.42	4.15	7.72	-	-	-	-
JK22	0.9	0.23	2.85	2.17	-	-	-	-
JK19/21	2.3	0.27	1.44	1.42	18.7	44.6	36.7	0.82
JK12	4.6	0.28	1.01	1.53	-	-	-	-
JK13	9.4	0.26	0.66	1.29	-	-	-	-
JK14	14.0	0.28	0.73	1.27	-	-	-	-
JK15	18.8	0.34	1.22	1.26	-	-	-	-
JK20/61	23.3	0.29	0.83	1.20	12.2	49.7	38.0	0.76

- : Not determined

TABLE 28

YIELDS, MASS BALANCES AND CONVERSIONS FROM INITIAL COAL EXTRACT SOLUTION CONCENTRATION EXPERIMENTS

	RUN NUMBER		JK44	JK48	JK46	JK42	JK43	JK47	JK45	JK41
	Concentration Coal Extract Solution in Anthracene Oil (% w/w)		0	0	20	40	60	60	80	100
HYDROCARBON GAS	CH_4	YIELDS (% w/w FEED)	0.8	1.0	1.6	1.8	2.5	2.7	2.9	3.2
	C_2H_6		1.3	1.3	1.7	1.6	2.0	2.1	2.3	2.4
	C_3H_8		1.2	1.1	1.1	1.1	1.8	1.5	1.8	2.5
	C_4H_{10}		0.3	0.3	0.4	0.5	0.8	0.2	0.9	0.9
	Sub-total		3.6	3.7	4.8	5.0	7.1	6.5	7.9	9.0
LIQUID PRODUCTS	IBP - 170°C		6.8	6.1	5.7	3.9	4.2	4.7	4.3	4.3
	170 - 250°C		17.7	17.9	15.4	11.6	9.3	10.7	7.9	5.4
	250 - 300°C		25.7	25.5	19.2	14.1	11.4	11.8	8.2	5.6
	300 - 355°C		26.7	29.5	26.2	24.8	19.5	20.0	14.5	9.2
	355 - 420°C		10.1	9.1	15.5	16.0	15.0	15.6	15.9	13.8
	420°C +		6.1	5.1	10.6	19.5	27.8	27.5	37.0	43.5
	Sub-total		93.1	93.2	92.6	89.9	87.2	90.3	87.8	81.8
HETERO-GAS	H_2O		0.8	1.9	1.7	0.2	1.7	1.9	2.3	2.2
	NH_3		1.2	1.2	1.2	1.3	1.5	1.5	1.4	1.6
	H_2S		0.6	0.9	0.4	0.3	0.6	0.6	0.5	0.5
	Sub-total		2.6	4.0	3.3	1.8	3.8	4.0	4.2	4.3
	TOTAL		99.3	100.9	100.7	96.7	98.1	100.8	99.9	95.1
	HYDROGEN CONSUMPTION		4.8	5.0	5.7	3.6	4.0	4.3	4.3	3.6
	% MASS BALANCE		94.5	95.9	95.0	93.1	94.1	96.5	95.6	91.5
	% CONVERSION		54.2	62.3	61.1	51.7	48.9	50.7	46.5	45.5

TABLE 29

YIELDS, MASS BALANCES AND CONVERSIONS FROM SECONDARY HYDROGENATION OF 355 - 420°C PRODUCT FRACTION AT DIFFERENT REACTION TIMES

Run Number: JK92

	WEIGHT BALANCE		1	2	3	4	5
	Reaction Time at Temperature (hr)		0	1	2	3	4
	Hydrogen Flow Time (min)		39	99	159	219	279
HYDROCARBON GAS	CH_4	YIELDS (% w/w FEED)	-	0.6	1.1	1.6	2.0
	C_2H_6		-	0.9	1.7	2.4	2.9
	C_3H_8		-	0.9	2.1	3.2	4.1
	C_4H_{10}		-	0.6	1.3	2.2	3.0
	Sub-total		-	3.0	6.2	9.4	12.0
LIQUID PRODUCTS	IBP - 170°C		-	2.9	4.9	8.2	9.2
	170 - 250°C		0.3	3.5	8.0	13.7	19.4
	250 - 300°C		0.6	5.8	11.8	18.4	22.5
	300 - 355°C		13.7	21.9	25.4	24.1	19.8
	355 - 420°C		69.6	45.0	38.4	23.3	15.9
	420°C +		15.8	17.8	5.7	3.5	1.7
	Sub-total		100.0	96.9	94.2	91.2	88.5
HETERO-GAS	H_2O		-	0.3	0.1	0.4	0.2
	NH_3		0.2	0.5	0.6	0.7	0.6
	H_2S		-	-	-	-	-
	Sub-total		0.2	0.8	0.7	1.1	0.8
	TOTAL		100.2	100.7	101.1	101.7	101.3
	HYDROGEN CONSUMPTION		0.2	1.1	1.8	2.9	3.3
	% MASS BALANCE (MB)		100.0	99.6	99.3	98.8	98.0
	% CONVERSION *		4.7	29.6	50.4	69.7	80.0

*% CONVERSION

$$= \frac{\text{wt b.}>355^{\circ}\text{C in feed} - (\text{wt b.}>355^{\circ}\text{C in prod})\left(\frac{100}{MB}\right)}{\text{wt b.}>355^{\circ}\text{C in feed}} \times 100$$

TABLE 30

YIELDS FROM SECONDARY HYDROGENATION OF 355 - 420°C PRODUCT FRACTION AT DIFFERENT CATALYST LOADINGS

Run Number		JKR165	JKR166	JKR167	JKR168	JKR169
Catalyst Loading (% w/w feed)		0	0	1	5	10
Gaseous C_1-C_4 Hydrocarbons	% of recovered prod.	0.5	0.6	2.0	3.0	5.3
Liquid Products:						
IBP - 170°C		1.1	1.1	1.6	2.0	2.3
170 - 250°C		0.8	0.8	1.1	1.5	2.2
250 - 300°C		1.0	0.8	1.3	2.0	2.8
300 - 355°C		6.9	6.3	7.8	10.2	11.7
355 - 420°C		74.3	75.0	70.6	66.0	60.4
420°C +		15.4	15.4	15.6	15.3	15.3

TABLE 31

YIELDS, MASS BALANCES AND CONVERSIONS FROM SECONDARY HYDROGENATION OF 300 - 355°C PRODUCT FRACTION AT DIFFERENT REACTION TIMES

Run Number: JK93

	WEIGHT BALANCE		1	2	3	4	5
	Reaction Time at Temperature (hr)		0	1	2	3	4
	Hydrogen Flow Time (min)		39	99	159	219	279
HYDROCARBON GAS	CH_4	YIELDS (% w/w FEED)	-	0.8	1.4	2.1	2.5
	C_2H_6		-	1.0	1.9	2.6	2.9
	C_3H_8		-	0.7	1.9	3.0	3.7
	C_4H_{10}		-	0.4	1.2	2.1	2.8
	Sub-total		-	2.9	6.4	9.8	11.9
LIQUID PRODUCTS	IBP - 170°C		0.5	4.6	8.8	13.4	16.5
	170 - 250°C		1.2	6.6	16.8	24.5	30.7
	250 - 300°C		4.4	16.0	30.9	32.9	29.0
	300 - 355°C		76.8	56.7	30.9	16.7	10.1
	355 - 420°C		16.8	12.7	6.2	2.9	1.2
	420°C +		-	0.5	0.3	0.1	0.1
	Sub-total		99.7	97.1	93.9	90.5	87.6
HETERO-GAS	H_2O		0.1	-	0.5	0.5	0.9
	NH_3		0.2	0.5	0.6	0.6	0.6
	H_2S		-	-	-	-	-
	Sub-total		0.3	0.5	1.1	1.1	1.5
	TOTAL		100.0	100.5	101.4	101.4	101.0
	HYDROGEN CONSUMPTION		0.2	0.5	2.0	2.9	3.4
	% MASS BALANCE (MB)		99.8	100.0	99.4	98.5	97.6
	% CONVERSION *		2.7	27.5	60.9	79.2	87.9

* % CONVERSION

$$= \frac{\text{wt b.}>300^{\circ}\text{C in feed} - (\text{wt b.}>300^{\circ}\text{C in prod})\left(\frac{100}{MB}\right)}{\text{wt b.}>300^{\circ}\text{C in feed}} \times 100$$

TABLE 32

YIELDS FROM SECONDARY HYDROGENATION OF 300 - 355°C PRODUCT FRACTION AT DIFFERENT CATALYST LOADINGS

Run Number		JKR82	JKR83	JKR84	JKR85	JKR95	JKR96
Catalyst Loading (% w/w feed)		0	0	0.2	1	5	10
Gaseous C_1-C_4 Hydrocarbons	% of recovered product	0.1	0.1	0.4	1.0	2.4	5.5
Liquid Products:							
IBP - 170°C		1.3	1.1	1.1	1.8	2.4	2.3
170 - 250°C		1.5	1.3	1.6	2.0	2.7	3.1
250 - 300°C		4.8	4.1	4.9	5.8	7.9	9.2
300 - 355°C		67.6	67.9	67.2	65.5	62.5	58.8
355 - 420°C		24.5	25.1	24.6	23.7	21.9	21.0
420°C +		0.2	0.4	0.2	0.2	0.2	0.1

TABLE 33

MEAN, $\bar{x}$, STANDARD DEVIATION, s, AND PERCENTAGE ERROR OF YIELDS AND CONVERSIONS IN REPEATED EXPERIMENTS

Run Numbers		JK5,10,25,56			JK7,39,62			JK6,27,60			JK65,75,91		
		$\bar{x}$	s	% error	$\bar{x}$	s	% error	$\bar{x}$	s	% error	$\bar{x}$	s	% error
Gaseous C_1-C_4 Hydrocarbons	Yields, % w/w feed	9.18	0.88	9.6	16.62	1.39	8.4	25.08	1.72	6.9	6.01	0.06	1.0
Liquid Products:													
IBP - 170°C		5.96	3.15	52.9	11.56	1.76	15.2	14.70	3.75	25.5	2.31	0.22	9.5
170 - 250°C		7.19	1.42	19.7	12.45	2.07	16.6	18.86	3.43	18.2	4.39	0.20	4.6
IBP - 250°C		13.15	2.44	18.6	24.01	0.84	3.5	33.56	1.07	3.2	6.70	0.41	6.1
250 - 300°C		10.22	1.07	10.5	16.23	1.05	6.5	18.06	0.72	4.0	3.80	0.11	2.9
300 - 355°C		12.63	0.91	7.2	12.00	0.81	6.8	11.59	0.51	4.4	7.70	0.09	1.2
355 - 420°C		8.10	0.68	8.4	6.32	0.37	5.9	0.88	1.52	172.7	14.27	0.09	0.6
420°C +		46.69	1.88	4.0	26.10	2.38	9.1	13.96	2.31	16.5	62.67	0.56	0.9
Sub-total		90.79	1.07	1.2	84.66	1.88	2.2	78.05	0.55	0.7	95.14	0.55	0.6
Hetero-gases		4.48	0.36	8.0	4.60	0.49	10.7	4.17	0.45	10.8	1.79	0.18	10.1
Hydrogen Consumption		4.45	0.46	10.3	5.88	0.58	9.9	7.27	0.55	7.6	2.94	0.43	14.6
% Conversion		46.45	2.15	4.6	70.07	2.74	3.9	84.00	2.63	3.1	26.07	0.65	2.5

TABLE 34

REACTION RATE CONSTANTS CALCULATED FROM THE KINETIC MODEL

Reaction Step	Rate Constant (min^{-1}) x 10^3
A → B	1.3
A → C	0.8
A → D	0.6
A → E	0.5
A → F	0.4
A → G	0.7
A → any	4.3
B → C	5.7
B → E	0.2
B → F	0.2
B → G	0.2
C → D	4.1
C → E	1.7
C → F	1.2
C → G	0.9
D → E	0.3
D → F	0.3
D → G	0.3

TABLE 35

OBSERVED AND PREDICTED YIELDS (g.) AT 450°C

H_2 flow time (min.)	Observed/ predicted	A	B	C	D	E	F	G
132	O	312.9	79.1	47.0	21.6	24.8	7.9	13.7
	P	308.5	69.5	41.2	25.3	21.3	16.8	24.8
207	O	215.8	61.0	57.1	43.8	46.0	28.8	56.0
	P	221.8	63.6	55.9	50.0	40.3	31.8	44.1
256	O	180.1	61.7	55.6	56.2	52.8	35.6	66.7
	P	178.8	57.6	58.3	64.9	51.9	41.0	55.0
264	O	164.5	53.4	50.3	69.1	65.5	34.6	71.8
	P	172.6	56.6	58.3	67.2	53.7	42.4	56.7
380	O	100.0	24.4	37.8	100.0	78.3	62.8	105.0
	P	103.6	41.2	51.7	94.6	77.3	61.3	77.7
99	O	71.5	180.8	88.1	23.4	14.2	11.7	12.2
	P	42.9	210.1	94.6	20.3	13.2	10.2	9.6
159	O	23.0	154.8	102.6	47.8	32.4	19.9	25.1
	P	33.0	145.7	107.3	45.5	27.9	21.9	19.8
219	O	14.0	94.7	97.8	74.7	55.8	33.1	38.4
	P	25.3	101.2	100.5	69.4	42.2	33.1	29.3
279	O	7.1	65.1	81.0	92.1	79.6	37.9	49.1
	P	19.4	70.4	86.0	89.0	55.0	43.3	37.9
99	O	2.0	51.5	229.9	64.9	26.7	18.6	11.6
	P	0.1	46.2	215.6	75.6	30.7	21.4	15.7
159	O	1.1	25.4	125.8	125.8	68.5	36.0	26.2
	P	0.1	31.5	144.3	114.3	50.8	36.9	27.4
219	O	0.5	11.8	68.8	135.2	100.7	55.0	40.3
	P	0	21.5	96.7	136.8	65.4	48.4	36.3
279	O	0.5	5.0	41.8	120.5	127.4	68.4	49.5
	P	0	14.6	64.9	148.6	76.2	57.3	43.5

TABLE 36

REACTION RATE CONSTANTS ESTIMATED FROM KINETIC MODEL

Reaction	Rate constant (min^{-1}) x 10^3		
	420°C	440°C	460°C
A → B	0.6	1.1	1.9
A → C	0.4	0.7	1.2
A → D	0.3	0.5	0.9
A → E	0.3	0.5	0.8
A → F	0.2	0.4	0.6
A → G	0.3	0.6	1.0
B → C	4.8	4.6	12.0
B → E	0.2	0.2	0.5
B → F	0.2	0.2	0.5
B → G	0.2	0.2	0.5
C → D	2.6	3.3	7.3
C → E	1.1	1.3	2.9
C → F	0.8	1.0	2.2
C → G	0.6	0.7	1.6
D → E	0.1	0.2	0.6
D → F	0.1	0.2	0.6
D → G	0.1	0.2	0.6

TABLE 37

OBSERVED AND PREDICTED YIELDS (g.) 420°C

H_2 flow time (min.)	Observed/ predicted	A	B	C	D	E+F	G
71	O	403.7	48.7	23.8	12.7	8.9	5.3
	P	379.8	58.3	26.1	10.3	16.5	10.7
128	O	342.8	49.5	29.1	26.7	36.6	15.3
	P	338.9	53.5	39.2	20.5	30.3	19.1
186	O	288.1	43.8	57.9	41.8	47.0	25.2
	P	301.8	48.8	47.4	31.7	44.7	27.1
317	O	234.4	40.7	63.4	51.3	66.0	46.1
	P	232.2	38.9	53.4	56.8	75.8	43.8

TABLE 38

OBSERVED AND PREDICTED YIELDS (g.) AT 440°C

H_2 flow time (min.)	Observed/ predicted	A	B	C	D	E+F	G
82	O	330.0	85.1	36.8	19.4	22.6	7.9
	P	323.2	70.0	36.2	20.3	31.3	20.6
145	O	271.4	70.4	53.6	34.7	47.9	30.1
	P	256.0	67.8	51.0	37.2	54.8	34.5
202	O	205.0	62.4	51.8	58.6	75.4	48.6
	P	207.3	63.3	57.6	52.3	75.1	45.7
328	O	131.0	31.7	60.2	81.5	120.5	83.4
	P	130.1	49.8	58.1	81.3	116.3	66.4

TABLE 39

OBSERVED AND PREDICTED YIELDS (g.) AT 460°C

H_2 flow time (min.)	Observed/ predicted	A	B	C	D	E+F	G
94	O	340.8	61.2	23.5	24.0	28.8	24.6
	P	332.3	59.4	38.7	20.8	31.5	20.1
158	O	206.4	46.4	58.5	29.8	103.2	62.9
	P	222.0	46.7	55.2	54.7	78.3	45.9
213	O	157.4	38.8	51.9	60.1	112.6	89.1
	P	157.0	35.8	52.2	78.9	114.6	64.3
334	O	70.2	4.4	58.3	90.8	168.7	126.1
	P	73.3	18.2	32.9	107.4	176.6	94.3

TABLE 40

PREDICTED, P, AND EXPERIMENTAL, E, YIELDS FOR INITIAL COAL EXTRACT SOLUTION CONCENTRATION EXPERIMENTS

Concentration Coal Extract Solution in Anthracene Oil (% w/w)		20		40		60		80	
		P	E	P	E	P	E	P	E
A (420°C +)	Yield (g)	69.2	53.0	107.0	97.1	148.4	138.3	188.9	185.0
B (355 - 420°C)		53.5	77.5	56.7	79.7	62.6	76.5	67.7	79.5
C (300 - 355°C)		123.0	131.1	101.5	123.6	84.5	98.8	66.6	72.5
D (250 - 300°C)		109.1	96.1	86.7	70.3	68.3	58.0	48.9	41.0
E (170 - 250°C)		77.4	77.0	63.4	57.8	52.2	50.0	40.4	39.5
F (IBP - 170°C)		30.6	28.5	27.9	19.4	26.3	22.3	24.5	21.5
G (C_1 - C_4 gas)		24.4	24.0	29.5	24.9	35.6	34.0	41.6	39.5

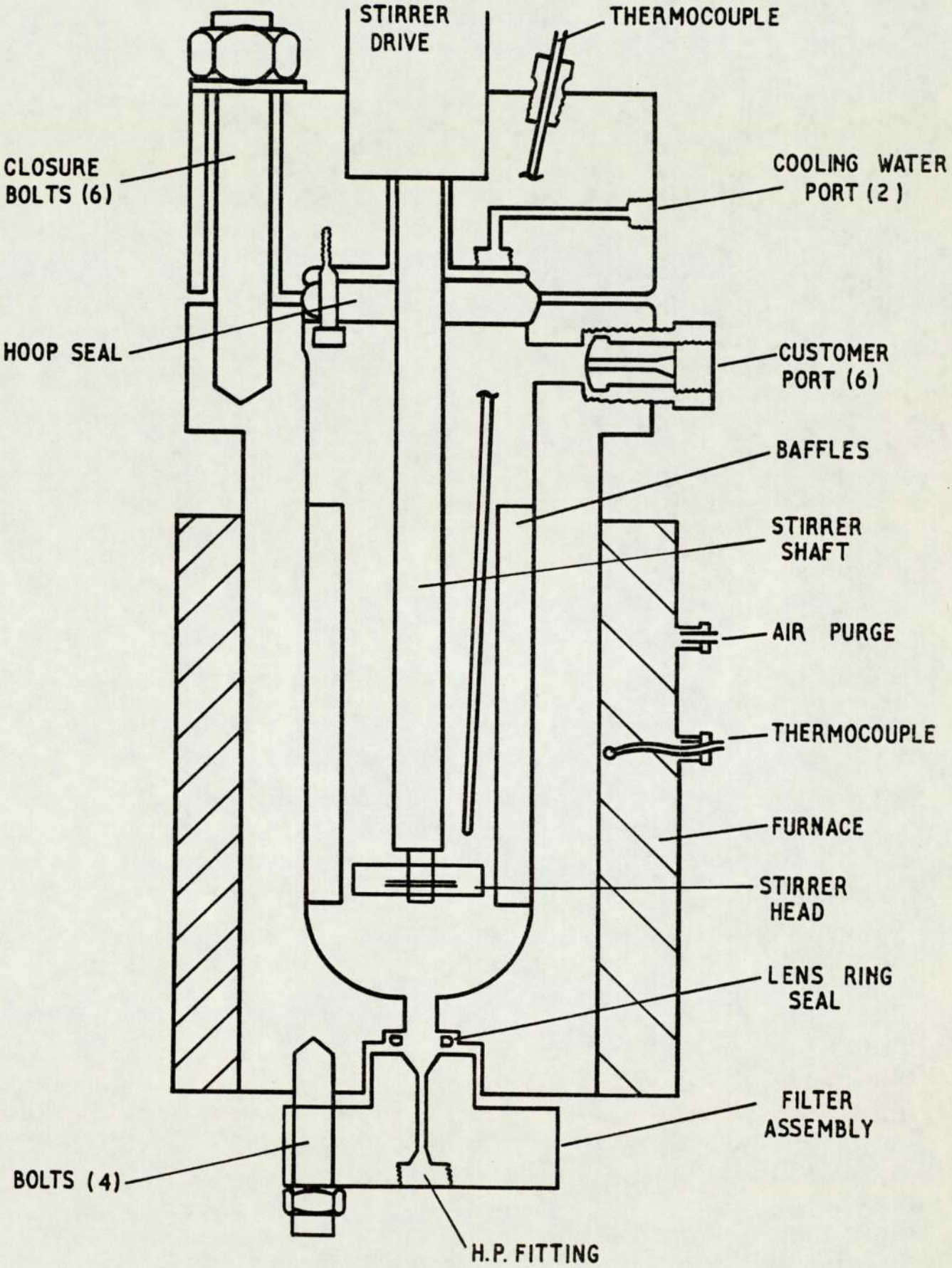

FIGURE 1 ONE LITRE AUTOCLAVE

APPROX. 1/2 SCALE

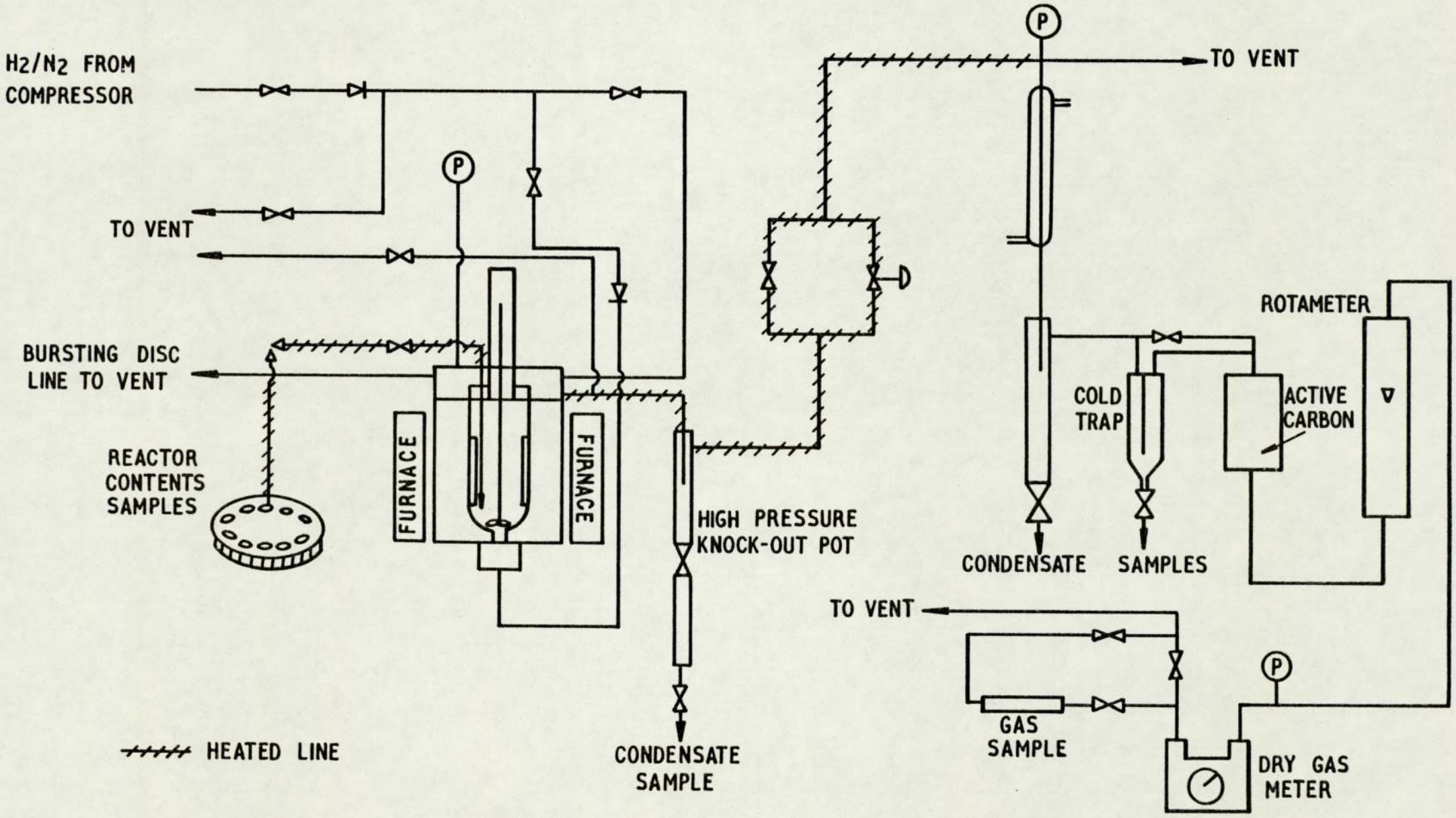

FIGURE 2. FLOW DIAGRAM OF ONE LITRE AUTOCLAVE SYSTEM

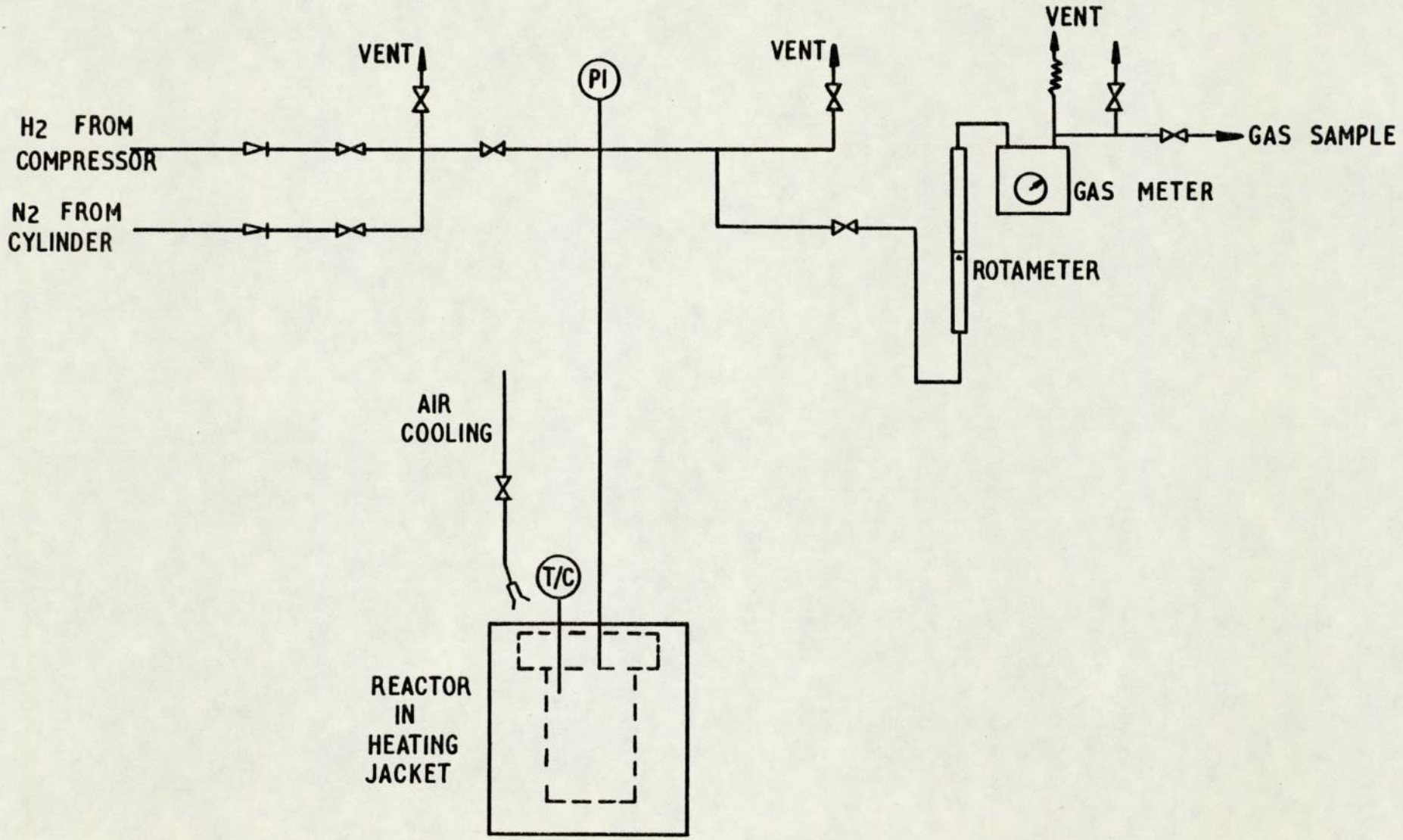

FIGURE 3. FLOW DIAGRAM OF 300ml AUTOCLAVE SYSTEM

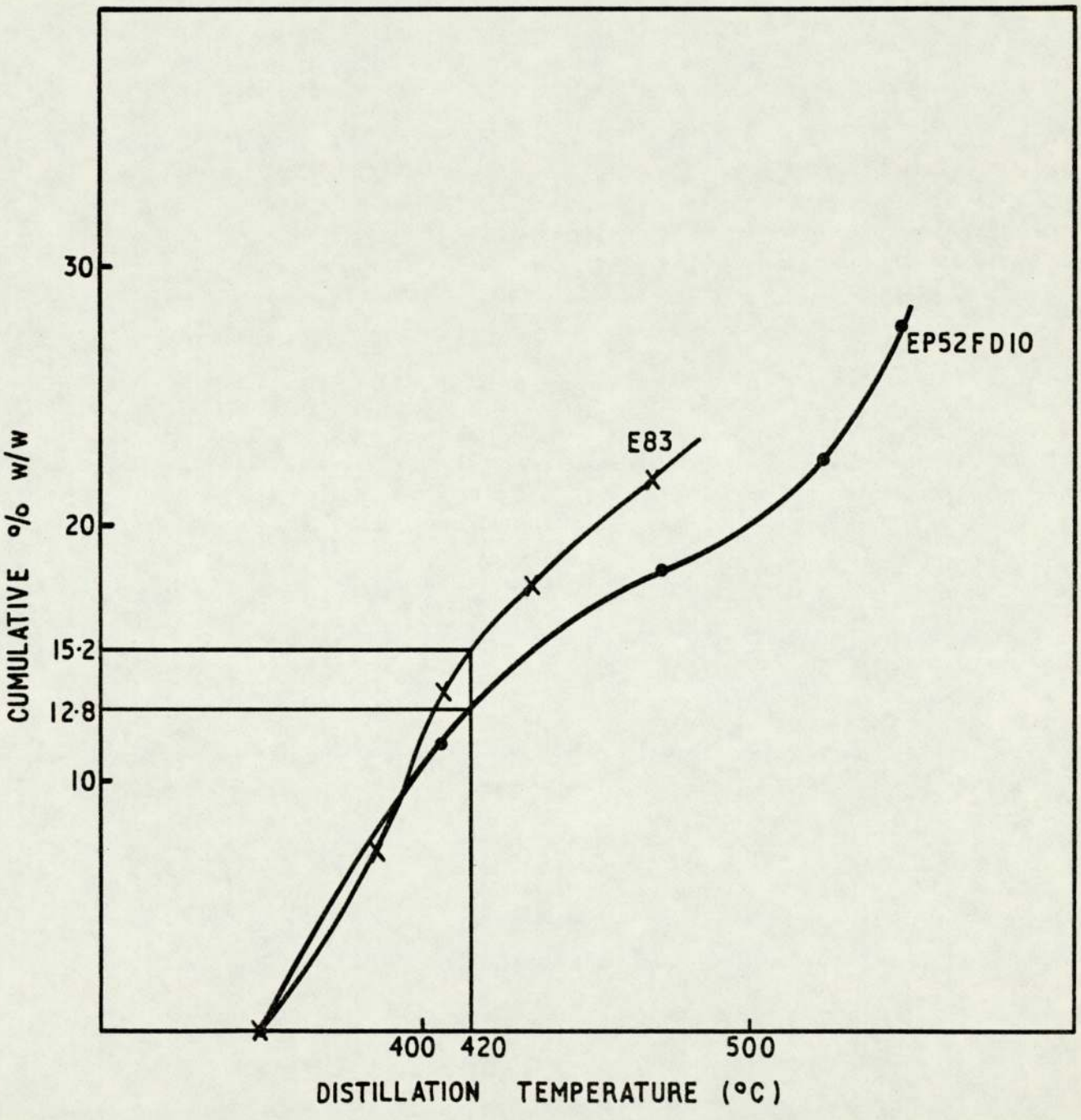

FIGURE 4. BOILING POINT DISTRIBUTION OF COAL EXTRACT SOLUTIONS

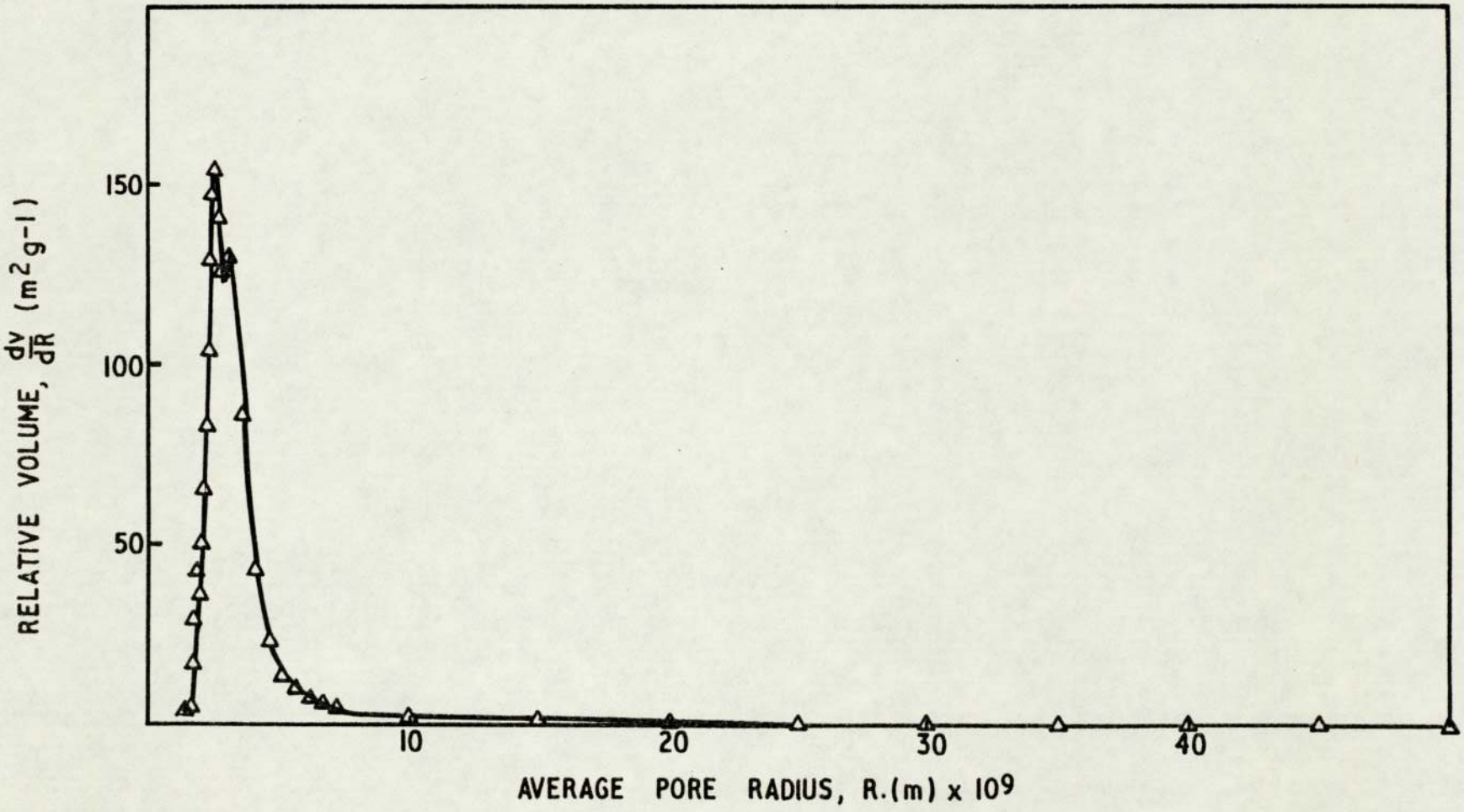

FIGURE 5. PORE SIZE DISTRIBUTION OF GROUND HARSHAW 0402T CATALYST

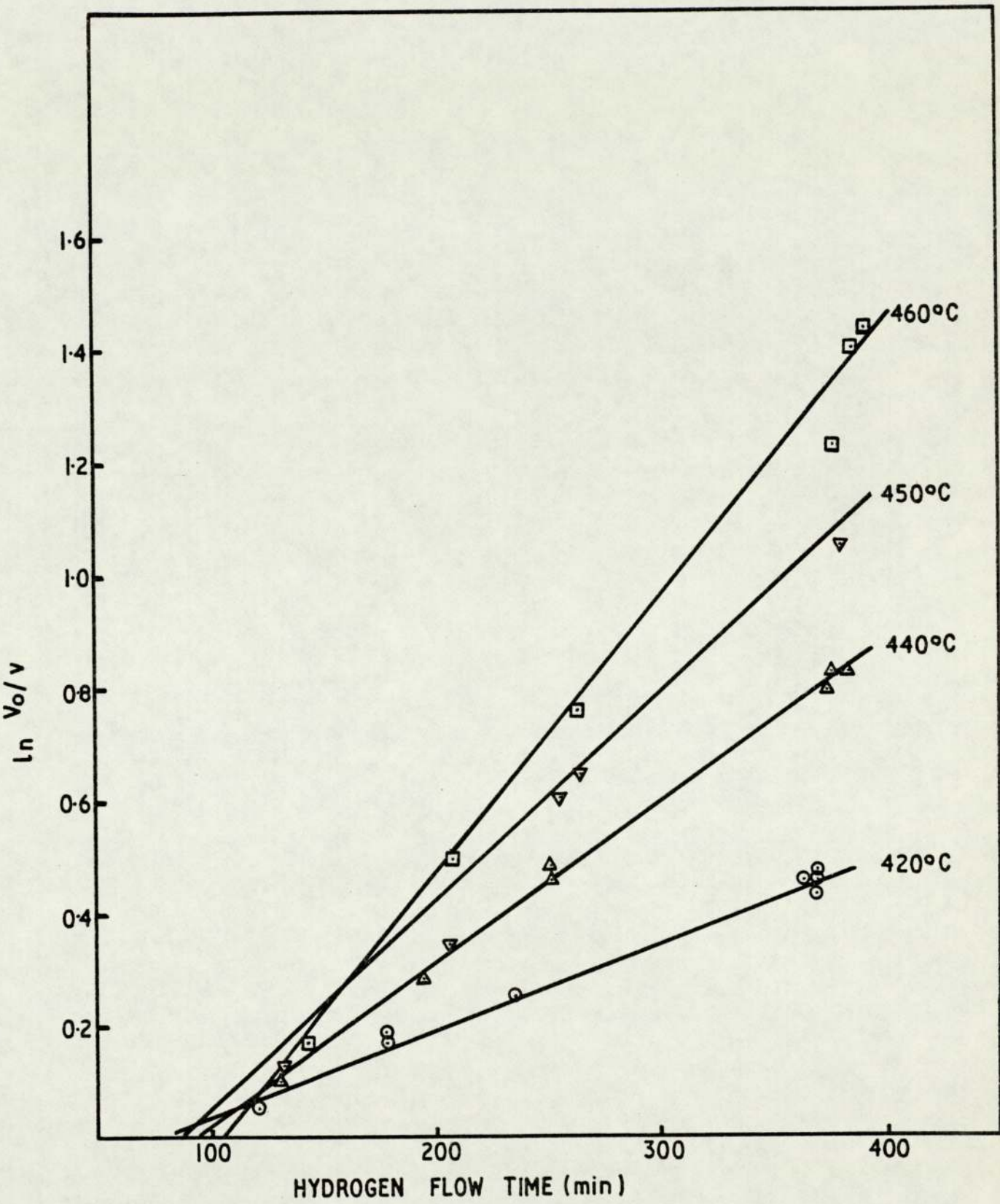

FIGURE 6. PLOTS OF Ln Vo/V v.t AT DIFFERENT REACTION TEMPERATURES

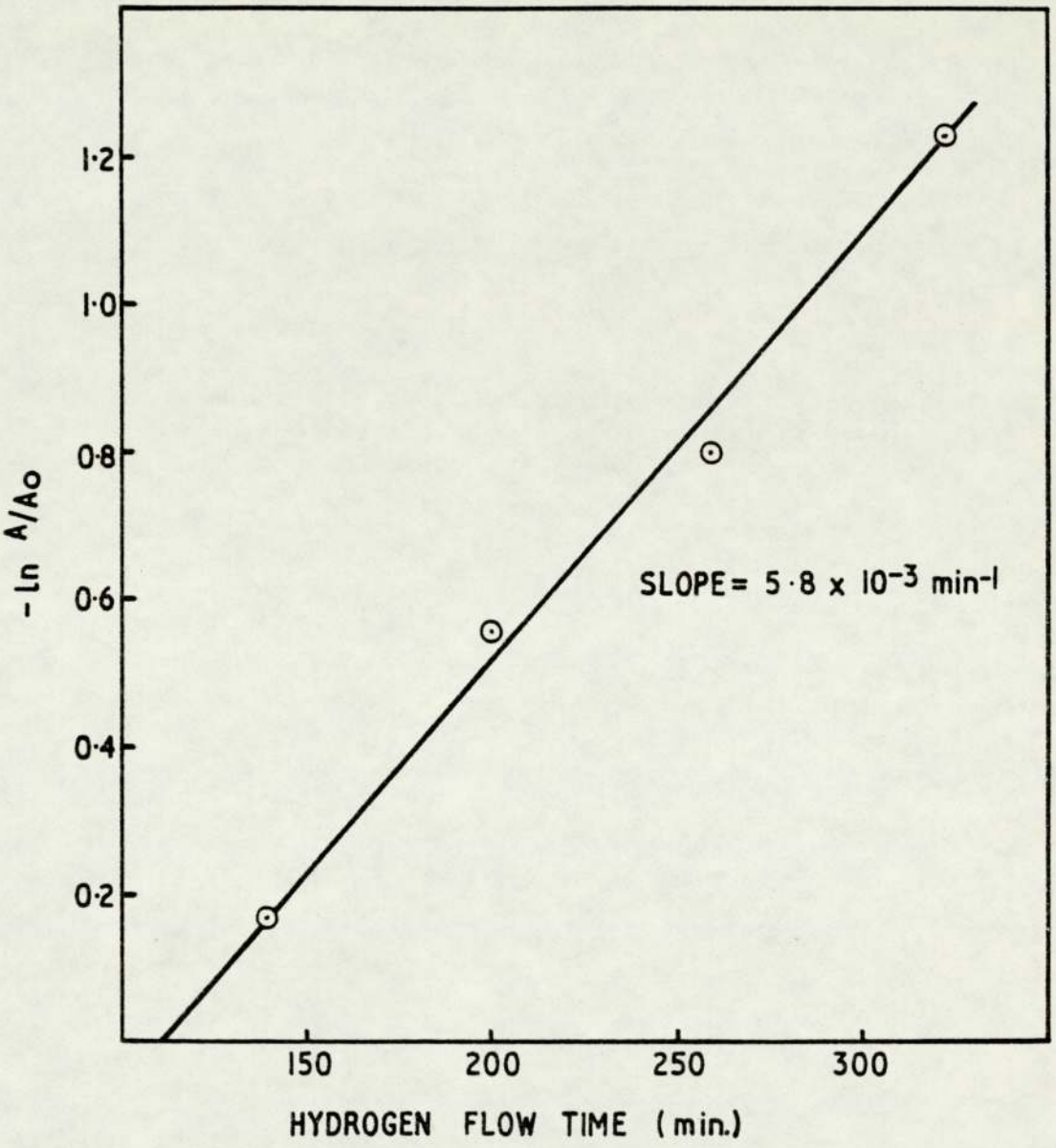

FIGURE 7. PLOT OF FIRST ORDER RATE EXPRESSION FROM PRELIMINARY EXPERIMENTS.

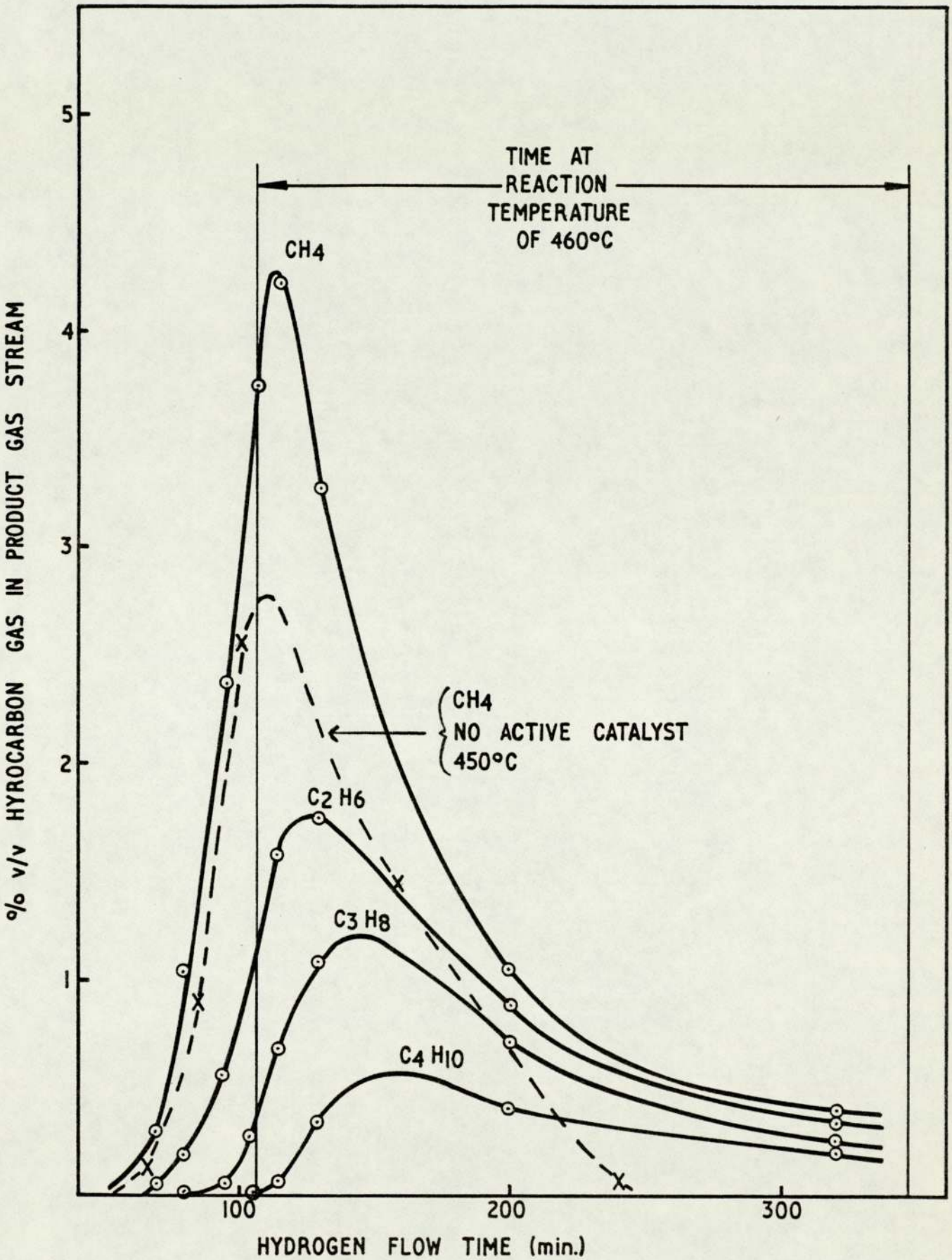

FIGURE 8. RATE OF FORMATION OF GASEOUS HYDROCARBONS DURING AN EXPERIMENT.

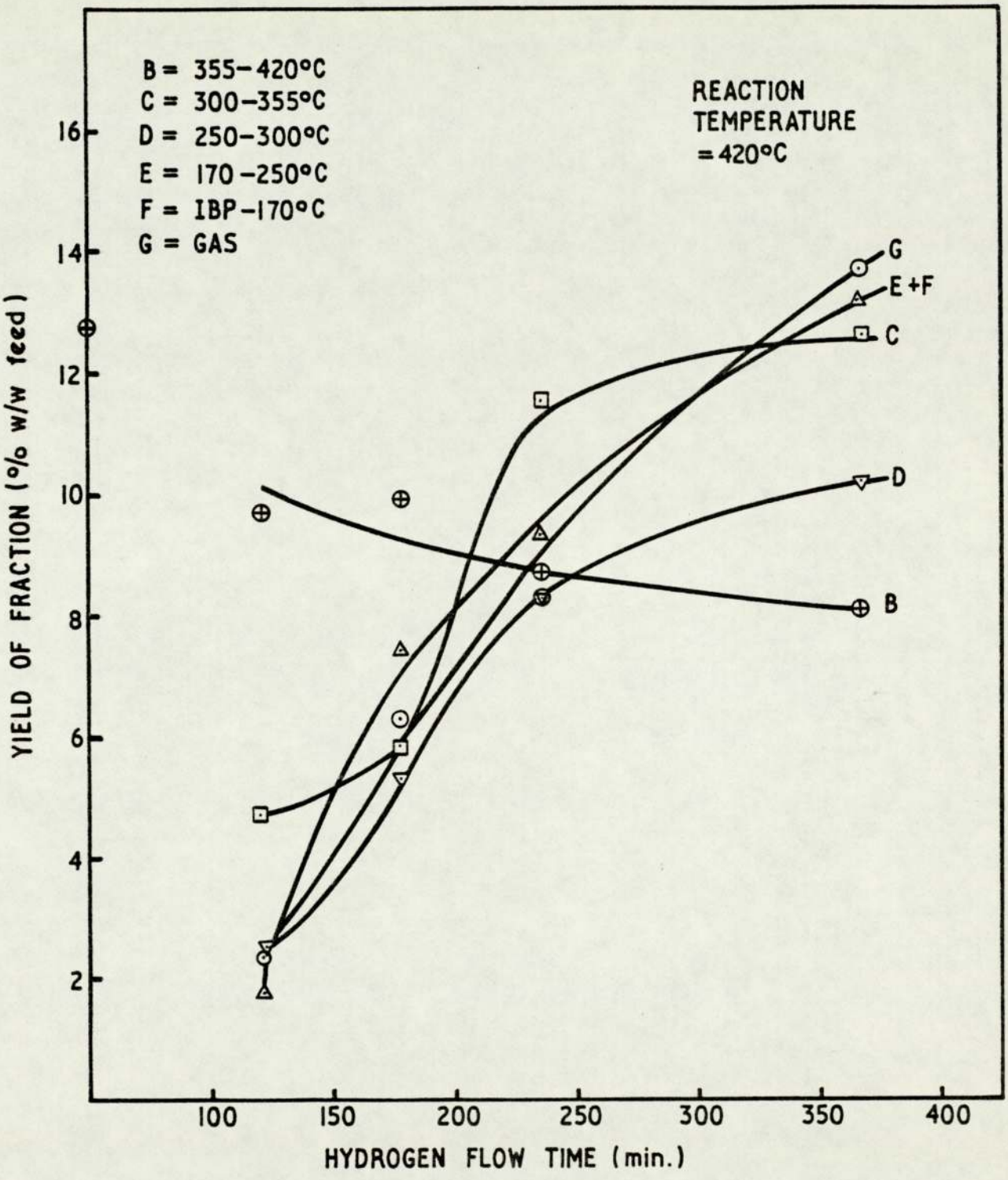

FIGURE 9. RATE OF CHANGE IN YIELD OF PRODUCT FRACTIONS.

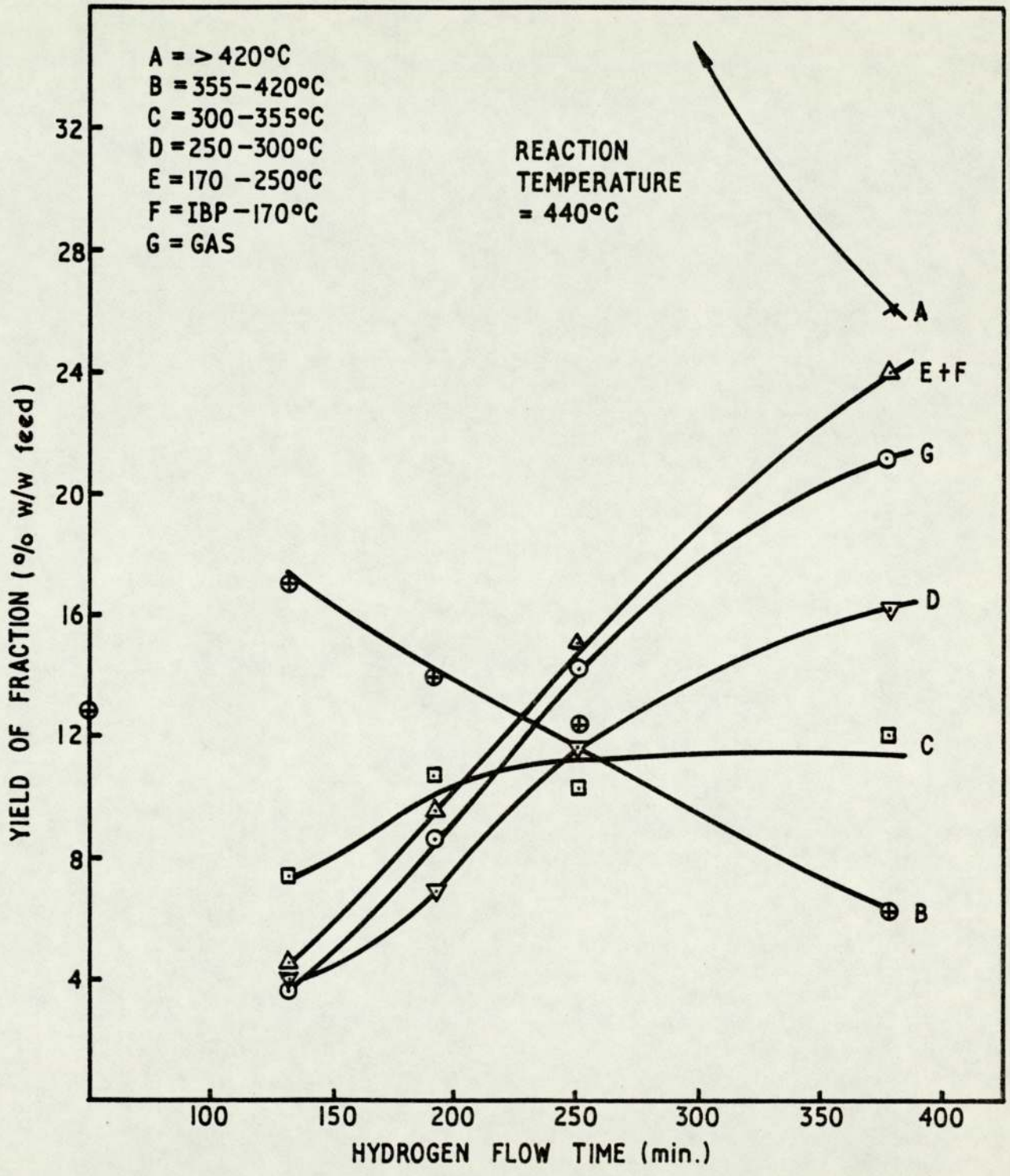

FIGURE 10. RATE OF CHANGE IN YIELD OF PRODUCT FRACTIONS.

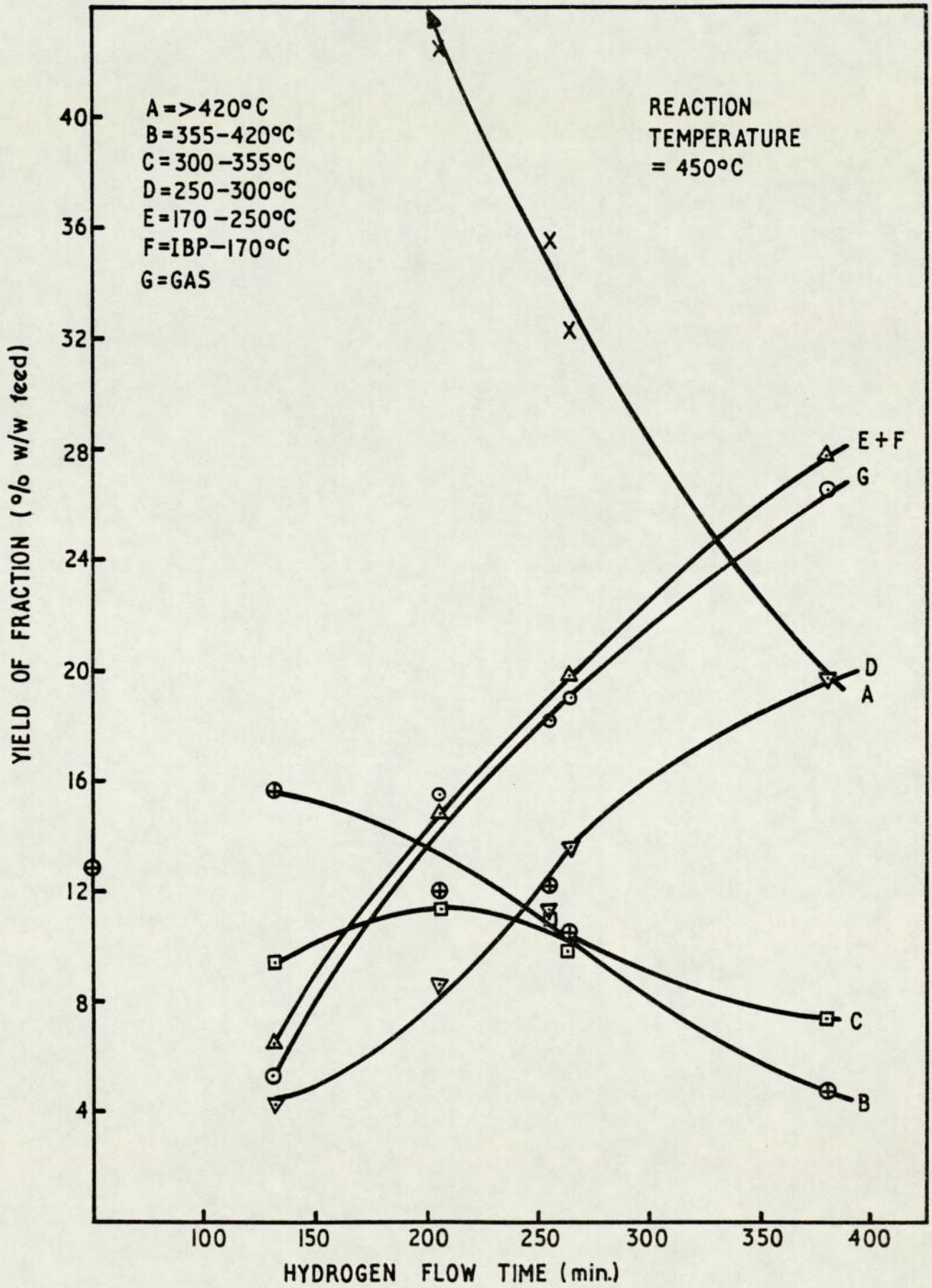

FIGURE II. RATE OF CHANGE IN YIELD OF PRODUCT FRACTIONS.

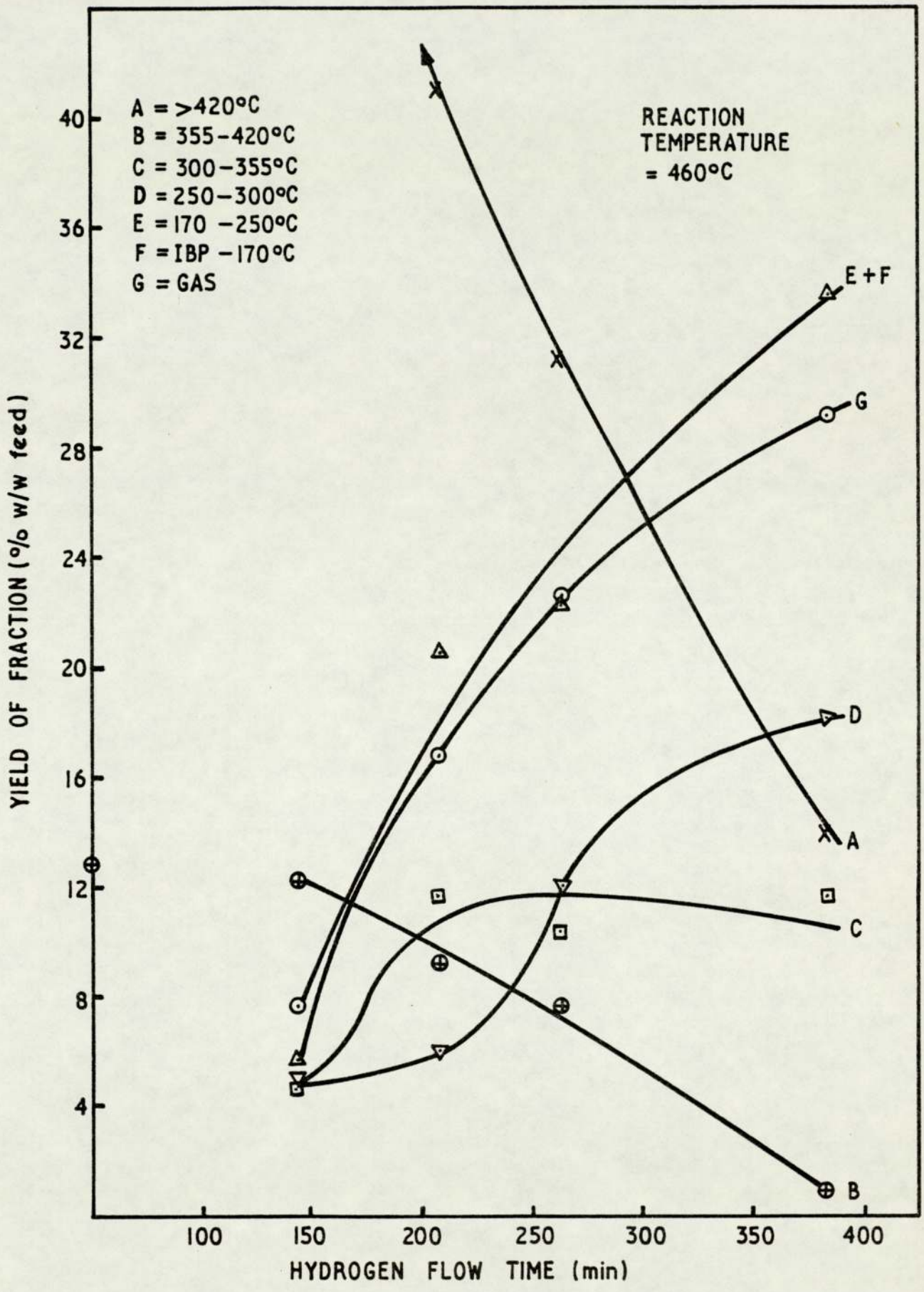

FIGURE 12. RATE OF CHANGE IN YIELD OF PRODUCT FRACTIONS.

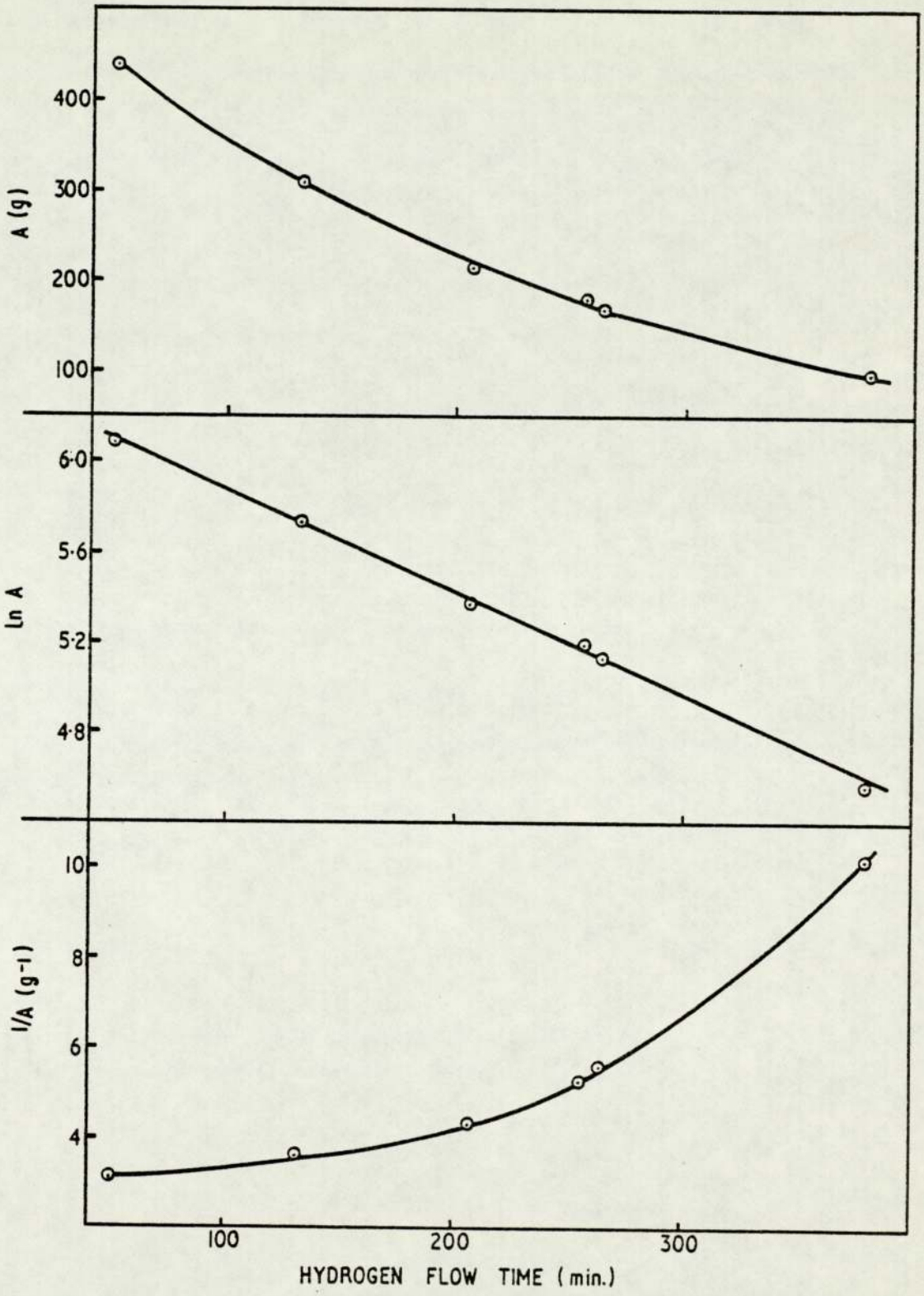

FIGURE 13. PLOTS OF ZERO, FIRST AND SECOND ORDER RATE EXPRESSIONS.

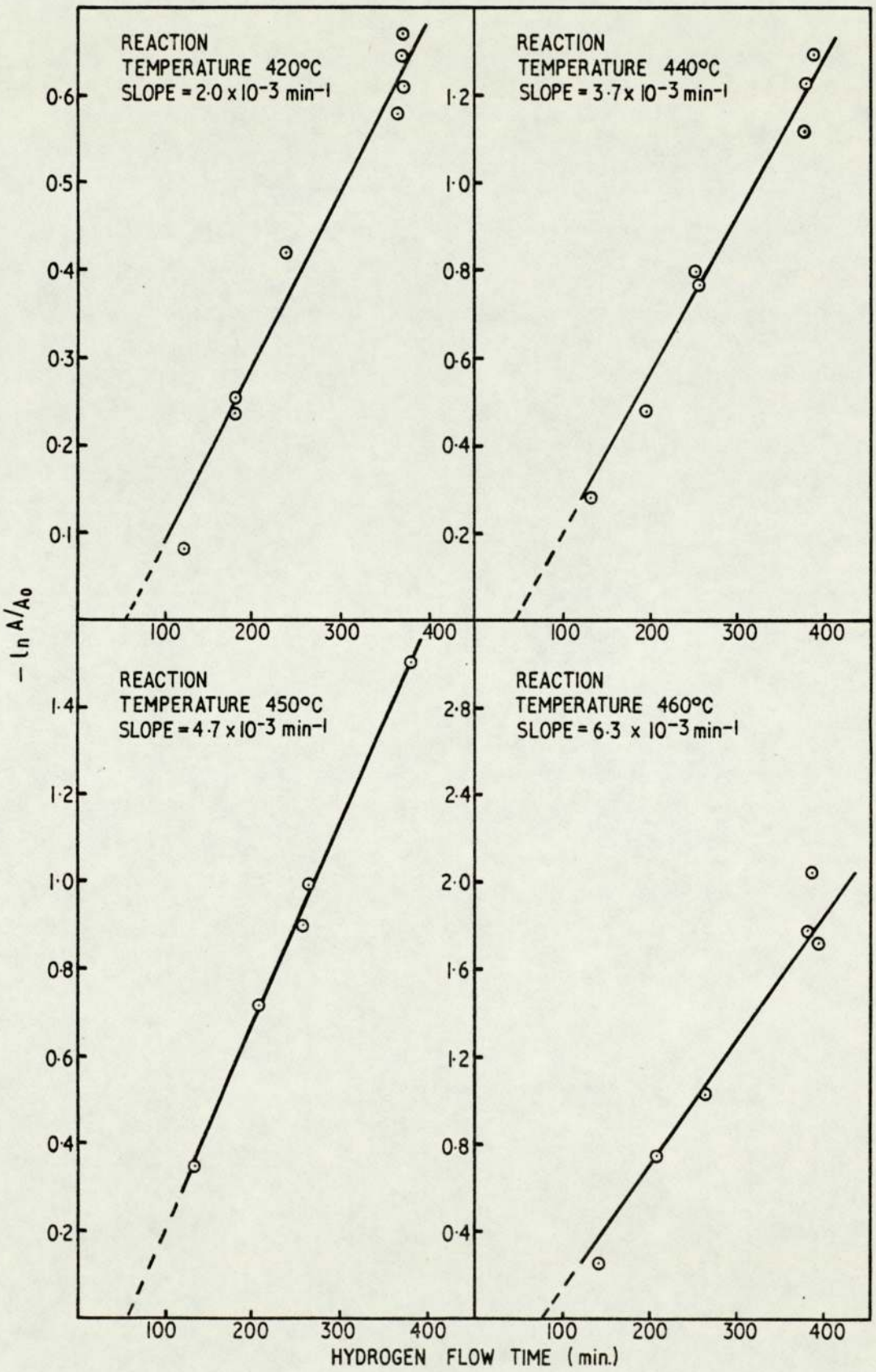

FIGURE 14. PLOTS OF FIRST ORDER RATE EXPRESSION AT DIFFERENT REACTION TEMPERATURES.

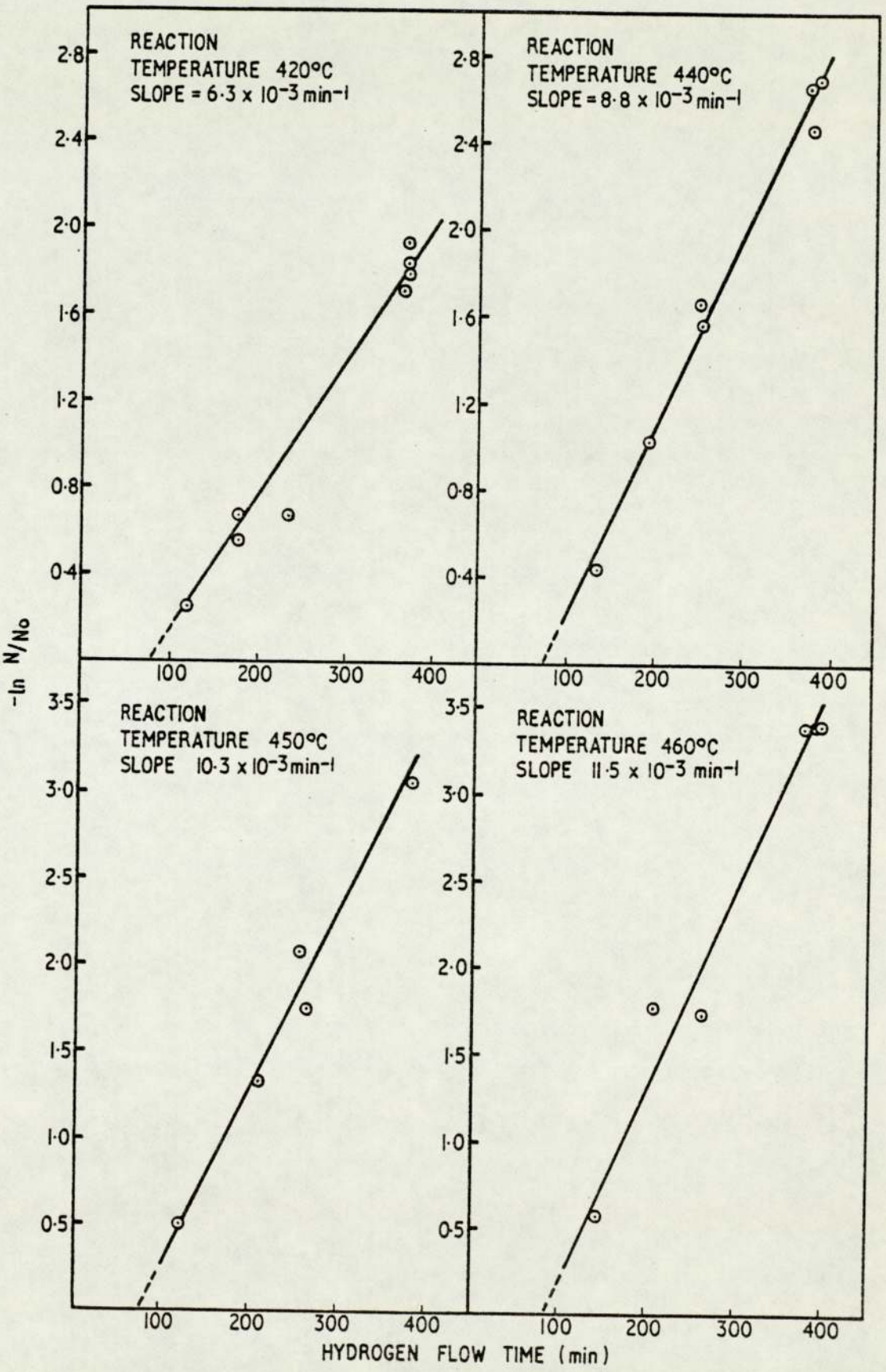

FIGURE 15. FIRST ORDER PLOTS FOR NITROGEN REMOVAL AT DIFFERENT TEMPERATURES.

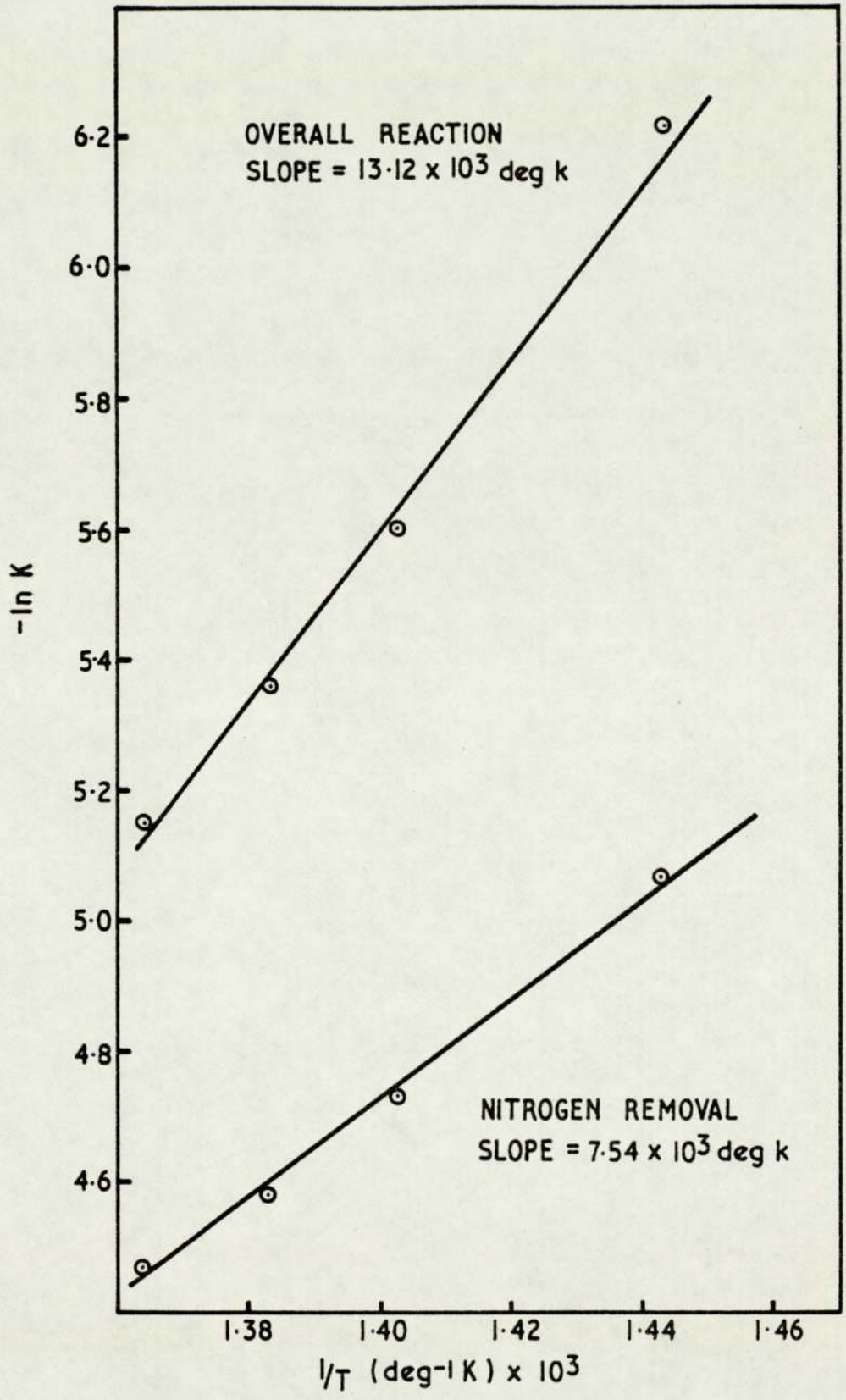

FIGURE 16. ARRHENIUS PLOTS FOR THE OVERALL REACTION AND FOR NITROGEN REMOVAL.

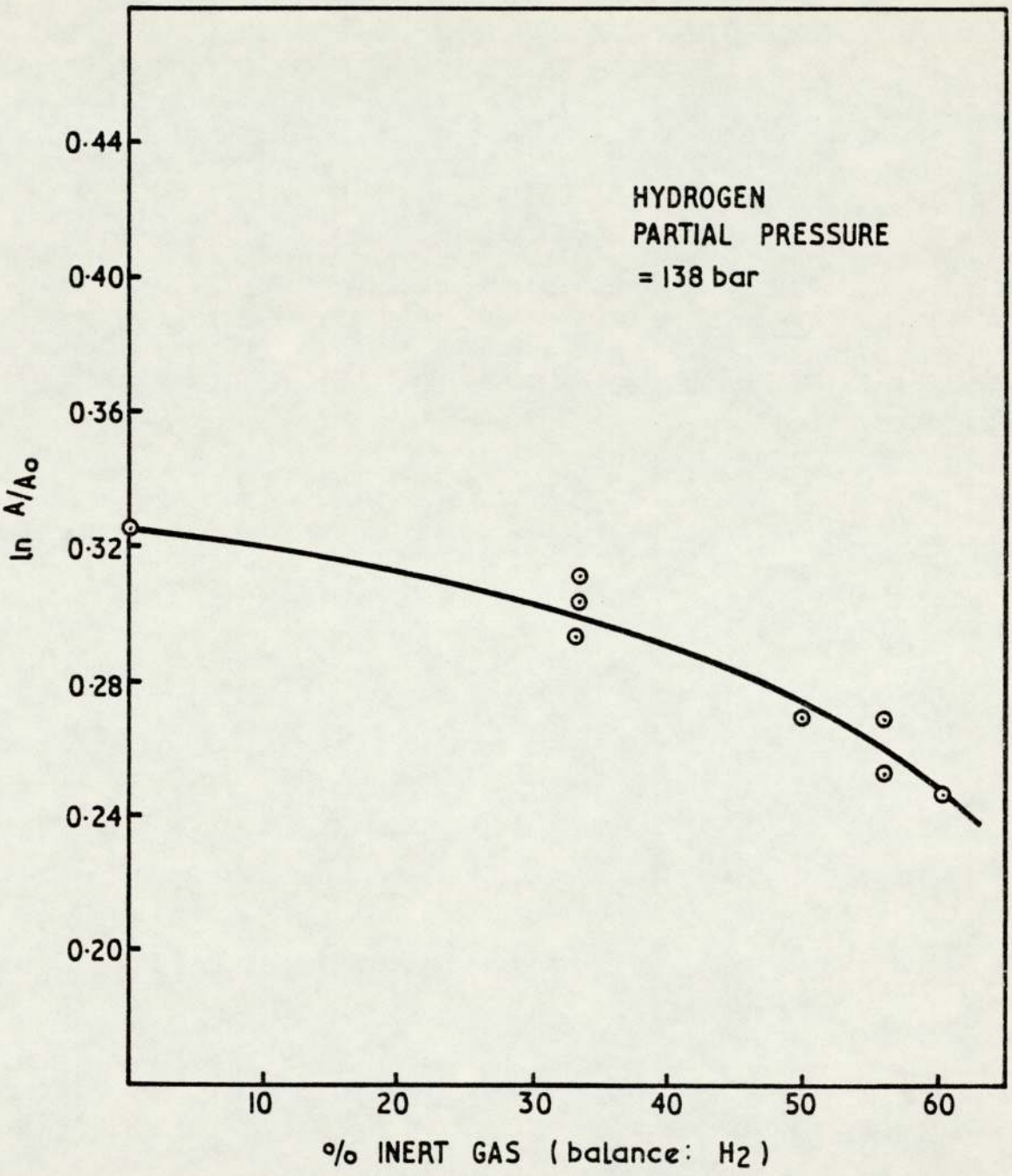

FIGURE 17. EFFECT ON RATE OF INCREASING INERT GAS PARTIAL PRESSURE AT CONSTANT HYDROGEN PARTIAL PRESSURE.

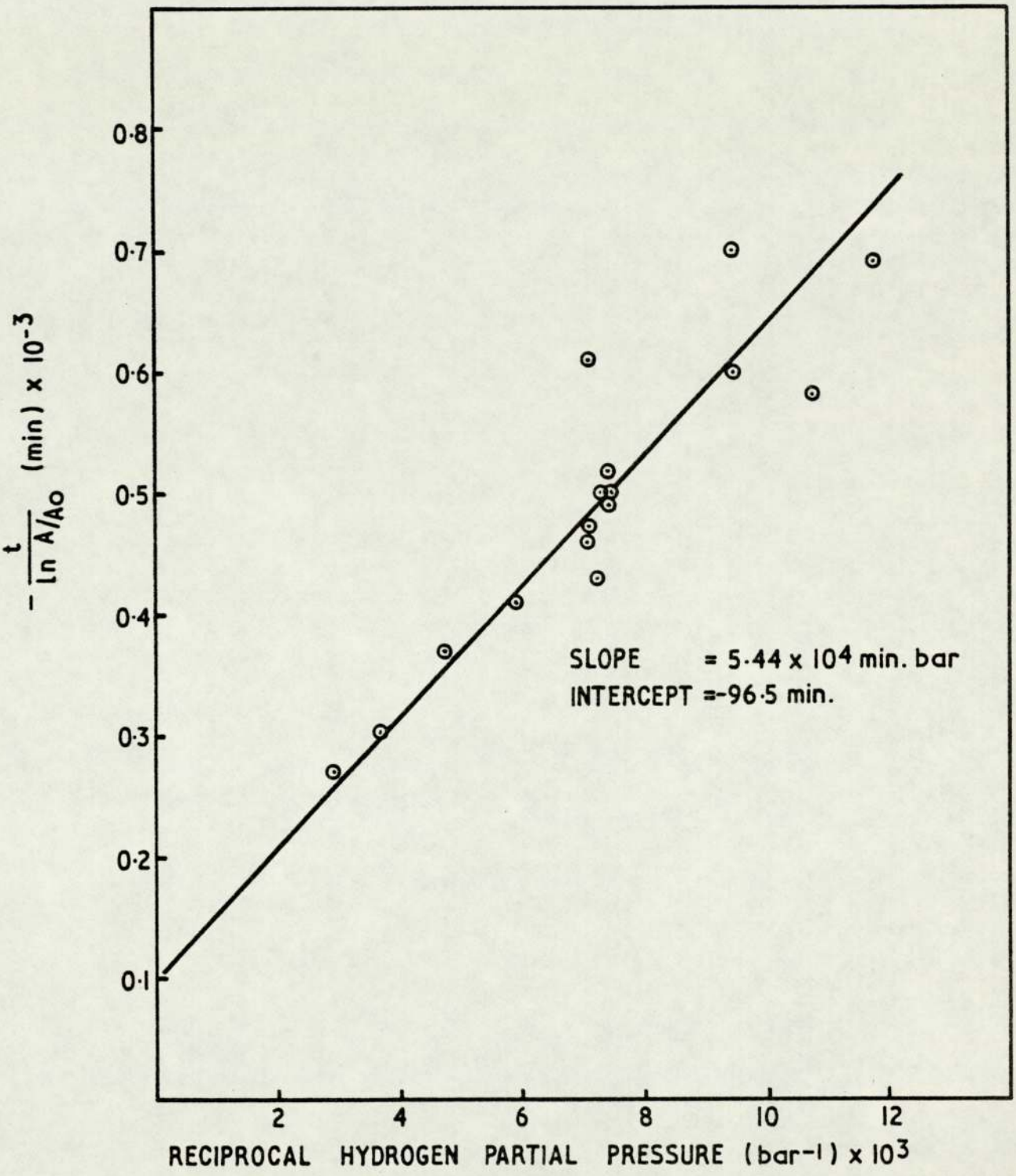

FIGURE 18. PLOT OF MODIFIED RATE EXPRESSION FOR PRESSURE EXPERIMENTS.

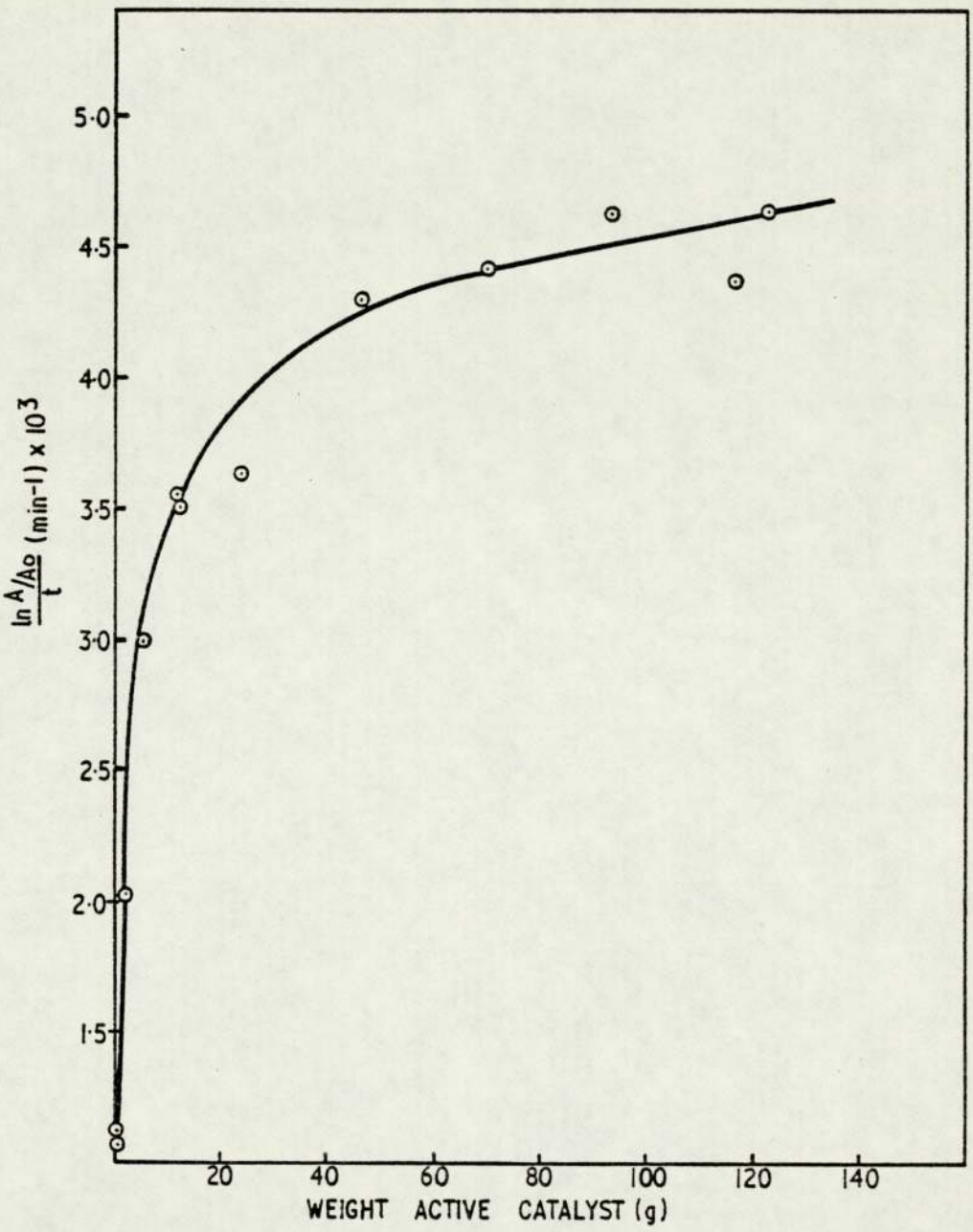

FIGURE 19. CHANGE IN REACTION RATE WITH CATALYST LOADING.

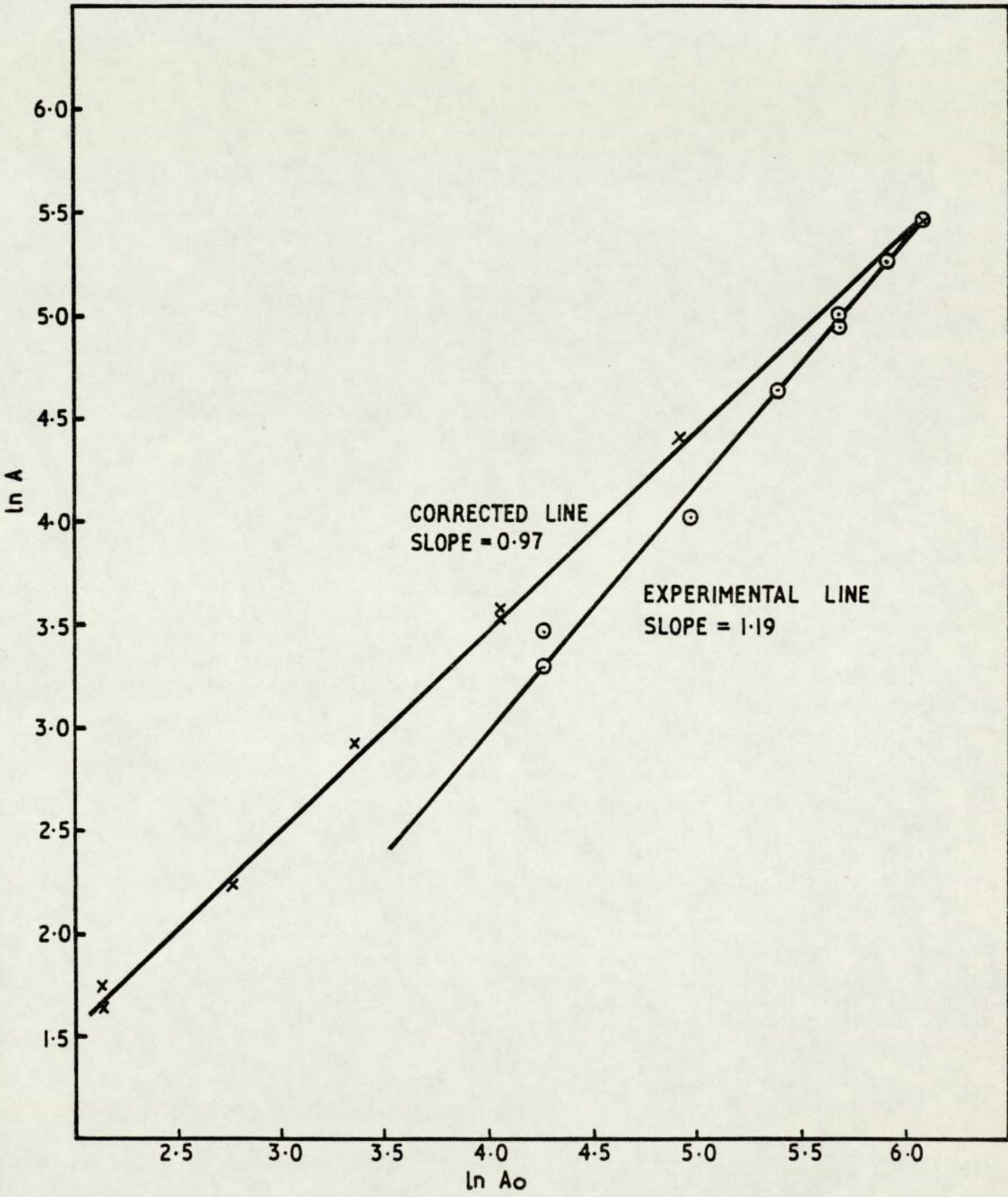

FIGURE 20. PLOT OF RATE EXPRESSION FOR INITIAL COAL EXTRACT SOLUTION CONCENTRATION EXPERIMENTS.

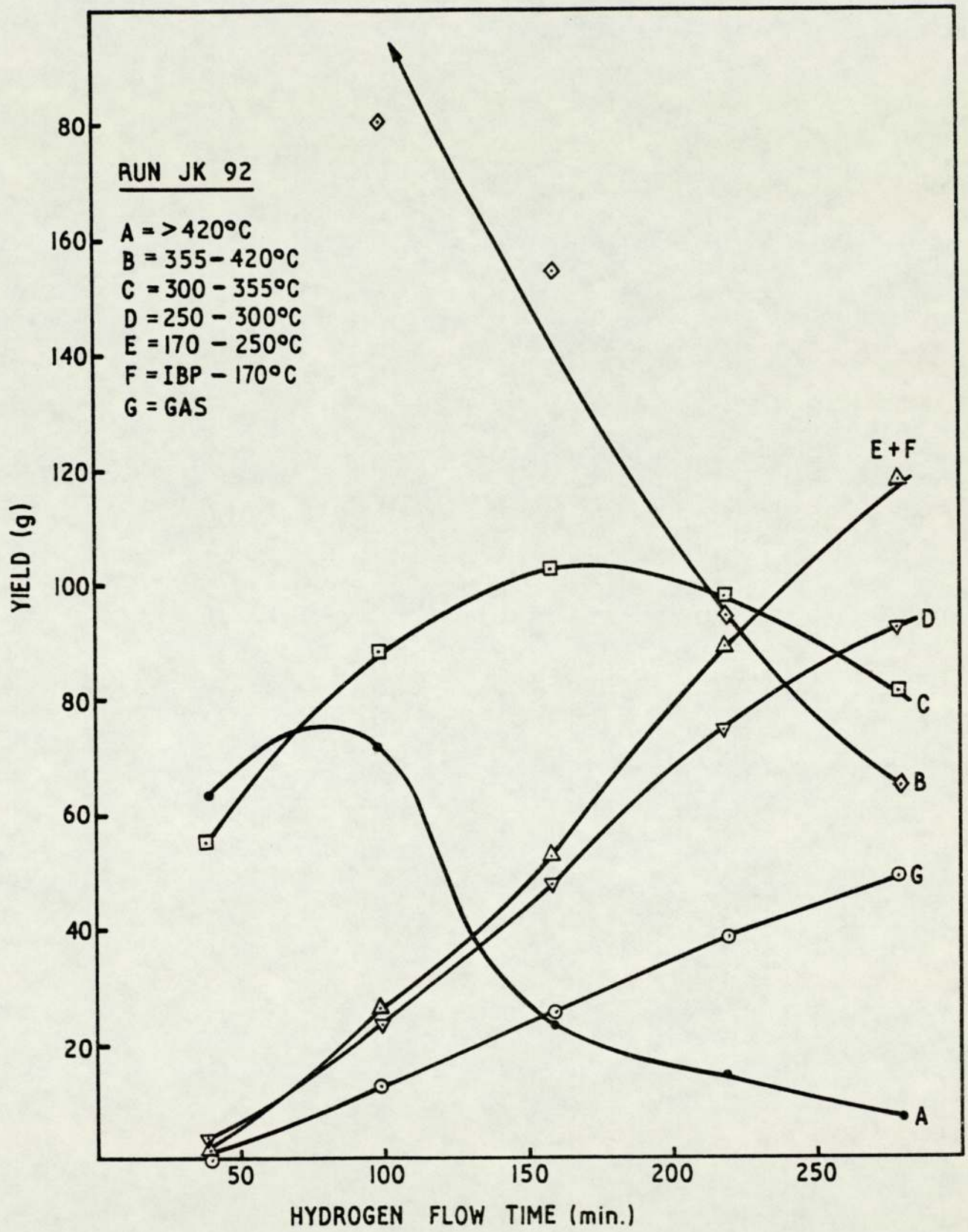

FIGURE 21. RATE OF CHANGE IN YIELD OF PRODUCT FRACTIONS FROM SECONDARY HYDROGENATION OF 355 - 420°C FRACTION.

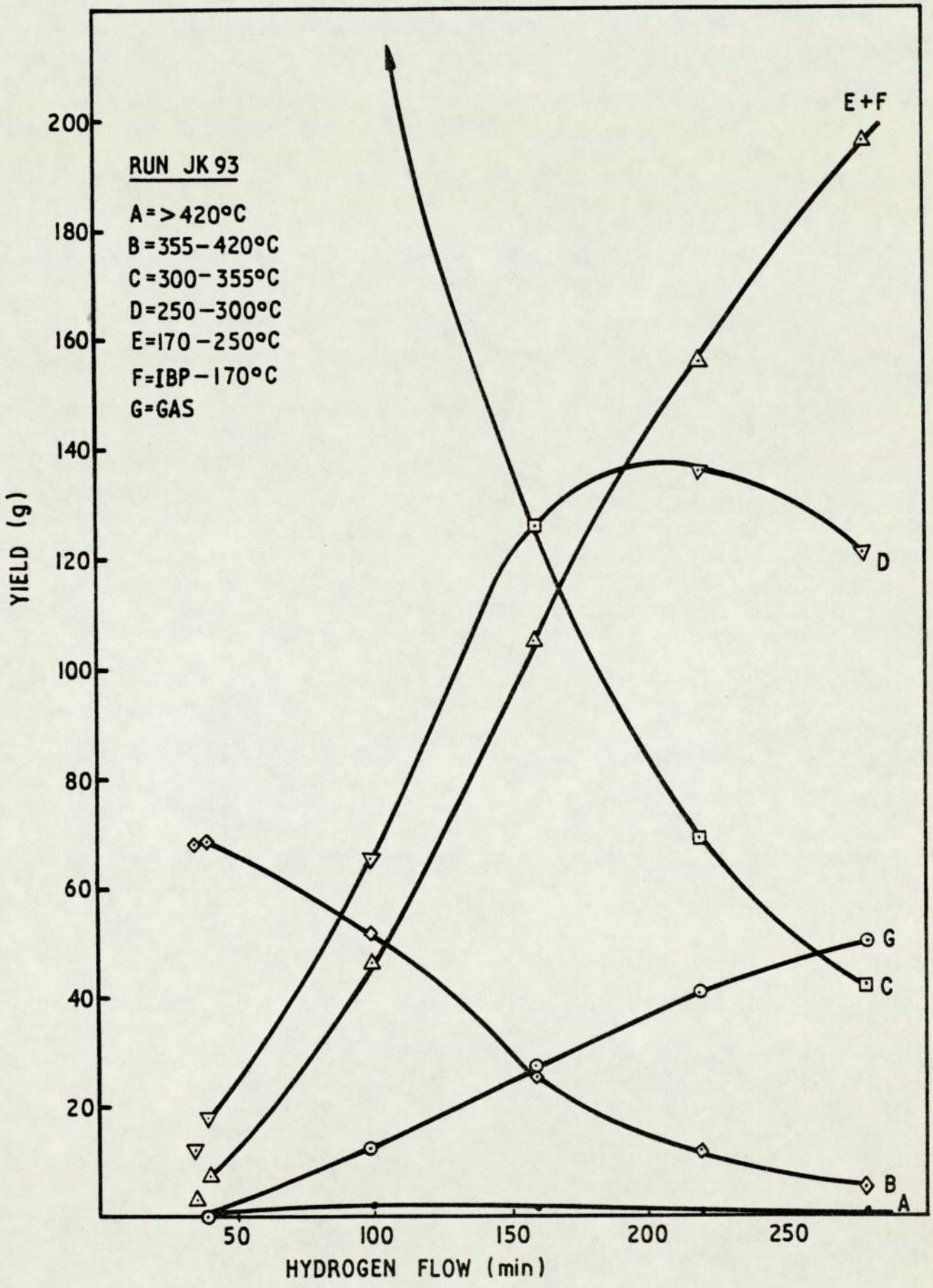

FIGURE 22. RATE OF CHANGE IN YIELD OF PRODUCT FRACTIONS FROM SECONDARY HYDROGENATION OF 300-355°C FRACTION.

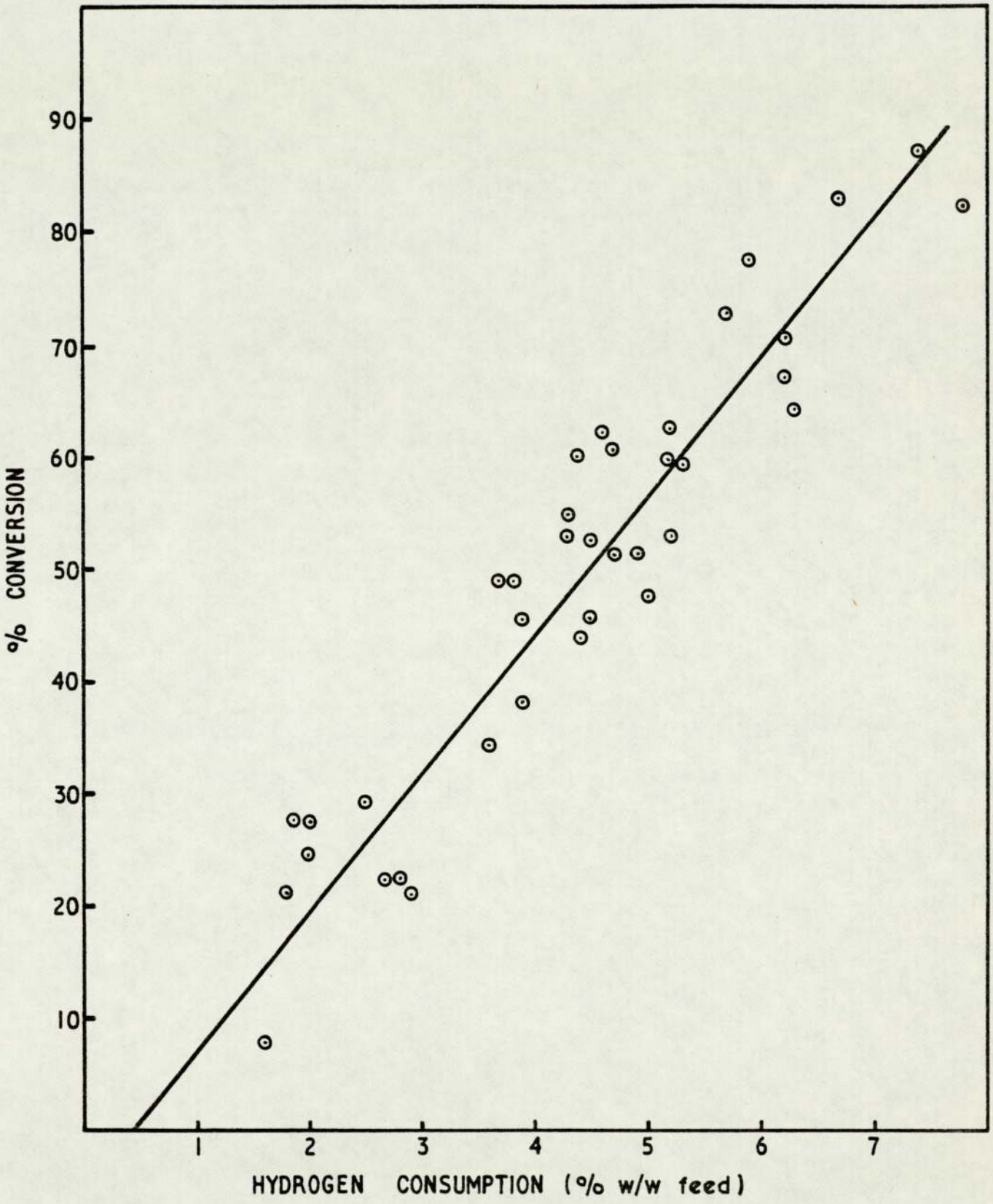

FIGURE 23. RELATIONSHIP BETWEEN HYDROGEN CONSUMPTION AND CONVERSION FOR LOW RANK COAL EXTRACT SOLUTION.

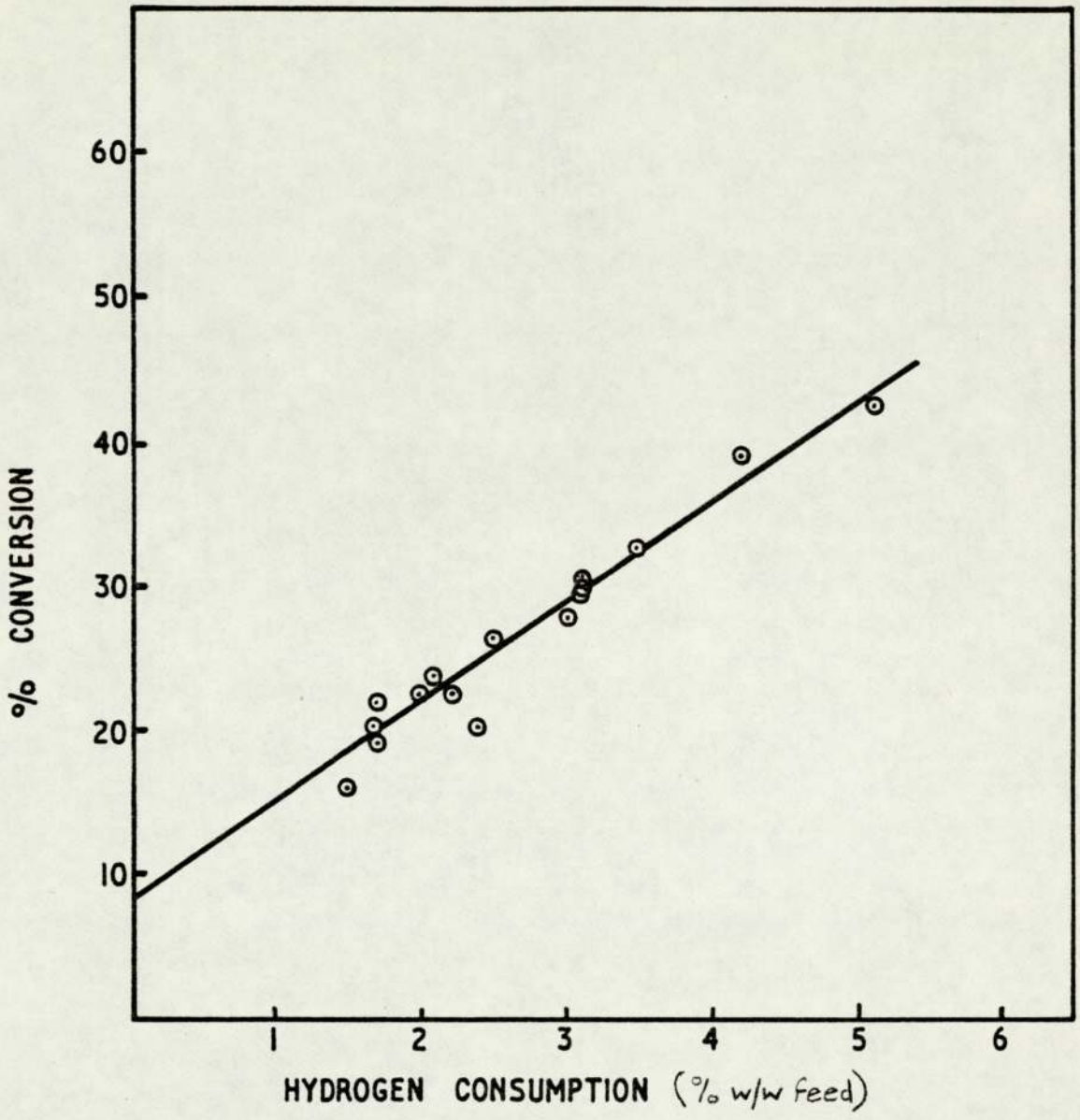

FIGURE 24. RELATIONSHIP BETWEEN HYDROGEN CONSUMPTION AND CONVERSION FOR HIGH RANK COAL EXTRACT SOLUTION.

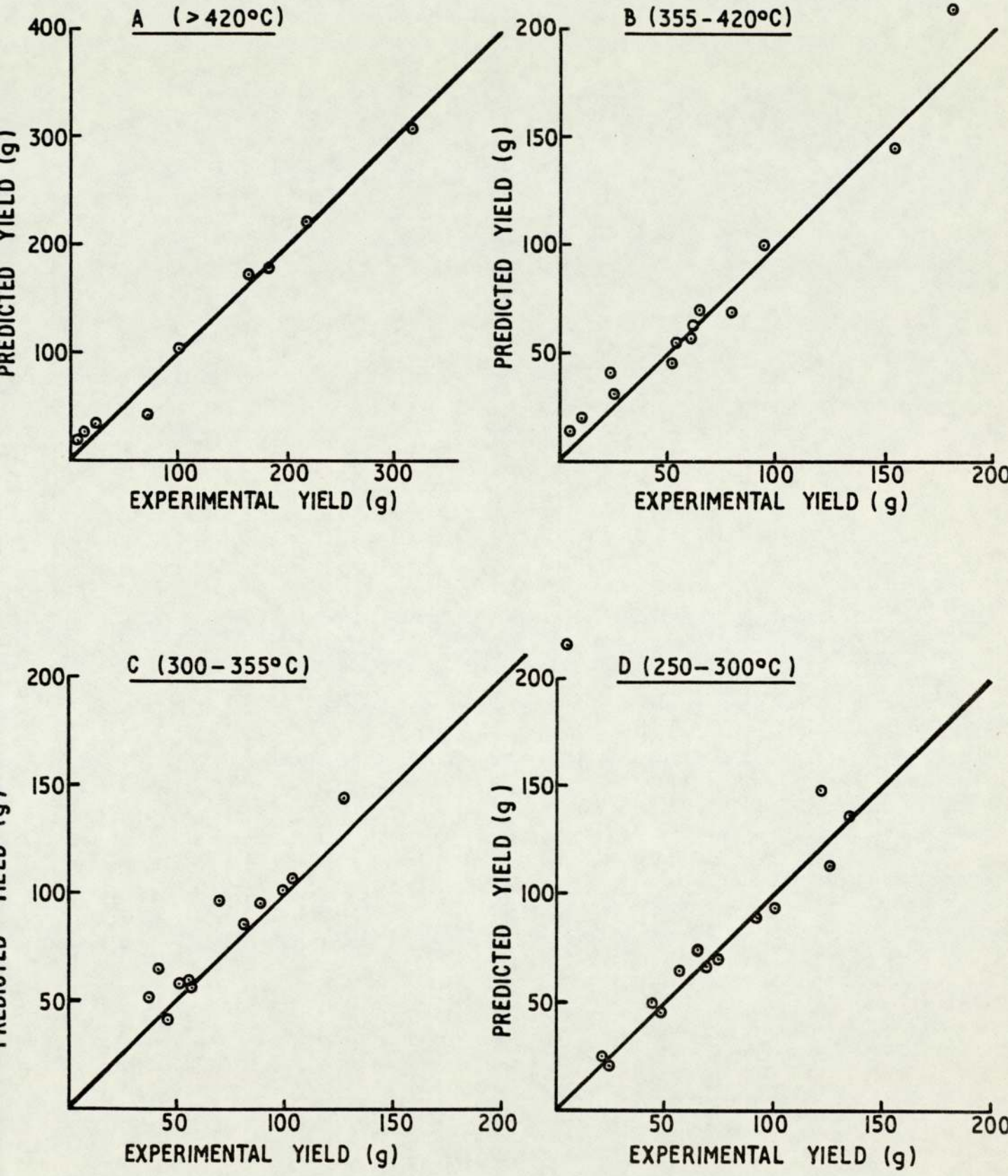

FIGURE 25. TEST OF KINETIC MODEL FOR FRACTIONS A,B,C AND D.

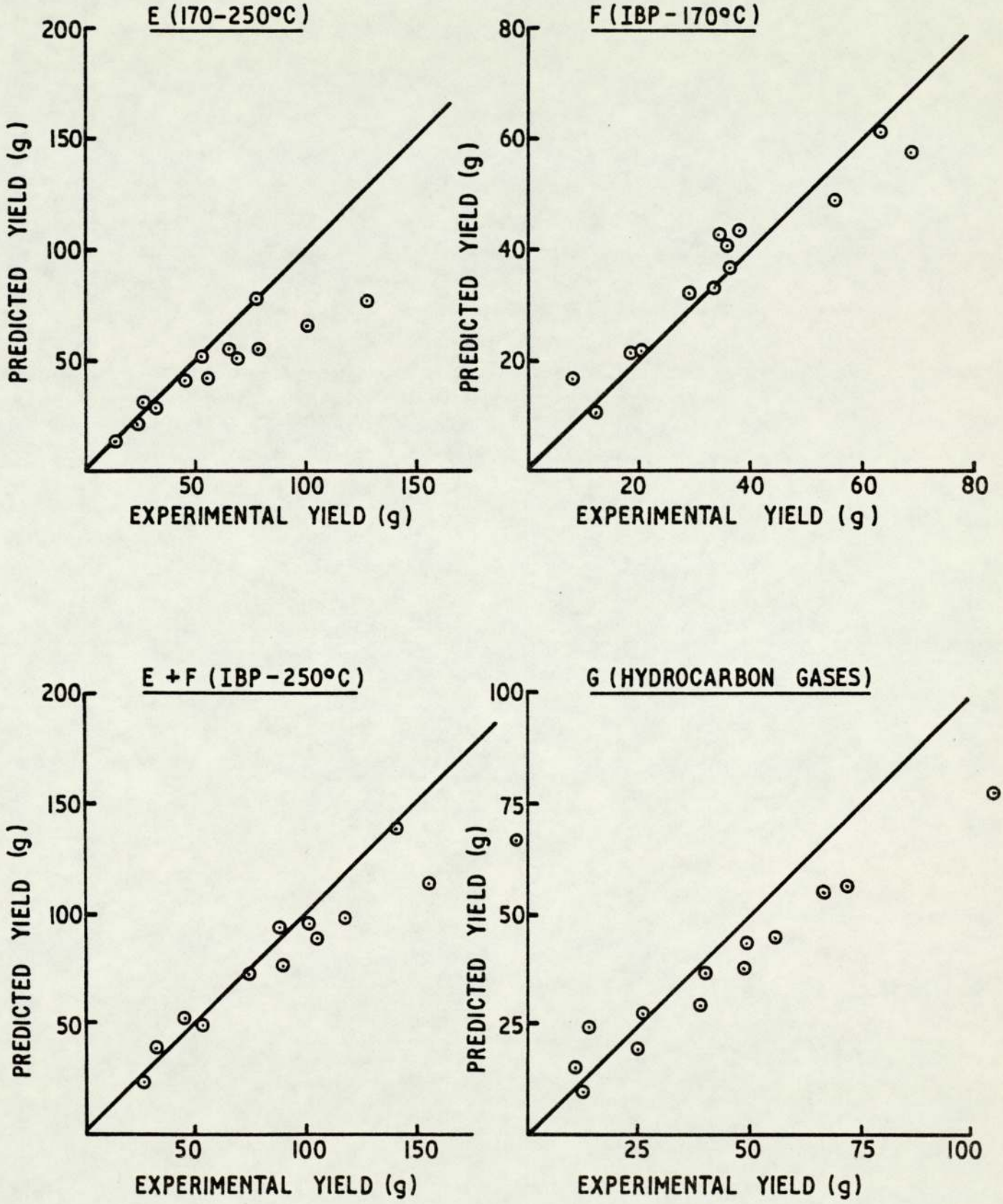

FIGURE 26. TEST OF KINETIC MODEL FOR FRACTIONS E, F, E + F AND G.

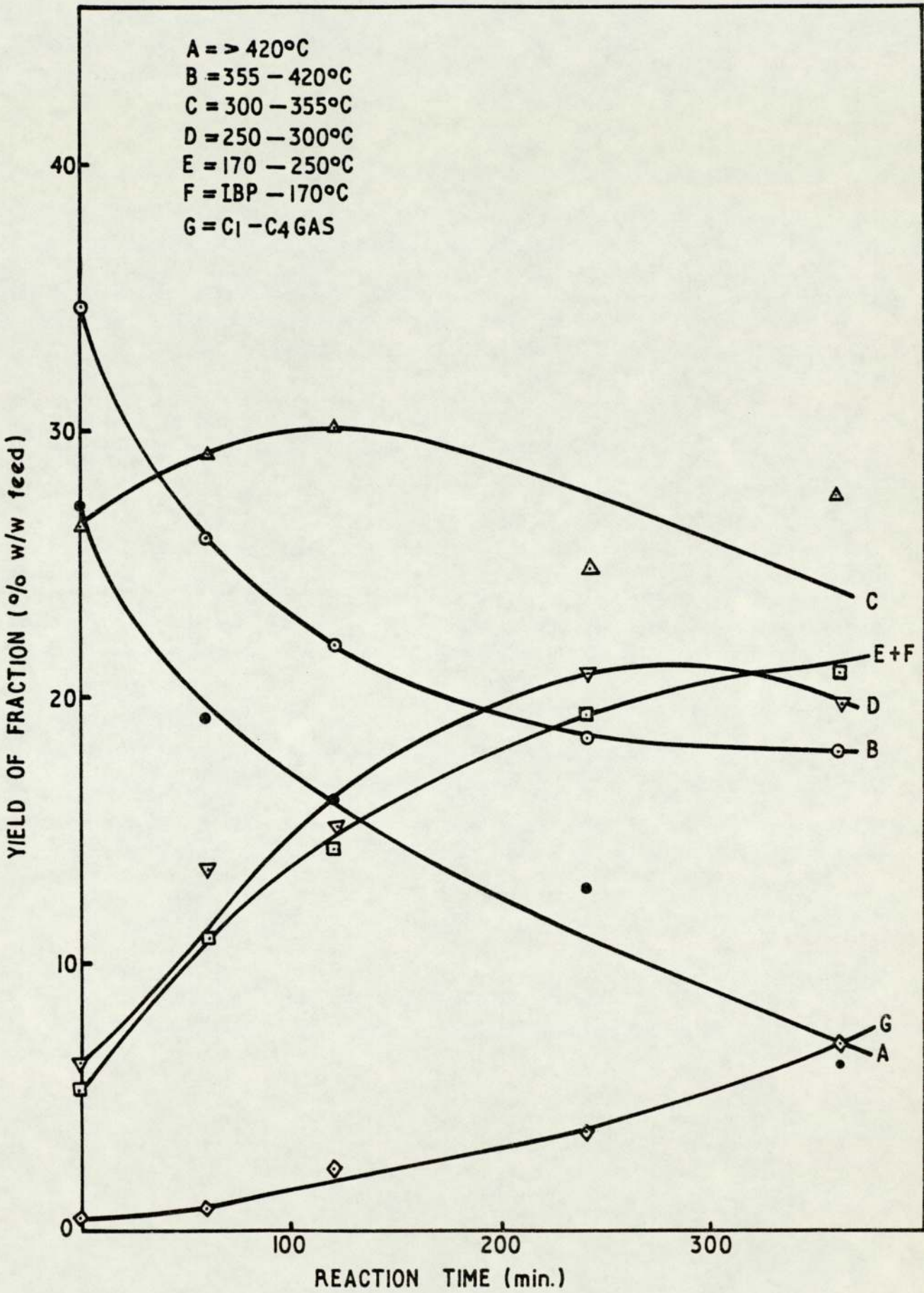

FIGURE 27. RATE OF CHANGE IN YIELD OF PRODUCT FRACTIONS — 2L CATALYST BASKET REACTOR.

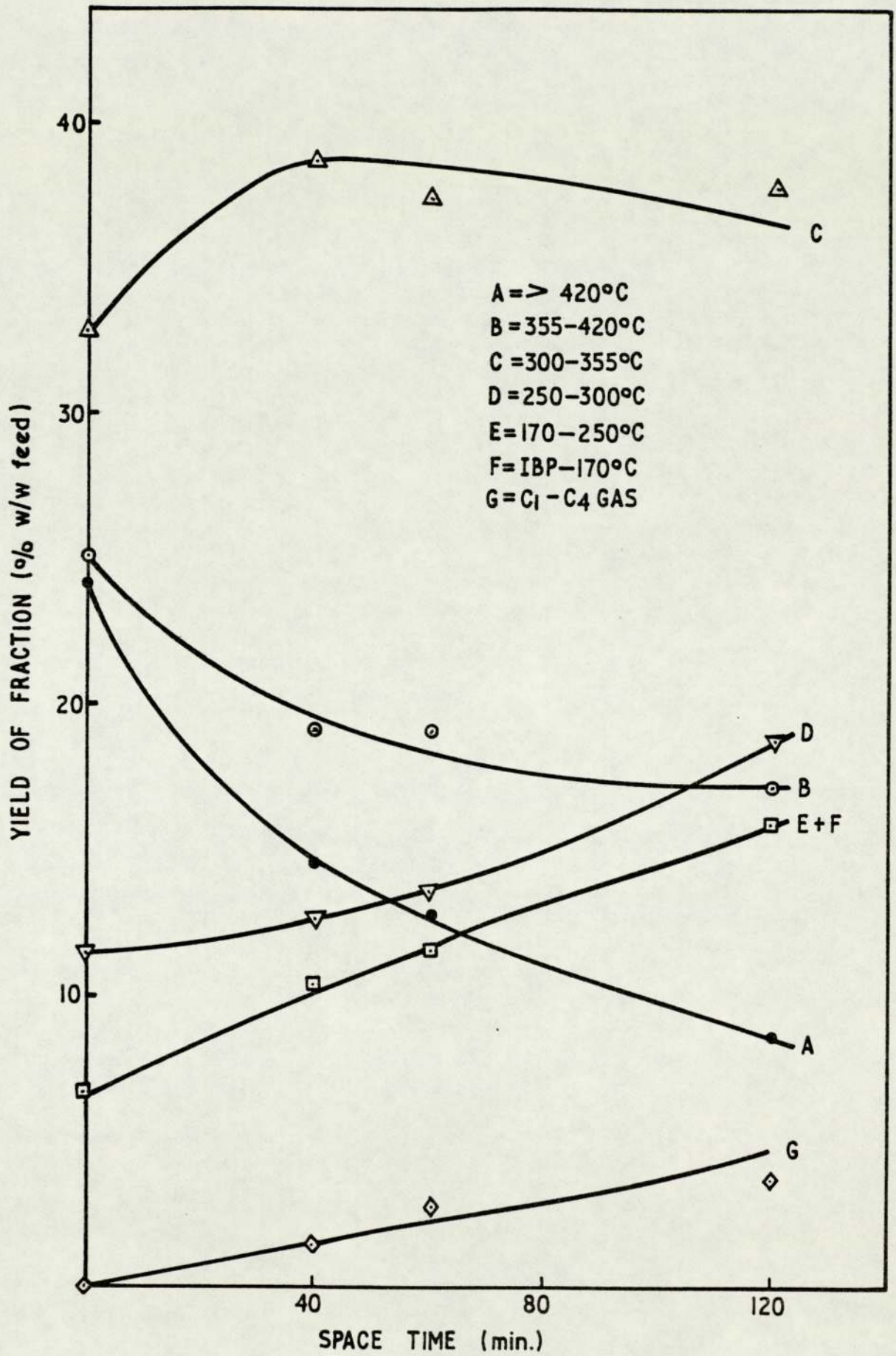

FIGURE 28. RATE OF CHANGE IN YIELD OF PRODUCT FRACTIONS — CONTINUOUS TRICKLE-BED REACTOR.

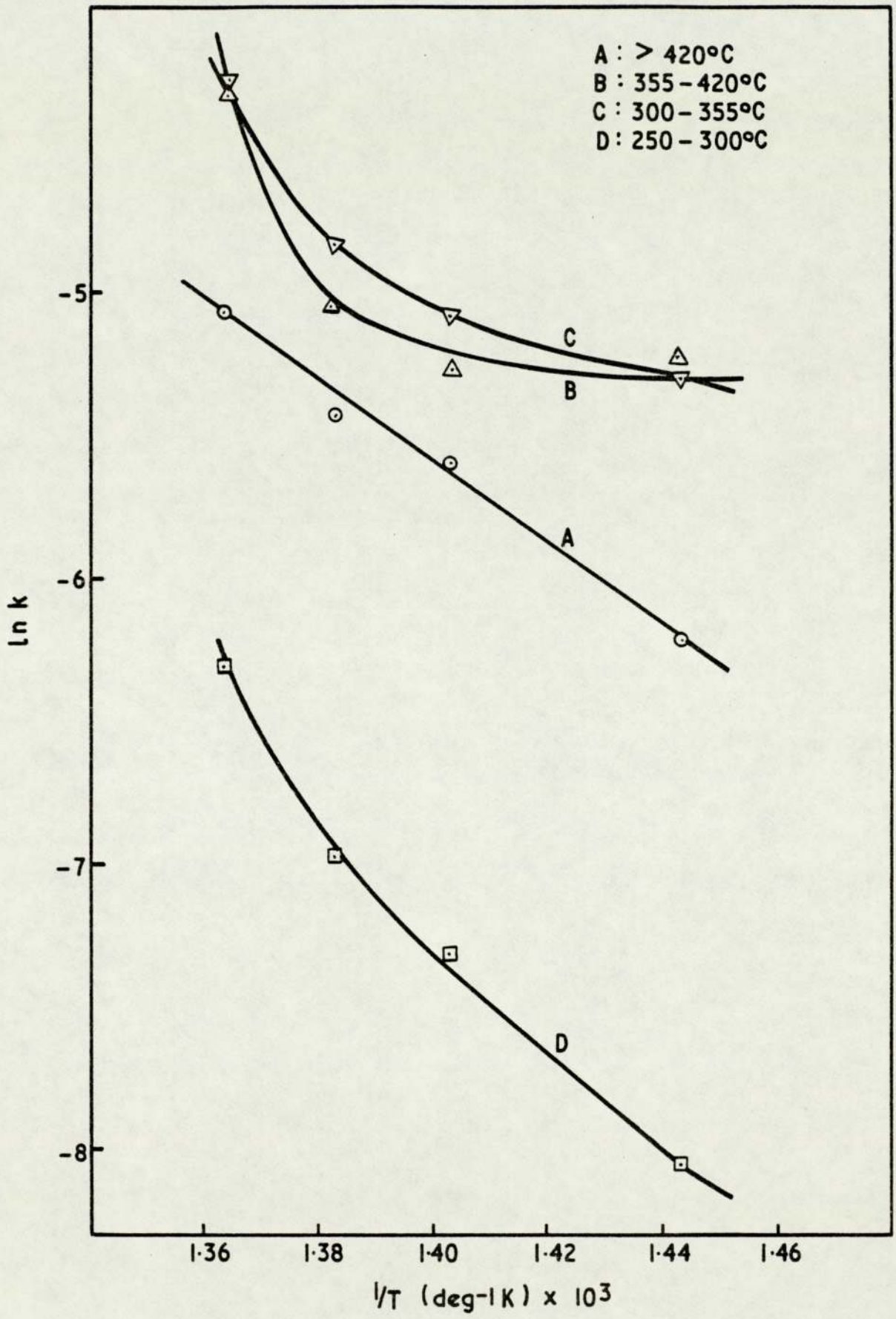

FIGURE 29. ARRHENIUS PLOTS FOR OVERALL REACTIONS OF A,B,C AND D.

APPENDIX 1

DETAILS OF SEALS AND CONNECTIONS

A.1.1 Main Closure Seal

The components making up the main closure seal were the body of the reactor, the autoclave head, a stainless steel hoop seal-ring and six closure bolts.

The thin cross-section of the ring was designed so that on increasing internal pressure on the inner face, the ring would tend to expand due to increased hoop stress, and bear against the seal faces on the autoclave head and body. Since the seal portion of the ring was radiused and the seals in the body and head were tapered, the resultant contact area was very small. This small contact area, together with the high load combined to give a high bearing stress in the seal area. With the high bearing stress (or contact load) the metal to metal seal resulted in a potentially leak-free design. However, in practice, any dirt or small scratch on any of the sealing faces could cause serious leaks.

After several experiments had been completed, the autoclave head became difficult to seal because of either the expansion of the autoclave or the contraction of the hoop seal or both. To remedy the situation, an oversize hoop seal was specially manufactured.

After initial teething troubles, this seal worked very satisfactorily.

A.1.2 "Cone and Thread" Connections

Most of the high pressure connections used were of the "Cone and Thread" type. Figure A1-1 shows the components of the fitting, which were:

(i) A threaded female opening with a female cone seat at the bottom.

(ii) Two opposed "weep holes" between the thread and seat through which any leak could be detected.

(iii) A male cone and a left-hand male thread on the end of the tubing.

(iv) A collar, chamferred at both ends and having a left-hand female thread which screwed on to the tube. The left-hand thread prevented unscrewing as the right-hand threaded gland unit was tightened.

(v) A gland unit having an internal 45° shoulder to mate with the collar chamfer to provide sealing thrust and end-load support.

The male cone had a slightly smaller included angle than the female cone. The initial line-contact between the two cones had a theoretical area equal to zero. Low-torque gland nut loads created stresses that produced localized yielding and plastic flow at the seal contact. As the gland unit was torqued to the specified value, the line contact broadened to an annular area seal just wide enough to support the sealing thrust, with the sealing stress equal to the yield strength of the material.

This mechanism obliterated surface imperfections remaining after coning so that leak-paths were eliminated. In practice, no leaks were ever found from this type of fitting when correctly assembled.

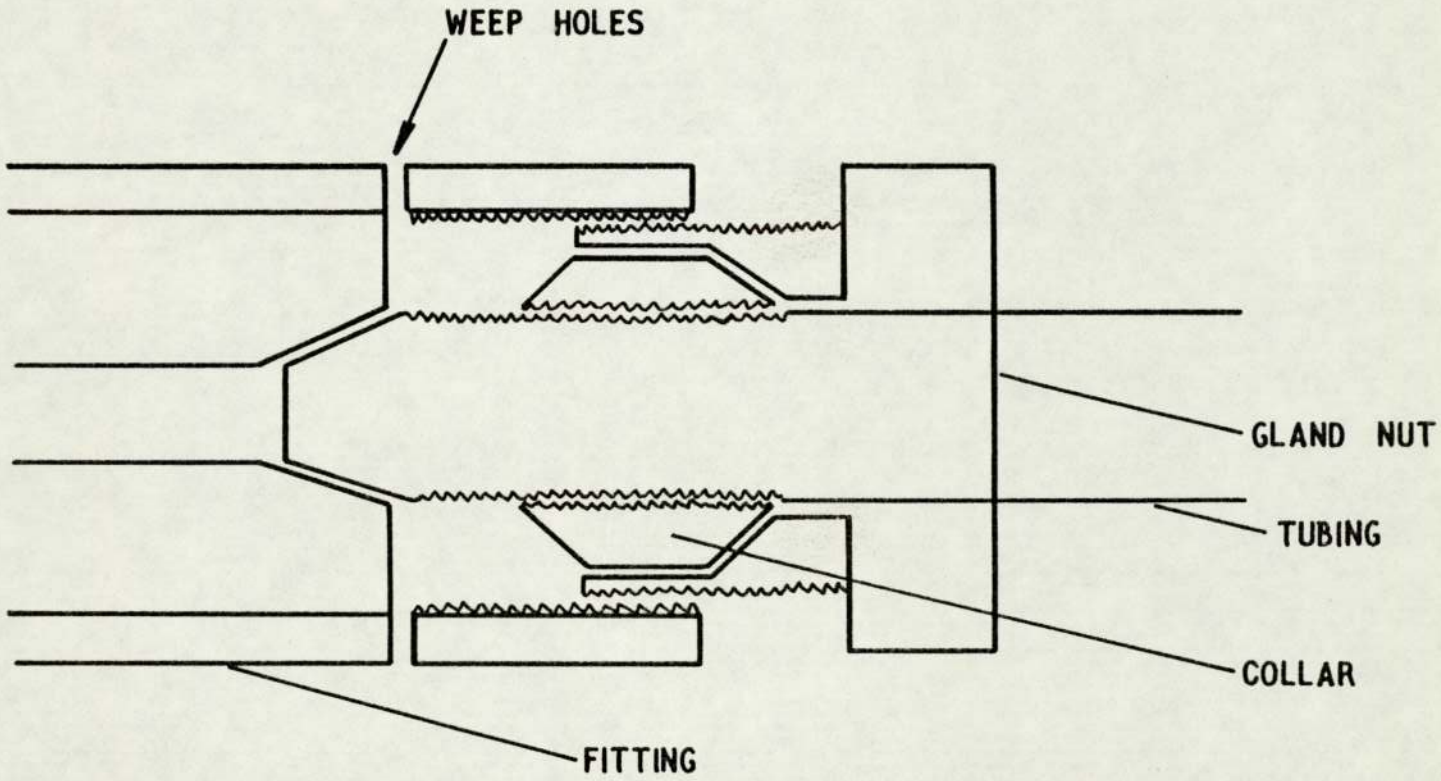

FIGURE AI-1 DETAILS OF "CONE AND THREAD" CONNECTION

APPENDIX 2

GAS FLOW MEASUREMENT

The rotameter used was calibrated for hydrogen duty. Since the exit gas from the autoclave usually consisted of only 90-95% hydrogen, re-calibration was necessary. Using actual volumes measured on a Parkinson Cowan dry gas meter, a rotameter reading of 10 l min^{-1} (the usual setting) gave an average actual volumetric flowrate of exit gas of 7.6 $lmin^{-1}$.

In the experiments where hydrogen/nitrogen mixtures were used, further recalibration was necessary. Figure A2-1 shows the actual flowrates for different hydrogen/nitrogen compositions at a constant rotameter setting of 10 $lmin^{-1}$. Both the theoretical and actual curves are shown, the former derived from the equation:

$$\frac{F_1}{F_2} = \sqrt{\frac{P_2}{P_1}}$$

where F and p were the volumetric flowrate and gas density respectively, and suffixes 1 and 2 refer to hydrogen and hydrogen + nitrogen respectively. The departure of the actual curve from the theoretical was attributed to other gases (methane, predominantly) in the exit gas and to the fact that the density of a gas affects the Reynolds Number so that the flow may have differed from the expected values calculated on the basis of density correction.

Equivalent volumetric flowrates of hydrogen/nitrogen mixtures and pure hydrogen were achieved without significant error by using rotameter settings of 10 $lmin^{-1}$ and 6 $lmin^{-1}$ respectively.

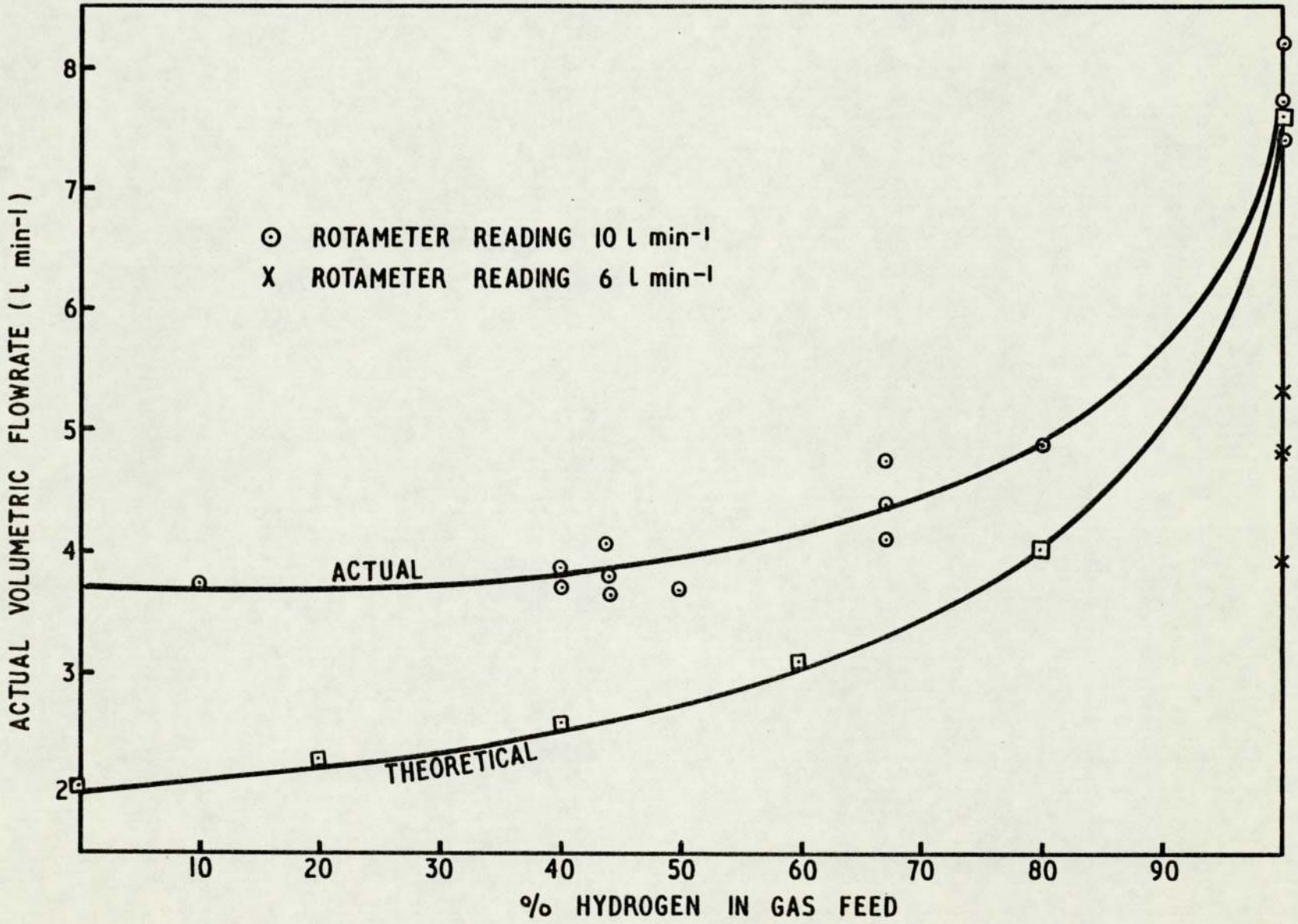

FIGURE A2-1 FLOWRATES WITH DIFFERENT HYDROGEN / NITROGEN MIXTURES

APPENDIX 3

CHOICE OF DISTILLATE FRACTIONS

The choice of distillate fractions should be such that minimum overlap of components between consecutive fractions is achieved.

G.L.C. analyses of several product distillates from the hydrogenation of low rank coal extract solution at different conditions were carried out with a view to determining temperatures at which component concentrations were low as it was these temperatures that were most suitable for fraction cut-points.

A typical chromatogram is shown in Figure A3-1. On it, suitable points for cutting the fractions are indicated with the corresponding temperatures, and these were chosen as standard:

Initial Boiling Point (I.B.P.) - 170°C

170 - 250°C

250 - 300°C

300 - 355°C

355 - 420°C

>420°C

A temperature of 420°C was chosen as the final cut-point because most of the components in anthracene oil boil below 420°C and it is assumed that all unreacted coal and/or coal derived material boils above this temperature. However, as was discussed in section 4.6.1, the small amount of material boiling above 420°C originally present in the oil makes a significant contribution to the total amount boiling above this temperature in the coal extract solution.

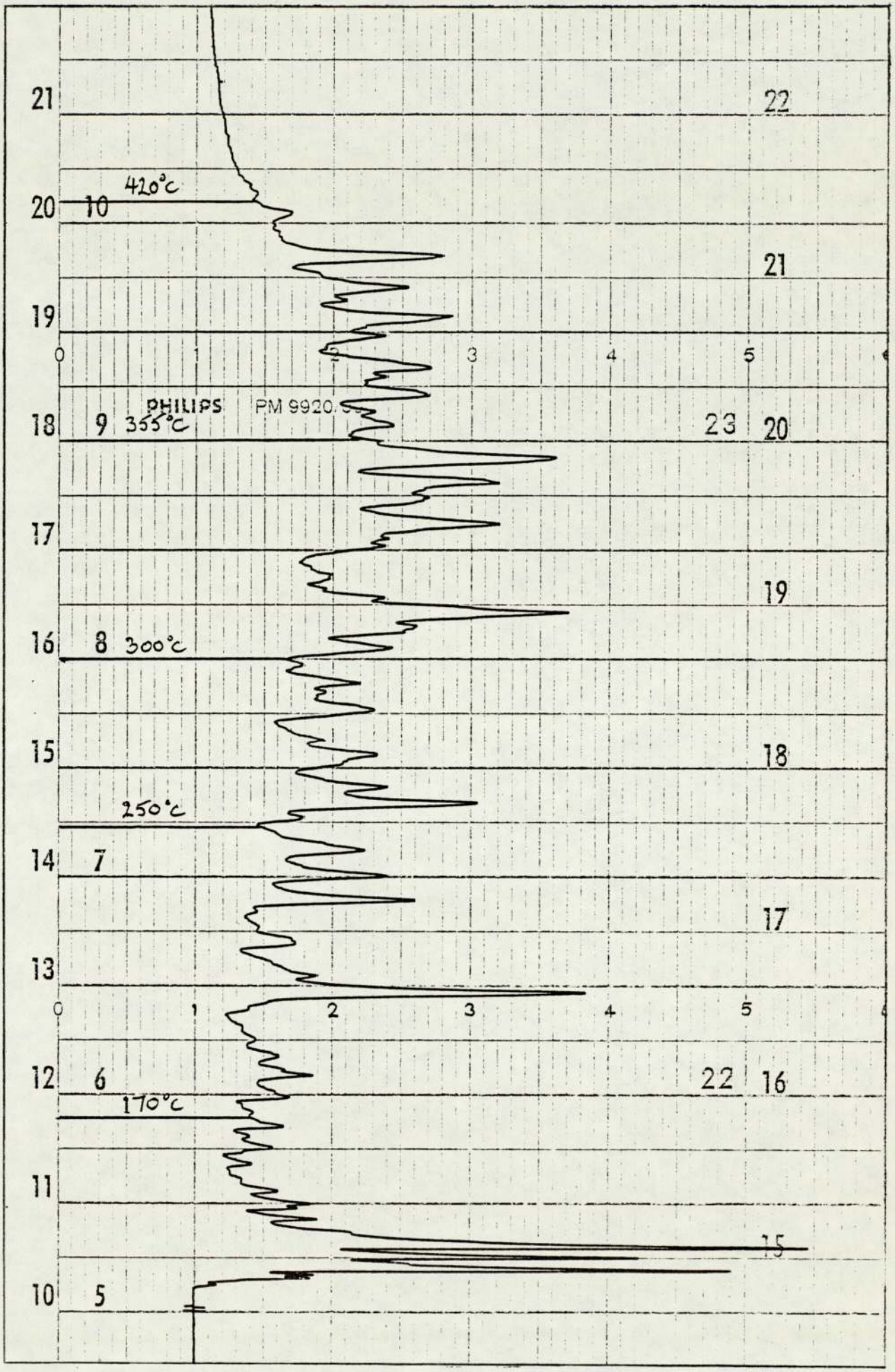

FIGURE A3-1. GAS-LIQUID CHROMATOGRAM OF TYPICAL PRODUCT DISTILLATE SHOWING FRACTION CUT-POINTS.

APPENDIX 4

TYPICAL COMPOUNDS PRESENT IN DIFFERENT DISTILLATION FRACTIONS

(Boiling points in brackets)

1. IBP - 170°C

Cyclopentane (50°C)

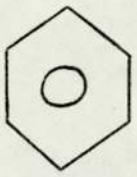

Benzene (80°C)

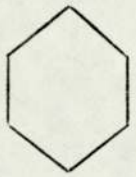

Cyclohexane (81°C)

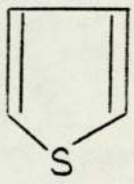

Thiophene (84°C)

2. 170 - 250°C

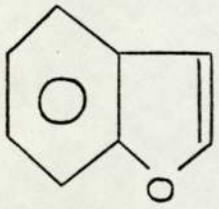

Benzofuran (171°C)

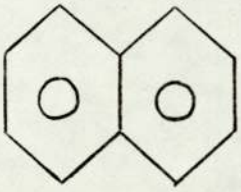

Naphthalene (218°C)

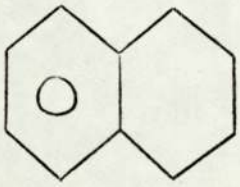

Tetralin (207°C)

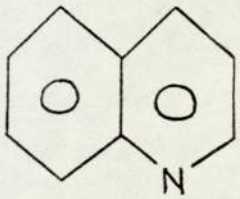

Quinoline (237°C)

3. 250 - 300°C

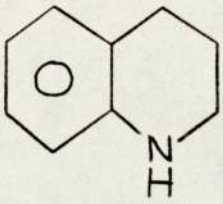

Tetrahydro-quinoline (251°C)

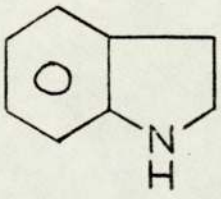

Indole (253°C)

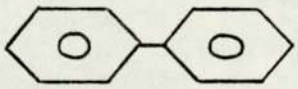

Diphenyl (255°C)

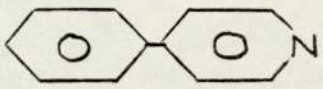

4-Phenylpyridine (275°C)

4. 300 - 355°C

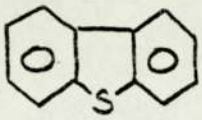

Dibenzo-thiophene

(332°C)

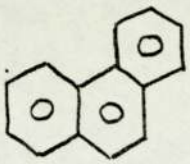

Phenanthrene

(338°C)

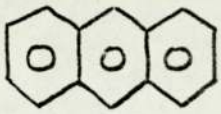

Anthracene

(340°C)

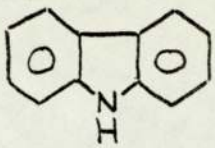

Carbazole

(354°C)

5. 355 - 420°C

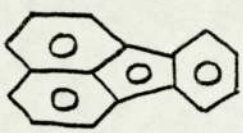

Fluoranthene

(382°C)

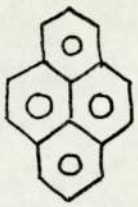

Pyrene

(393°C)

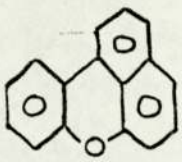

Benzo(kl)-xanthen

(400°C)

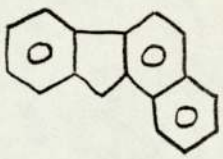

Benzo(a)-fluorene

(413°C)

6. 420°C +

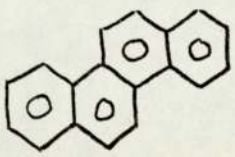

Chrysene

(448°C)

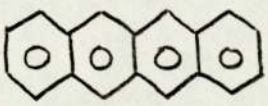

Naphthacene

(450°C)

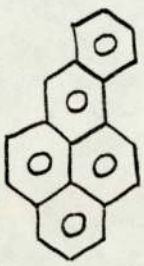

Benzo(a)-pyrene

(496°C)

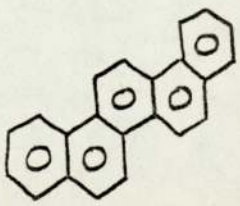

Picene

(520°C)

The above is intended only as an indication of the type of compounds that are present in each distillation fraction and not all the compounds listed are necessarily to be found in the product.

It should be pointed out that the relationship between the number of cyclic rings and boiling range is complicated by the presence of paraffinic side chains, for example:

Phenanthrene	b.p. 338°C
3-Methyl-phenanthrene	b.p. 352°C
3,6-Dimethyl-phenanthrene	b.p. 363°C
1,2,8-Trimethyl-phenanthrene	b.p. 409°C

REFERENCES

1. "Reserves of Oil & Gas in U.K.", HMSO (1974).
2. P. Savage, Chem. Age, p.14. 22 March (1974).
3. B.C. Thompson, World Coal, 3, 8, p.14 (1977).
4. M.P.E. Berthelot, Bull. Soc. Chim, 11, 278 (1869).
5. F. Bergius, Ger.P 301,231 (1913).
6. F. Bergius, Fuel, 4, 458 (1925).
7. M. Pier, Fuel, 14, 136 (1935).
8. N. Booth, F.A. Williams. J. Inst. Fuel, 11,493 (1938).
9. K. Gordon, J. Inst. Fuel, 9,69 (1935).
10. H.E. Blayden, J. Gibson, H.L. Riley. Proc. conf. Ultrafine Str. of Coals & Cokes. BCURA, London, p.76 (1944).
11. P.B. Hirsch. Proc. R. Soc., London, A226,143 (1954).
12. I.G.C. Dryden in "Chem. Coal Util.", H.H. Lowry, Ed. Suppl. Vol., Wiley, N.Y., Ch.6 (1963).
13. J.L. Ayre, R.H. Essenhigh. Fuel Soc. J., 8,44 (1957).
14. D.W. van Krevelen. Fuel, 42,5,427 (1963).
15. W.F.K. Wynne-Jones, H.E. Blaydon, F. Shaw, Brennst-Chem., 33,201 (1952).
16. R. Hayatsu, et al. Nature, 257,5525,378 (1975).
17. R.J. Pugmire, et al. Fuel, 56,295 (1977).
18. M. Orchin, et al. USBM Bull., 505 (1951).
19. F. Heathcoat, R.V. Wheeler, J. Chem. Soc., 2839 (1932).
20. C.W. Shacklock, T.J. Drakeley, J. Soc. Chem. Ind., 46,478T (1927).
21. L. Birkofer, F. Orywal. Brennst-Chem, 48,8,225 (1967).
22. G.R. Hill, L.B. Lyon, Ind. Eng. Chem., 54,6,37 (1962).
23. A.L. Yergey, et al. Ind. Eng. Chem., Proc. Des. Dev., 13,3,233 (1974).
24. A. Lissner, A. Nemes. Brennst. Chem., 16,101 (1935).

25. C.E. Snape, C.R.E., Private Communication (1977).

26. C. Golumbic. USBM Invest., 4662 (1950).

27. A.P. Oele, et al. Fuel, 30,169 (1951).

28. I.G.C. Dryden. Nature, 162,959 (1948).

29. O. Kruber, A. Raeithel. Chem. Ber., 86,366 (1953); 85,327 (1952); 71B,2478 (1938).

30. A. Gillet. Research, 2,407 (1949).

31. E. Rusin. Koks Smola Gaz., 17,9,271 (1972).

32. G.O. Davies, F.J. Derbyshire, R. Price. J. Inst. Fuel, L404,121 (1977).

33. M. Orchin, H.H. Storch. Ind. Eng. Chem., 40, 1385 (1949).

34. G.P. Curran, R.T. Struck, E. Gorin. A.C.S., Div. Fuel Chem., 10,2,C-130 (1966).

35. A.M. Squires. Appl. Energy, 4,3,161 (1978).

36. D.C. Cronauer, et al. Ind. Eng. Chem., Prod. Des. Dev., 17,3,281 (1978).

37. V. Ipatieff, M.I. Levine. J. Phys. Chem. (USSR), 6,632 (1935).

38. V. Ipatieff, V.P. Teodorovitch, M.I. Levine. Oil & Gas J., 32,20 (1933).

39. V. Ipatieff, M.I. Levine. Khim. Tver. Top., 7,866 (1937).

40. P.K. Frolich, et al. Ind. Eng. Chem., 23,548 (1931).

41. I.B. Rapoport. "Chem. & Technol. of Synth. Liq. Fuels." Publ. for Nat. Sci. Foundation, Washington D.C. by Israel Programme for Scientific Translations, Jeruselem. First Publ. 1955.

42. J.A. Guin, et al. A.C.S., Div. Fuel. Chem., 21,5,170 (1976).

43. J.W. Prather, et al. Ind. Eng. Chem., Proc. Des. Dev., 16,3 (1977).

44. M.D. Gray, J. Owen. Paper to ECSC Round Table Conf., Rome (1973).

45. A. Pott, H. Broche. B.P. 293808 (1927); French P. 657409 (1928).

46. E. Gorin. US P. 3,143,489 (1964).

47. W.C. Bull. Paper to Coal Tech. Gp., ACS Pittsburg. (1964).

48. D.L. Kloepper, et al. Spencer Chem. Div. of Gulf Oil Corp., Report No.9 for O.C.R. (1965).

49. R. Wolk, N. Stewart, S. Alpert. EPRI J., p.12 May (1976).

50. Conoco Coal Dev. Co., Cat. Tech. Summary: Clean Fuels West Report, Spring (1976).

51. L.E. Furlong, et al. Paper to Nat. Meet. A.I.ChE., L.A., Calif. Nov. (1975).

52. W. Kawa, et al. A.C.S., Div. Fuel Chem., 19,1,192 (1974).

53. J.G. Gatsis. USP 3,671,418 (1972).

54. D.K. Mukherjee, P.B. Chowdhury. Fuel, 55,1,4 (1976).

55. A.R. Tarrer, J.A. Guin. A.C.S., Div. Fuel Chem. 21,5 (1976).

56. J.A. Guin, et al. Ind. Eng. Chem., Proc. Des. Dev., 17,2,118 (1978).

57. W.K.T. Gleim. A.C.S., Div. Fuel. Chem., 21,5 (1976).

58. V. Ipatieff, H. Pines, E. Meisinger. J.ACS, 71,2934 (1949).

59. H.W. Slotboom, J.M.L. Penninger, Ind. Eng. Chem., Proc. Des. Dev. 13,3,296 (1974).

60. D.L. Trimm, Chem. Engr. 261,200 (1972).

61. A.G. Deem, J.E. Kaveckis, Ind. Eng. Chem. 33,1373 (1941).

62. O. Weisser, S. Landa 'Sulphide Catalysts - their properties & applications', Pergamon. (1973).

63. W.H. Wiser. Fuel, 47,6,475 (1968).

64. H. Adkins, G. Krsek. J.A.C.S. 71,3051, (1949).

65. S.M. Kovach, J. Bennett, A.C.S. Div. Fuel Chem., 20,1,143 (1975).

66. C.C. Kang, E.S. Johanson. A.C.S. Div. Fuel Chem. 21,32 (1976).

67. E.C. McColgan, B.I. Parsons. Mines Branch. Res. Rep. R-273, Ottawa (1974).

68. M. Boudart, et al. EPRI. Rep. 415, PB247, 618/2WE Oct. (1975).

69. V.G. Lipovich, et al. Neftepererabotkai Neftekhimiya, 12, (1975), Trans. in Int. Chem. Eng., 18,1,98 (1978).

70. S. Friedman, et al. J. Org. Chem., 24,1287 (1959).

71. S.J. Lapporte, W.R. Schnett. J. Org. Chem., 28,1947 (1963).

72. C.G. Frye, J. Chem. Eng. Data, 7,592 (1962).

73. C.C. Hall, Fuel, 12,76 (1933).

74. S.A. Qader, G.R. Hill. ACS, Div. Fuel Chem., 14,4(I), 84 (1970).

75. H.G.J. Potgieter. Fuel, 52,2,134 (1973).

76. D.M. Maiorov. J. Appl. Chem. USSR, 29,1195 (1956).

77. J.M.L. Penninger, H.W. Slotboom. Erdöl und Kohle, 26,8,445 (1973).

78. A.A. Krichko, L.S. Soretova. Noiye Sposoby Poluch. Khim. Prod. Osu. Goryuch. Iskop, Akad Nauk SSSR. Inst. Goryuch. Iskop. 68 (1966).

79. P. Blom, et al. J.S. Afr. Chem. Inst., 28,1,130 (1975).

80. S.A. Qader, D.B. McComber, W.H. Wiser. ACS, Div. Fuel Chem. 18,4,127 (1973).

81. H.W. Haynes, C.S. Huang, K.C. Wang. ACS, Div. Fuel Chem., 21,5,228 (1976).

82. W. Wu, H.W. Haynes. ACS, Symp. Series, 20,65 (1975).

83. E.S. Moore. "Coal". 2nd Ed. Wiley, N.Y. (1940).

64. H.D. Glass. Fuel, 34,253 (1955).

85. W. van Loon, H.H. Smeets. Fuel, 19,119 (1950).

86. H.C. Howard in "Chem. Coal Util.," H.H. Lowry, Ed. Suppl. Vol., Wiley, N.Y., Ch.6 (1963).

87. R. Holroyd, R.V. Wheeler, Fuel, 9,104 (1930).

88. D. Fitzgerald, D.W. van Krevelen. Fuel, 38,17 (1959).

89. P.C. Yellow. BCURA, Mon. Bull., 29,9,285 (1965).

90. W.H. Wiser, G.R. Hill, N.J. Kertamus. ACS, Div. Fuel Chem., 10,2,121 (1966).

91. D.R. Stephens. "Prospects for in-Situ Coal Liquefaction", Calif. Univ., Livermore (1975).

92. N.C.B. Report "Mining Beyond 2000 A.D.," PL8531 (RLC/P/77/12) (1977).

93. E.F. Pevere, G.B. Arnold. USP 2,595,979 (1952).

94. E.L. Clark, et al. Ind. Eng. Chem. 42,861 (1950).

95. R.W. Rieve, H. Shalit. USP 3,619,404 (1971).

96. W.C. Schroeder. Hydroc. Proc., 55,1,131 (1976).

97. E.L. Clark, et al. Ind. Eng. Chem., 42,861 (1950).

98. L. Horton, J.G. King, F.A. Williams. BP 407,400 (1934).

99. I.G. Farbenindustrie A-G. Ger. P. 68,641 (1941).

100. Kohlenveredlung A-G. BP 291,481 (1928).

101. Standard Oil Dev. Co. B.P. 693,582 (1953).

102. E.F. Pevere, H.V. Hess, G.B. Arnold. USP 2,658,861 (1953).

103. C. Krauch, M. Pier. USP 1,890,435 (1932).

104. T.M. Davidson, G.P. Lewis. BP 220,732 (1923).

105. M. Melamid. BP 235,828 (1924).

106. M. Letort, A. Boyer, P. Payen. Bull. Soc. Chim. France, 8-9, 1589 (1963).

107. F. Fisher, H. Schrader. Brennst. Chem., 2,257 (1921).

108. H.R. Appell, I. Wender. ACS, Div. Fuel Chem., 12,3,220 (1968).

109. H.R. Appell, I. Wender, R.D. Miller. ACS, 163rd Nat. Meet., Boston, Mass. (1972).

110. H.R. Appell, E.C. Moroni, R.D. Miller. ACS, Div. Fuel Chem. 20,1,58 (1975).

111. J.G. Handwerk, et al. ACS, Div. Fuel Chem. 20,1,26 (1975).

112. Y.C. Fu, E.G. Illig. ACS. Div. Fuel Chem. 20,1,47 (1975).

113. Fuel Research Station. Annual Report (1933).

114. K. Gordon. Coll. Guard, 143,2115 (1931).

115. E.J. Lush. J. Soc. Chem. Ind., 43,53T (1924).

116. H.H. Storch, et al. Ind. Eng. Chem. 32,346 (1940).

117. L.L. Anderson, et al. ACS, Div. Fuel Chem., 12,3,181 (1968).

118. S.A. Qader, G.R. Hill, ACS, Div. Fuel Chem., 13,1,87 (1969).

119. S.A. Qader, W.H. Wiser, G.R. Hill, ACS. Div. Fuel Chem., 12,2,28 (1968).

120. M.G. Pelipetz, et al. Ind. Eng. Chem., 40,1259 (1948).

121. T. Ishii,Y. Maekawa, G. Takeda. Kagaku Kogaku, 29,12,988 (1965).

122. R. Yoshida, et al. Nippon Kagaku Kaishi, 10, 1885 (1972).

123. M.G. Pelipetz, et al. Ind. Eng. Chem., 45,806 (1953).

124. S. Weller, M.G. Pelipetz, S. Friedman. Ind. Eng. Chem., 43,1572 (1951).

125. J.A. Brooks, et al. "Cat. Dev. for Coal Lique." Amoco PB-254 400 (1976).

126. D.K. Mukherjee, P. Samuel, A. Lahiri, Proc. Symp. Chem. Oil Coal, 128, (1969) - publ. (1972).

127. S.R. Gun, et al. Indian J. Tech., 15,218 (1977).

128. R.T. Struck, et al. Ind. Eng. Chem. Proc. Des. Dev. 8,4,546 (1969).

129. W.T. House. ACS, Div. Fuel Chem., 14,4(I), 68 (1970).

130. M. Janardanarao, et al. Erdöl und Kohle, 27,6,309 (1974).

131. B.C. Peters, ERDA Rep. FE-1534-44-49 (1977).

132. V.M. Kuganov, Khimiya i Tekhnologiya Toplivi Masel, 3,1, (1973).

133. S.G. Gagarin, et al. Khimiya Tverdogo Toplivi, 10,1,94 (1976).

134. Y.T. Shah, et al. Ind. Eng. Chem., Proc. Des. Dev., 17,3,288 (1978).

135. V.W. Weekman, Jr. Ind. Eng. Chem., Proc. Des. Dev., 7,90 (1968).

136. V.W. Weekman, D.M. Nace. A.I.ChEJ., 16,397 (1970).

137. B.E. Strangeland, J.R. Kittrell. Ind. Eng. Chem., Proc. Des. Dev., 11,1,15 (1972).

138. V.W. Weekman, Jr. Ind. Eng. Chem., Proc. Des. Dev., 8,3,385 (1969).

139. S.A. Qader, et al. J. Inst. Petrol, 56,550,187 (1970).

140. Y.M. Zhorov, et al. Neftepererab. Neftekhim, 5 (1970). Trans. in Int. Chem. Eng., 11,256 (1971).

141. B.E. Strangeland, Ind. Eng. Chem., Proc. Des. Dev., 13,1,71 (1974).

142. T. Suzaki, I. Takahashi. U.S. Naval Tech. Mission to Japan, X-38(N)-7, Encl. (B), 16,149 (1946).

143. K. Mitsui, U.S. Naval Tech. Mission to Japan, X-38(N)-7, Encl. (B), 10,PB58,701, 95, (1945).

144. H.H. Storch, C.O. Hawk, W.E. O'Neill. J.A.C.S., 64,230, (1942).

145. H.H. Storch, et al. U.S.B.M. Tech. Pap. 654, (1943).

146. S.A. Qader, W.H. Wiser, G.R. Hill. Fuel, 7,390, (1968).

147. Y. Maekawa, et al. Nenryo Kyokaishi, 46,488,927, (1967).

148. S.A. Qader, W.H. Wiser, G.R. Hill. A.C.S., Div. Fuel Chem., 12,2,28 (1968).

149. R.H. Heck, T.R. Stein. ACS, Div. Pet. Chem., Symp. on Refining of Coal and Shale Liquids, Chicago, (1977).

150. W.A. Wilson, et al. Ind. Eng. Chem., 49,4, (1957).

151. S.A. Qader, D.B. McOmber. A.C.S., Div. Pet. Chem., 20,2,479, (1975).

152. H.W. Haynes, C.S. Huang, W.C. Wang. A.C.S., Div. Fuel Chem., 21,5,228, (1976).

153. A.K. Aboul-Gheit, K. Adbou. J. Inst. Pet., 59,568,188 (1973).

154. B.C. Gates, et al. E.R.D.A. Quart. Rep., July-Sept. (1976).

155. B. Ozimek, B. Radomyski. Chem. Stosow, 19,1,97 (1975).

156. K.W. Han, V.B. Dixit, C.Y. Wen. Ind. Eng. Chem., Proc. Des. Dev. 17,1, (1978).

157. J.Y.F. Low, et al. ACS, Div. Fuel Chem., 20,1,122 (1975).

158. S.A. Qader, G.R. Hill. A.C.S., Div. Fuel Chem., 15,1,26, (1971).

159. S.A. Qader, W.H. Wiser, G.R. Hill. Ind. Eng. Chem., Proc. Des. Dev, 7,3,390 (1968).

160. R.C. Koltz, et al. A.C.S., Div. Fuel Chem., 21,5, (1976).

161. S.A. Qader, et al. A.C.S., Div. Fuel Chem., 12,3,164 (1968).

162. D.K. Mukherjee, et al. Proc. Symp. Chem. Oil Coal, 143 (1969).

163. J.A. Mima, et al. Chem. Eng. Prog., Symp. Series, 63,76,55 (1967).

164. Y. Maekawa, T. Ishii, G. Takeya. J.Chem. Eng. Japan, 10,2,101, (1977).

165. H. Hoog, J.Inst. Pet., 36,738 (1950).

166. M.D. Schlesinger, L. Frank, R. Hiteshue. USBM Rep. 6021 (1962).

167. H.F. Feldman, D.A. Williams. A.J.ChE, 68th Nat. Meet. (1971).

168. J.A. Ruether. Ind. Eng. Chem., Proc. Des. Dev., 16,2,249 (1977).

169. J.O.H. Newman. Jack Charrington Memorial Fellowship paper (1975).

170. L. Horton, J.G. King, F.A. Williams. J. Inst. Fuel, 7,85 (1933).

171. F. Bertolacini. Amoco AF-190, Feb. (1976).

172. T.K. Sherwood, G.J. Farkas. Chem. Eng. Sci., 21,573 (1966).

(173) K.G. Denbigh, Trans. Faraday Soc., 40,352 (1944); 43,648 (1947). K.G. Denhigh, M. Hicks, F.M. Page, Trans. Faraday Soc., 44,479 (1948).

(174) E.L. Clark, Ind. Eng. Chem., 39,1555 (1947).

(175) J. Bridgwater, J.J. Carberry, Brit. Chem. Eng., 12,58 (1967) 12,217 (1967).

(176) L.J. Hillenbrand, ERDA Annual Report US/DE/FE-2321-19, May (1977).

(177) D. Jacques, C.R.E. Private Communication (1979).

(178) P.H. Calderbank, et al. Trans. Inst. Chem. Engrs. (London), 66, (1963).

(179) E.J. Davis, F.J. Derbyshire, NCB Internal Report No. CPS.53 (1976).

(180) Standard Methods for Testing Tar and its Products, p.510, test 3-67, (1967).

(181) H. Kolbel, W. Siemes, Umschan, 24,746 (1957).

(182) W. Siemes, W. Weiss, Dechema Monographien, 32,451 (1959).

(183) I. Furusawa, J.M. Smith, A.I.ChE.J., 20,88 (1974).

(184) I. Langmuir, J.A.C.S., 40,1361 (1918).

(185) P.H. Calderbank, Trans. Inst. Chem. Engrs. (London), 37,173 (1959).

(186) C. Karr, ACS, Div. Fuel Chem., 14,4 (I), 58 (1970).

(187) P.H. Calderbank, F. Evans, J. Rennie, Proc. Int. Symp. Distil., Brighton, Inst. Chem. Engrs, London. Pts. I & II, p.51 (1960).

(188) CRE, ECSC Research Project 7220-EC/810, ¼ly report, July-Dec. (1977).

(189) L.C. Dick, I.C.I. Petrochemicals Div., Private Communication (1977).

(190) W.J. Sweeney, A. Voorhies, Jr. Ind. Eng. Chem., 26,195 (1934).

(191) P.H. Calderbank, S.J.R. Jones, Trans. Inst. Chem. Engrs. (London), 39,363 (1961).

(192) G.B. White, A.J. Pitt, F.J. Derbyshire, C.R.E., Internal Report No. CPS.35 (1975).